CHAPTER
8

FLOW IN PIPES

F luid flow in circular and noncircular pipes is commonly encountered in practice. The hot and cold water that we use in our homes is pumped through pipes. Water in a city is distributed by extensive piping networks. Oil and natural gas are transported hundreds of miles by large pipelines. Blood is carried throughout our bodies by arteries and veins. The cooling water in an engine is transported by hoses to the pipes in the radiator where it is cooled as it flows. Thermal energy in a hydronic space heating system is transferred to the circulating water in the boiler, and then it is transported to the desired locations through pipes.

Fluid flow is classified as *external* and *internal,* depending on whether the fluid is forced to flow over a surface or in a conduit. Internal and external flows exhibit very different characteristics. In this chapter we consider *internal flow* where the conduit is completely filled with the fluid, and flow is driven primarily by a pressure difference. This should not be confused with *open-channel flow* where the conduit is partially filled by the fluid and thus the flow is partially bounded by solid surfaces, as in an irrigation ditch, and flow is driven by gravity alone.

We start this chapter with a general physical description of internal flow and the *velocity boundary layer.* We continue with a discussion of the dimensionless *Reynolds number* and its physical significance. We then discuss the characteristics of flow inside pipes and introduce the *pressure drop* correlations associated with it for both laminar and turbulent flows. Then we present the minor losses and determine the pressure drop and pumping power requirements for real-world piping systems. Finally, we present an overview of flow measurement devices.

OBJECTIVES

When you finish reading this chapter, you should be able to

■ Have a deeper understanding of laminar and turbulent flow in pipes and the analysis of fully developed flow

■ Calculate the major and minor losses associated with pipe flow in piping networks and determine the pumping power requirements

■ Understand the different velocity and flow rate measurement techniques and learn their advantages and disadvantages

Circular pipe

Water
50 atm

Rectangular
duct

Air
1.2 atm

FIGURE 8–1
Circular pipes can withstand large
pressure differences between the
inside and the outside without
undergoing any significant distortion,
but noncircular pipes cannot.

V_{avg}

FIGURE 8–2
Average velocity V_{avg} is defined as the
average speed through a cross section.
For fully developed laminar pipe flow,
V_{avg} is half of maximum velocity.

8–1 ▪ INTRODUCTION

Liquid or gas flow through *pipes* or *ducts* is commonly used in heating and
cooling applications and fluid distribution networks. The fluid in such appli-
cations is usually forced to flow by a fan or pump through a flow section.
We pay particular attention to *friction,* which is directly related to the *pres-
sure drop* and *head loss* during flow through pipes and ducts. The pressure
drop is then used to determine the pumping power requirement. A typical
piping system involves pipes of different diameters connected to each other
by various fittings or elbows to route the fluid, valves to control the flow
rate, and pumps to pressurize the fluid.

The terms *pipe, duct,* and *conduit* are usually used interchangeably for
flow sections. In general, flow sections of circular cross section are referred
to as *pipes* (especially when the fluid is a liquid), and flow sections of non-
circular cross section as *ducts* (especially when the fluid is a gas). Small-
diameter pipes are usually referred to as *tubes.* Given this uncertainty, we
will use more descriptive phrases (such as *a circular pipe* or *a rectangular
duct*) whenever necessary to avoid any misunderstandings.

You have probably noticed that most fluids, especially liquids, are trans-
ported in *circular pipes.* This is because pipes with a circular cross section
can withstand large pressure differences between the inside and the outside
without undergoing significant distortion. *Noncircular pipes* are usually
used in applications such as the heating and cooling systems of buildings
where the pressure difference is relatively small, the manufacturing and
installation costs are lower, and the available space is limited for ductwork
(Fig. 8–1).

Although the theory of fluid flow is reasonably well understood, theoreti-
cal solutions are obtained only for a few simple cases such as fully devel-
oped laminar flow in a circular pipe. Therefore, we must rely on experimen-
tal results and empirical relations for most fluid flow problems rather than
closed-form analytical solutions. Noting that the experimental results are
obtained under carefully controlled laboratory conditions and that no two
systems are exactly alike, we must not be so naive as to view the results
obtained as "exact." An error of 10 percent (or more) in friction factors cal-
culated using the relations in this chapter is the "norm" rather than the
"exception."

The fluid velocity in a pipe changes from *zero* at the surface because of
the no-slip condition to a maximum at the pipe center. In fluid flow, it is
convenient to work with an *average* velocity V_{avg}, which remains constant in
incompressible flow when the cross-sectional area of the pipe is constant
(Fig. 8–2). The average velocity in heating and cooling applications may
change somewhat because of changes in density with temperature. But, in
practice, we evaluate the fluid properties at some average temperature and
treat them as constants. The convenience of working with constant proper-
ties usually more than justifies the slight loss in accuracy.

Also, the friction between the fluid particles in a pipe does cause a slight
rise in fluid temperature as a result of the mechanical energy being con-
verted to sensible thermal energy. But this temperature rise due to *frictional
heating* is usually too small to warrant any consideration in calculations and
thus is disregarded. For example, in the absence of any heat transfer, no
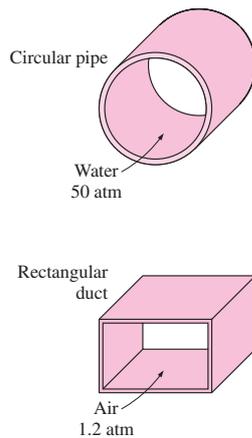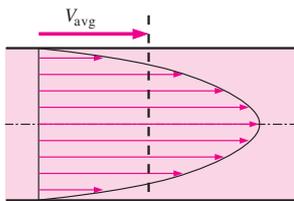
noticeable difference can be detected between the inlet and outlet temperatures of water flowing in a pipe. The primary consequence of friction in fluid flow is pressure drop, and thus any significant temperature change in the fluid is due to heat transfer.

The value of the average velocity V_{avg} at some streamwise cross-section is determined from the requirement that the *conservation of mass* principle be satisfied (Fig. 8–2). That is,

$$\dot{m} = \rho V_{avg} A_c = \int_{A_c} \rho u(r) \, dA_c \qquad (8\text{–}1)$$

where $\dot{m}$ is the mass flow rate, ρ is the density, A_c is the cross-sectional area, and $u(r)$ is the velocity profile. Then the average velocity for incompressible flow in a circular pipe of radius R can be expressed as

$$V_{avg} = \frac{\int_{A_c} \rho u(r) \, dA_c}{\rho A_c} = \frac{\int_0^R \rho u(r) 2\pi r \, dr}{\rho \pi R^2} = \frac{2}{R^2} \int_0^R u(r) r \, dr \qquad (8\text{–}2)$$

Therefore, when we know the flow rate or the velocity profile, the average velocity can be determined easily.

8–2 ■ LAMINAR AND TURBULENT FLOWS

If you have been around smokers, you probably noticed that the cigarette smoke rises in a smooth plume for the first few centimeters and then starts fluctuating randomly in all directions as it continues its rise. Other plumes behave similarly (Fig. 8–3). Likewise, a careful inspection of flow in a pipe reveals that the fluid flow is streamlined at low velocities but turns chaotic as the velocity is increased above a critical value, as shown in Fig. 8–4. The flow regime in the first case is said to be **laminar,** characterized by *smooth streamlines* and *highly ordered motion,* and **turbulent** in the second case, where it is characterized by *velocity fluctuations* and *highly disordered motion.* The **transition** from laminar to turbulent flow does not occur suddenly; rather, it occurs over some region in which the flow fluctuates between laminar and turbulent flows before it becomes fully turbulent. Most flows encountered in practice are turbulent. Laminar flow is encountered when highly viscous fluids such as oils flow in small pipes or narrow passages.

We can verify the existence of these laminar, transitional, and turbulent flow regimes by injecting some dye streaks into the flow in a glass pipe, as the British engineer Osborne Reynolds (1842–1912) did over a century ago. We observe that the dye streak forms a *straight and smooth line* at low velocities when the flow is laminar (we may see some blurring because of molecular diffusion), has *bursts of fluctuations* in the transitional regime, and *zigzags rapidly and randomly* when the flow becomes fully turbulent. These zigzags and the dispersion of the dye are indicative of the fluctuations in the main flow and the rapid mixing of fluid particles from adjacent layers.

The *intense mixing* of the fluid in turbulent flow as a result of rapid fluctuations enhances momentum transfer between fluid particles, which increases the friction force on the surface and thus the required pumping power. The friction factor reaches a maximum when the flow becomes fully turbulent.
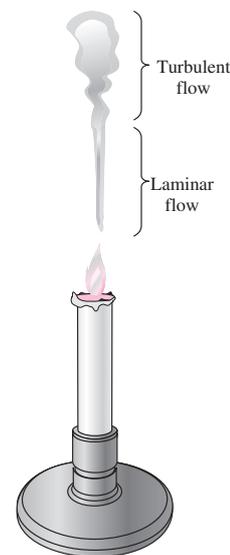
FIGURE 8–3
Laminar and turbulent flow regimes of candle smoke.
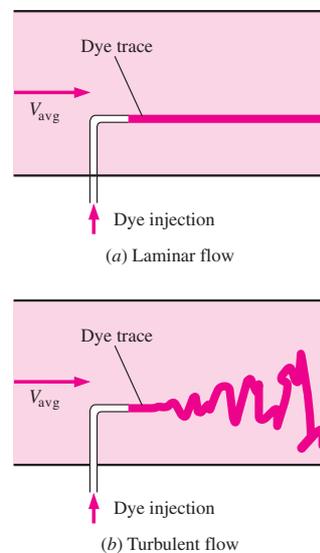
FIGURE 8–4
The behavior of colored fluid injected into the flow in laminar and turbulent flows in a pipe.
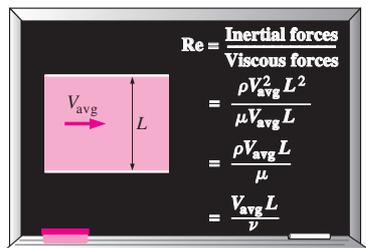
Reynolds Number

The transition from laminar to turbulent flow depends on the *geometry, surface roughness, flow velocity, surface temperature,* and *type of fluid,* among other things. After exhaustive experiments in the 1880s, Osborne Reynolds discovered that the flow regime depends mainly on the ratio of *inertial forces* to *viscous forces* in the fluid. This ratio is called the **Reynolds number** and is expressed for internal flow in a circular pipe as (Fig. 8–5)

$$\text{Re} = \frac{\text{Inertial forces}}{\text{Viscous forces}} = \frac{V_{\text{avg}}D}{\nu} = \frac{\rho V_{\text{avg}}D}{\mu} \qquad (8\text{--}3)$$

where V_{avg} = average flow velocity (m/s), D = characteristic length of the geometry (diameter in this case, in m), and $\nu = \mu/\rho$ = kinematic viscosity of the fluid (m^2/s). Note that the Reynolds number is a *dimensionless* quantity (Chap. 7). Also, kinematic viscosity has the unit m^2/s, and can be viewed as *viscous diffusivity* or *diffusivity for momentum*.

At large Reynolds numbers, the inertial forces, which are proportional to the fluid density and the square of the fluid velocity, are large relative to the viscous forces, and thus the viscous forces cannot prevent the random and rapid fluctuations of the fluid. At *small* or *moderate* Reynolds numbers, however, the viscous forces are large enough to suppress these fluctuations and to keep the fluid "in line." Thus the flow is *turbulent* in the first case and *laminar* in the second.

The Reynolds number at which the flow becomes turbulent is called the **critical Reynolds number,** Re_{cr}. The value of the critical Reynolds number is different for different geometries and flow conditions. For internal flow in a circular pipe, the generally accepted value of the critical Reynolds number is $\text{Re}_{\text{cr}} = 2300$.

For flow through noncircular pipes, the Reynolds number is based on the **hydraulic diameter** D_h defined as (Fig. 8–6)

Hydraulic diameter:
$$D_h = \frac{4A_c}{p} \qquad (8\text{--}4)$$

where A_c is the cross-sectional area of the pipe and p is its wetted perimeter. The hydraulic diameter is defined such that it reduces to ordinary diameter D for circular pipes,

Circular pipes:
$$D_h = \frac{4A_c}{p} = \frac{4(\pi D^2/4)}{\pi D} = D$$

It certainly is desirable to have precise values of Reynolds numbers for laminar, transitional, and turbulent flows, but this is not the case in practice. It turns out that the transition from laminar to turbulent flow also depends on the degree of disturbance of the flow by *surface roughness, pipe vibrations,* and *fluctuations in the flow.* Under most practical conditions, the flow in a circular pipe is laminar for Re $\lesssim$ 2300, turbulent for Re $\gtrsim$ 4000, and transitional in between. That is,

$$\begin{array}{ll} \text{Re} \lesssim 2300 & \text{laminar flow} \\ 2300 \lesssim \text{Re} \lesssim 4000 & \text{transitional flow} \\ \text{Re} \gtrsim 4000 & \text{turbulent flow} \end{array}$$

FIGURE 8–5
The Reynolds number can be viewed as the ratio of inertial forces to viscous forces acting on a fluid element.
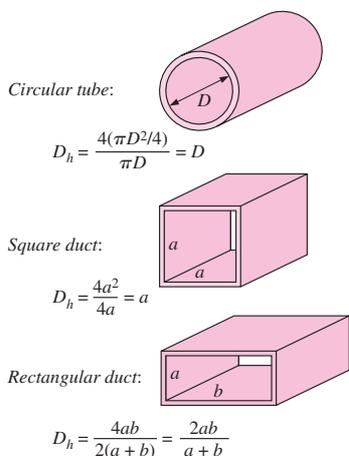
FIGURE 8–6
The hydraulic diameter $D_h = 4A_c/p$ is defined such that it reduces to ordinary diameter for circular tubes.

In transitional flow, the flow switches between laminar and turbulent randomly (Fig. 8–7). It should be kept in mind that laminar flow can be maintained at much higher Reynolds numbers in very smooth pipes by avoiding flow disturbances and pipe vibrations. In such carefully controlled experiments, laminar flow has been maintained at Reynolds numbers of up to 100,000.

8–3 ■ THE ENTRANCE REGION

Consider a fluid entering a circular pipe at a uniform velocity. Because of the no-slip condition, the fluid particles in the layer in contact with the surface of the pipe come to a complete stop. This layer also causes the fluid particles in the adjacent layers to slow down gradually as a result of friction. To make up for this velocity reduction, the velocity of the fluid at the midsection of the pipe has to increase to keep the mass flow rate through the pipe constant. As a result, a velocity gradient develops along the pipe.

The region of the flow in which the effects of the viscous shearing forces caused by fluid viscosity are felt is called the **velocity boundary layer** or just the **boundary layer.** The hypothetical boundary surface divides the flow in a pipe into two regions: the **boundary layer region,** in which the viscous effects and the velocity changes are significant, and the **irrotational (core) flow region,** in which the frictional effects are negligible and the velocity remains essentially constant in the radial direction.

The thickness of this boundary layer increases in the flow direction until the boundary layer reaches the pipe center and thus fills the entire pipe, as shown in Fig. 8–8. The region from the pipe inlet to the point at which the boundary layer merges at the centerline is called the **hydrodynamic entrance region,** and the length of this region is called the **hydrodynamic entry length** L_h. Flow in the entrance region is called *hydrodynamically developing flow* since this is the region where the velocity profile develops. The region beyond the entrance region in which the velocity profile is fully developed and remains unchanged is called the **hydrodynamically fully developed region.** The flow is said to be **fully developed** when the normalized temperature profile remains unchanged as well. Hydrodynamically developed flow is equivalent to fully developed flow when the fluid in the pipe is not heated or cooled since the fluid temperature in this case remains
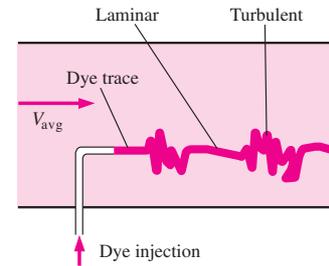
FIGURE 8–7
In the transitional flow region of $2300 \leq Re \leq 4000$, the flow switches between laminar and turbulent randomly.
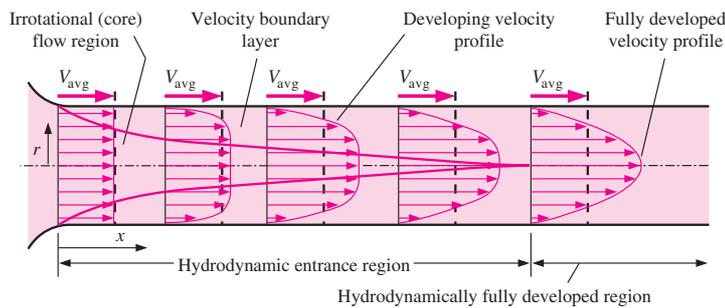
FIGURE 8–8
The development of the velocity boundary layer in a pipe. (The developed average velocity profile is parabolic in laminar flow, as shown, but somewhat flatter or fuller in turbulent flow.)
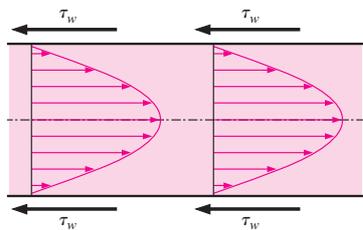
FIGURE 8–9
In the fully developed flow region of a pipe, the velocity profile does not change downstream, and thus the wall shear stress remains constant as well.

essentially constant throughout. The velocity profile in the fully developed region is *parabolic* in laminar flow and somewhat *flatter* (or *fuller*) in turbulent flow due to eddy motion and more vigorous mixing in the radial direction. The time-averaged velocity profile remains unchanged when the flow is fully developed, and thus

Hydrodynamically fully developed: $\dfrac{\partial u(r, x)}{\partial x} = 0 \rightarrow u = u(r)$ **(8–5)**

The shear stress at the pipe wall τ_w is related to the slope of the velocity profile at the surface. Noting that the velocity profile remains unchanged in the hydrodynamically fully developed region, the wall shear stress also remains constant in that region (Fig. 8–9).

Consider fluid flow in the hydrodynamic entrance region of a pipe. The wall shear stress is the *highest* at the pipe inlet where the thickness of the boundary layer is smallest, and decreases gradually to the fully developed value, as shown in Fig. 8–10. Therefore, the pressure drop is *higher* in the entrance regions of a pipe, and the effect of the entrance region is always to *increase* the average friction factor for the entire pipe. This increase may be significant for short pipes but is negligible for long ones.

Entry Lengths

The hydrodynamic entry length is usually taken to be the distance from the pipe entrance to where the wall shear stress (and thus the friction factor) reaches within about 2 percent of the fully developed value. In *laminar flow,* the hydrodynamic entry length is given approximately as [see Kays and Crawford (1993) and Shah and Bhatti (1987)]

$$L_{h, \text{laminar}} \cong 0.05\text{Re}D$$ **(8–6)**
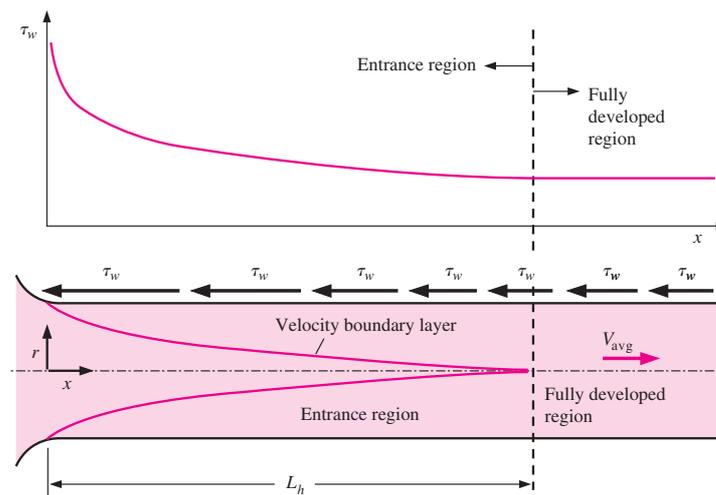
FIGURE 8–10
The variation of wall shear stress in the flow direction for flow in a pipe from the entrance region into the fully developed region.

For Re = 20, the hydrodynamic entry length is about the size of the diameter, but increases linearly with velocity. In the limiting laminar case of Re = 2300, the hydrodynamic entry length is 115D.

In *turbulent flow,* the intense mixing during random fluctuations usually overshadows the effects of molecular diffusion. The hydrodynamic entry length for turbulent flow can be approximated as [see Bhatti and Shah (1987) and Zhi-qing (1982)]

$$L_{h, \text{turbulent}} = 1.359D\text{Re}_D^{1/4} \tag{8–7}$$

The entry length is much shorter in turbulent flow, as expected, and its dependence on the Reynolds number is weaker. In many pipe flows of practical engineering interest, the entrance effects become insignificant beyond a pipe length of 10 diameters, and the hydrodynamic entry length is approximated as

$$L_{h, \text{turbulent}} \approx 10D \tag{8–8}$$

Precise correlations for calculating the frictional head losses in entrance regions are available in the literature. However, the pipes used in practice are usually several times the length of the entrance region, and thus the flow through the pipes is often assumed to be fully developed for the entire length of the pipe. This simplistic approach gives *reasonable* results for long pipes but sometimes poor results for short ones since it underpredicts the wall shear stress and thus the friction factor.

8–4 ▪ LAMINAR FLOW IN PIPES

We mentioned in Section 8–2 that flow in pipes is laminar for Re ≲ 2300, and that the flow is fully developed if the pipe is sufficiently long (relative to the entry length) so that the entrance effects are negligible. In this section we consider the steady laminar flow of an incompressible fluid with constant properties in the fully developed region of a straight circular pipe. We obtain the momentum equation by applying a momentum balance to a differential volume element, and obtain the velocity profile by solving it. Then we use it to obtain a relation for the friction factor. An important aspect of the analysis here is that it is one of the few available for viscous flow.

In fully developed laminar flow, each fluid particle moves at a constant axial velocity along a streamline and the velocity profile $u(r)$ remains unchanged in the flow direction. There is no motion in the radial direction, and thus the velocity component in the direction normal to flow is everywhere zero. There is no acceleration since the flow is steady and fully developed.

Now consider a ring-shaped differential volume element of radius r, thickness dr, and length dx oriented coaxially with the pipe, as shown in Fig. 8–11. The volume element involves only pressure and viscous effects and thus the pressure and shear forces must balance each other. The pressure force acting on a submerged plane surface is the product of the pressure at the centroid of the surface and the surface area. A force balance on the volume element in the flow direction gives

$$(2\pi r\, dr\, P)_x - (2\pi r\, dr\, P)_{x+dx} + (2\pi r\, dx\, \tau)_r - (2\pi r\, dx\, \tau)_{r+dr} = 0 \tag{8–9}$$
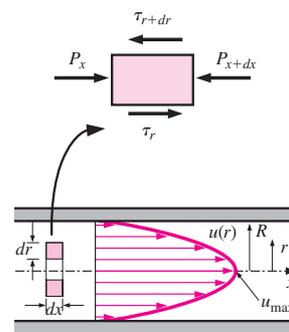
FIGURE 8–11
Free-body diagram of a ring-shaped differential fluid element of radius r, thickness dr, and length dx oriented coaxially with a horizontal pipe in fully developed laminar flow.
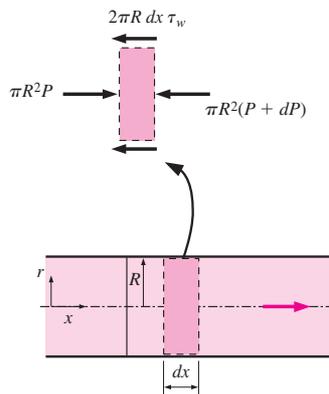
Force balance:

$$\pi R^2 P - \pi R^2 (P + dP) - 2\pi R\, dx\, \tau_w = 0$$

Simplifying:

$$\frac{dP}{dx} = -\frac{2\tau_w}{R}$$

FIGURE 8–12
Free-body diagram of a fluid disk element of radius R and length dx in fully developed laminar flow in a horizontal pipe.

which indicates that in fully developed flow in a horizontal pipe, the viscous and pressure forces balance each other. Dividing by $2\pi dr dx$ and rearranging,

$$r\frac{P_{x+dx} - P_x}{dx} + \frac{(r\tau)_{r+dr} - (r\tau)_r}{dr} = 0 \tag{8–10}$$

Taking the limit as $dr, dx \rightarrow 0$ gives

$$r\frac{dP}{dx} + \frac{d(r\tau)}{dr} = 0 \tag{8–11}$$

Substituting $\tau = -\mu(du/dr)$ and taking $\mu =$ constant gives the desired equation,

$$\frac{\mu}{r}\frac{d}{dr}\left(r\frac{du}{dr}\right) = \frac{dP}{dx} \tag{8–12}$$

The quantity du/dr is negative in pipe flow, and the negative sign is included to obtain positive values for τ. (Or, $du/dr = -du/dy$ since $y = R - r$.) The left side of Eq. 8–12 is a function of r, and the right side is a function of x. The equality must hold for any value of r and x, and an equality of the form $f(r) = g(x)$ can be satisfied only if both $f(r)$ and $g(x)$ are equal to the same constant. Thus we conclude that $dP/dx =$ constant. This can be verified by writing a force balance on a volume element of radius R and thickness dx (a slice of the pipe), which gives (Fig. 8–12)

$$\frac{dP}{dx} = -\frac{2\tau_w}{R} \tag{8–13}$$

Here τ_w is constant since the viscosity and the velocity profile are constants in the fully developed region. Therefore, $dP/dx =$ constant.

Equation 8–12 can be solved by rearranging and integrating it twice to give

$$u(r) = \frac{1}{4\mu}\left(\frac{dP}{dx}\right) + C_1 \ln r + C_2 \tag{8–14}$$

The velocity profile $u(r)$ is obtained by applying the boundary conditions $\partial u/\partial r = 0$ at $r = 0$ (because of symmetry about the centerline) and $u = 0$ at $r = R$ (the no-slip condition at the pipe surface). We get

$$u(r) = -\frac{R^2}{4\mu}\left(\frac{dP}{dx}\right)\left(1 - \frac{r^2}{R^2}\right) \tag{8–15}$$

Therefore, the velocity profile in fully developed laminar flow in a pipe is *parabolic* with a maximum at the centerline and minimum (zero) at the pipe wall. Also, the axial velocity u is positive for any r, and thus the axial pressure gradient dP/dx must be negative (i.e., pressure must decrease in the flow direction because of viscous effects).

The average velocity is determined from its definition by substituting Eq. 8–15 into Eq. 8–2, and performing the integration. It gives

$$V_{\text{avg}} = \frac{2}{R^2}\int_0^R u(r)r\, dr = \frac{-2}{R^2}\int_0^R \frac{R^2}{4\mu}\left(\frac{dP}{dx}\right)\left(1 - \frac{r^2}{R^2}\right)r\, dr = -\frac{R^2}{8\mu}\left(\frac{dP}{dx}\right) \tag{8–16}$$

Combining the last two equations, the velocity profile is rewritten as

$$u(r) = 2V_{\text{avg}}\left(1 - \frac{r^2}{R^2}\right) \tag{8–17}$$

This is a convenient form for the velocity profile since V_{avg} can be determined easily from the flow rate information.

The maximum velocity occurs at the centerline and is determined from Eq. 8–17 by substituting $r = 0$,

$$u_{max} = 2V_{avg} \tag{8–18}$$

Therefore, *the average velocity in fully developed laminar pipe flow is one-half of the maximum velocity.*

Pressure Drop and Head Loss

A quantity of interest in the analysis of pipe flow is the *pressure drop* ΔP since it is directly related to the power requirements of the fan or pump to maintain flow. We note that $dP/dx = $ constant, and integrating from $x = x_1$ where the pressure is P_1 to $x = x_1 + L$ where the pressure is P_2 gives

$$\frac{dP}{dx} = \frac{P_2 - P_1}{L} \tag{8–19}$$

Substituting Eq. 8–19 into the V_{avg} expression in Eq. 8–16, the pressure drop can be expressed as

Laminar flow:
$$\Delta P = P_1 - P_2 = \frac{8\mu L V_{avg}}{R^2} = \frac{32\mu L V_{avg}}{D^2} \tag{8–20}$$

The symbol Δ is typically used to indicate the difference between the final and initial values, like $\Delta y = y_2 - y_1$. But in fluid flow, ΔP is used to designate pressure drop, and thus it is $P_1 - P_2$. A pressure drop due to viscous effects represents an irreversible pressure loss, and it is called **pressure loss** ΔP_L to emphasize that it is a *loss* (just like the head loss h_L, which is proportional to it).

Note from Eq. 8–20 that the pressure drop is proportional to the viscosity μ of the fluid, and ΔP would be zero if there were no friction. Therefore, the drop of pressure from P_1 to P_2 in this case is due entirely to viscous effects, and Eq. 8–20 represents the pressure loss ΔP_L when a fluid of viscosity μ flows through a pipe of constant diameter D and length L at average velocity V_{avg}.

In practice, it is found convenient to express the pressure loss for all types of fully developed internal flows (laminar or turbulent flows, circular or noncircular pipes, smooth or rough surfaces, horizontal or inclined pipes) as (Fig. 8–13)

Pressure loss:
$$\Delta P_L = f \frac{L}{D} \frac{\rho V_{avg}^2}{2} \tag{8–21}$$

where $\rho V_{avg}^2 / 2$ is the *dynamic pressure* and f is the **Darcy friction factor,**

$$f = \frac{8\tau_w}{\rho V_{avg}^2} \tag{8–22}$$

It is also called the **Darcy–Weisbach friction factor,** named after the Frenchman Henry Darcy (1803–1858) and the German Julius Weisbach (1806–1871), the two engineers who provided the greatest contribution in its development. It should not be confused with the *friction coefficient* C_f

Pressure loss: $\Delta P_L = f \dfrac{L}{D} \dfrac{\rho V_{avg}^2}{2}$

Head loss: $h_L = \dfrac{\Delta P_L}{\rho g} = f \dfrac{L}{D} \dfrac{V_{avg}^2}{2g}$
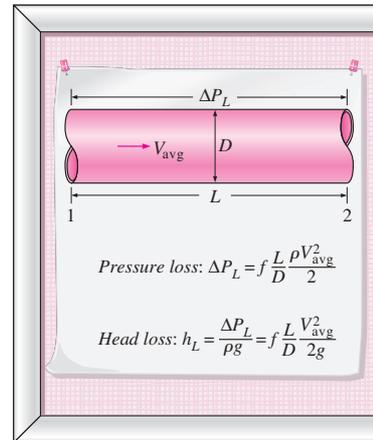
FIGURE 8–13
The relation for pressure loss (and head loss) is one of the most general relations in fluid mechanics, and it is valid for laminar or turbulent flows, circular or noncircular pipes, and pipes with smooth or rough surfaces.

[also called the *Fanning friction factor*, named after the American engineer John Fanning (1837–1911)], which is defined as $C_f = 2\tau_w/(\rho V_{avg}^2) = f/4$.

Setting Eqs. 8–20 and 8–21 equal to each other and solving for f gives the friction factor for fully developed laminar flow in a circular pipe,

Circular pipe, laminar:
$$f = \frac{64\mu}{\rho D V_{avg}} = \frac{64}{Re} \qquad \textbf{(8–23)}$$

This equation shows that *in laminar flow, the friction factor is a function of the Reynolds number only and is independent of the roughness of the pipe surface.*

In the analysis of piping systems, pressure losses are commonly expressed in terms of the *equivalent fluid column height*, called the **head loss** h_L. Noting from fluid statics that $\Delta P = \rho g h$ and thus a pressure difference of ΔP corresponds to a fluid height of $h = \Delta P/\rho g$, the pipe head loss is obtained by dividing ΔP_L by ρg to give

Head loss:
$$h_L = \frac{\Delta P_L}{\rho g} = f\frac{L}{D}\frac{V_{avg}^2}{2g} \qquad \textbf{(8–24)}$$

The head loss h_L represents *the additional height that the fluid needs to be raised by a pump in order to overcome the frictional losses in the pipe*. The head loss is caused by viscosity, and it is directly related to the wall shear stress. Equations 8–21 and 8–24 are valid for both laminar and turbulent flows in both circular and noncircular pipes, but Eq. 8–23 is valid only for fully developed laminar flow in circular pipes.

Once the pressure loss (or head loss) is known, the required pumping power *to overcome the pressure loss* is determined from

$$\dot{W}_{pump, L} = \dot{V}\Delta P_L = \dot{V}\rho g h_L = \dot{m}g h_L \qquad \textbf{(8–25)}$$

where $\dot{V}$ is the volume flow rate and $\dot{m}$ is the mass flow rate.

The average velocity for laminar flow in a horizontal pipe is, from Eq. 8–20,

Horizontal pipe:
$$V_{avg} = \frac{(P_1 - P_2)R^2}{8\mu L} = \frac{(P_1 - P_2)D^2}{32\mu L} = \frac{\Delta P\, D^2}{32\mu L} \qquad \textbf{(8–26)}$$

Then the volume flow rate for laminar flow through a horizontal pipe of diameter D and length L becomes

$$\dot{V} = V_{avg}A_c = \frac{(P_1 - P_2)R^2}{8\mu L}\pi R^2 = \frac{(P_1 - P_2)\pi D^4}{128\mu L} = \frac{\Delta P\, \pi D^4}{128\mu L} \qquad \textbf{(8–27)}$$

This equation is known as **Poiseuille's law,** and this flow is called *Hagen–Poiseuille flow* in honor of the works of G. Hagen (1797–1884) and J. Poiseuille (1799–1869) on the subject. Note from Eq. 8–27 that *for a specified flow rate, the pressure drop and thus the required pumping power is proportional to the length of the pipe and the viscosity of the fluid, but it is inversely proportional to the fourth power of the radius (or diameter) of the pipe*. Therefore, the pumping power requirement for a piping system can be reduced by a factor of 16 by doubling the pipe diameter (Fig. 8–14). Of course the benefits of the reduction in the energy costs must be weighed against the increased cost of construction due to using a larger-diameter pipe.

The pressure drop ΔP equals the pressure loss ΔP_L in the case of a horizontal pipe, but this is not the case for inclined pipes or pipes with variable cross-sectional area. This can be demonstrated by writing the energy

FIGURE 8–14
The pumping power requirement for a laminar flow piping system can be reduced by a factor of 16 by doubling the pipe diameter.

equation for steady, incompressible one-dimensional flow in terms of heads as (see Chap. 5)

$$\frac{P_1}{\rho g} + \alpha_1 \frac{V_1^2}{2g} + z_1 + h_{\text{pump}, u} = \frac{P_2}{\rho g} + \alpha_2 \frac{V_2^2}{2g} + z_2 + h_{\text{turbine}, e} + h_L \quad \textbf{(8–28)}$$

where $h_{\text{pump}, u}$ is the useful pump head delivered to the fluid, $h_{\text{turbine}, e}$ is the turbine head extracted from the fluid, h_L is the irreversible head loss between sections 1 and 2, V_1 and V_2 are the average velocities at sections 1 and 2, respectively, and α_1 and α_2 are the *kinetic energy correction factors* at sections 1 and 2 (it can be shown that $\alpha = 2$ for fully developed laminar flow and about 1.05 for fully developed turbulent flow). Equation 8–28 can be rearranged as

$$P_1 - P_2 = \rho(\alpha_2 V_2^2 - \alpha_1 V_1^2)/2 + \rho g[(z_2 - z_1) + h_{\text{turbine}, e} - h_{\text{pump}, u} + h_L] \quad \textbf{(8–29)}$$

Therefore, the pressure drop $\Delta P = P_1 - P_2$ and pressure loss $\Delta P_L = \rho g h_L$ for a given flow section are equivalent if (1) the flow section is horizontal so that there are no hydrostatic or gravity effects ($z_1 = z_2$), (2) the flow section does not involve any work devices such as a pump or a turbine since they change the fluid pressure ($h_{\text{pump}, u} = h_{\text{turbine}, e} = 0$), (3) the cross-sectional area of the flow section is constant and thus the average flow velocity is constant ($V_1 = V_2$), and (4) the velocity profiles at sections 1 and 2 are the same shape ($\alpha_1 = \alpha_2$).

Inclined Pipes

Relations for inclined pipes can be obtained in a similar manner from a force balance in the direction of flow. The only additional force in this case is the component of the fluid weight in the flow direction, whose magnitude is

$$W_x = W \sin \theta = \rho g V_{\text{element}} \sin \theta = \rho g (2\pi r \, dr \, dx) \sin \theta \quad \textbf{(8–30)}$$

where θ is the angle between the horizontal and the flow direction (Fig. 8–15). The force balance in Eq. 8–9 now becomes

$$(2\pi r \, dr \, P)_x - (2\pi r \, dr \, P)_{x+dx} + (2\pi r \, dx \, \tau)_r$$
$$- (2\pi r \, dx \, \tau)_{r+dr} - \rho g(2\pi r \, dr \, dx) \sin \theta = 0 \quad \textbf{(8–31)}$$

which results in the differential equation

$$\frac{\mu}{r} \frac{d}{dr}\left(r \frac{du}{dr}\right) = \frac{dP}{dx} + \rho g \sin \theta \quad \textbf{(8–32)}$$

Following the same solution procedure, the velocity profile can be shown to be

$$u(r) = -\frac{R^2}{4\mu}\left(\frac{dP}{dx} + \rho g \sin \theta\right)\left(1 - \frac{r^2}{R^2}\right) \quad \textbf{(8–33)}$$

It can also be shown that the *average velocity* and the *volume flow rate* relations for laminar flow through inclined pipes are, respectively,

$$V_{\text{avg}} = \frac{(\Delta P - \rho g L \sin \theta)D^2}{32\mu L} \quad \text{and} \quad \dot{V} = \frac{(\Delta P - \rho g L \sin \theta)\pi D^4}{128\mu L} \quad \textbf{(8–34)}$$

which are identical to the corresponding relations for horizontal pipes, except that ΔP is replaced by $\Delta P - \rho g L \sin \theta$. Therefore, the results already obtained for horizontal pipes can also be used for inclined pipes provided that ΔP is replaced by $\Delta P - \rho g L \sin \theta$ (Fig. 8–16). Note that $\theta > 0$ and thus $\sin \theta > 0$ for uphill flow, and $\theta < 0$ and thus $\sin \theta < 0$ for downhill flow.

FIGURE 8–15
Free-body diagram of a ring-shaped differential fluid element of radius r, thickness dr, and length dx oriented coaxially with an inclined pipe in fully developed laminar flow.

Horizontal pipe: $\dot{V} = \dfrac{\Delta P \, \pi D^4}{128\mu L}$

Inclined pipe: $\dot{V} = \dfrac{(\Delta P - \rho g L \sin \theta)\pi D^4}{128\mu L}$

Uphill flow: $\theta > 0$ and $\sin \theta > 0$

Downhill flow: $\theta < 0$ and $\sin \theta < 0$

FIGURE 8–16
The relations developed for fully developed laminar flow through horizontal pipes can also be used for inclined pipes by replacing ΔP with $\Delta P - \rho g L \sin \theta$.

In inclined pipes, the combined effect of pressure difference and gravity drives the flow. Gravity helps downhill flow but opposes uphill flow. Therefore, much greater pressure differences need to be applied to maintain a specified flow rate in uphill flow although this becomes important only for liquids, because the density of gases is generally low. In the special case of *no flow* ($\dot{V} = 0$), we have $\Delta P = \rho g L \sin \theta$, which is what we would obtain from fluid statics (Chap. 3).

Laminar Flow in Noncircular Pipes

The friction factor *f* relations are given in Table 8–1 for *fully developed laminar flow* in pipes of various cross sections. The Reynolds number for flow in these pipes is based on the hydraulic diameter $D_h = 4A_c/p$, where A_c is the cross-sectional area of the pipe and *p* is its wetted perimeter.

TABLE 8–1

Friction factor for fully developed *laminar flow* in pipes of various cross sections ($D_h = 4A_c/p$ and Re $= V_{avg} D_h/\nu$)

Tube Geometry	a/b or θ°	Friction Factor f
Circle	—	64.00/Re
Rectangle	a/b	
	1	56.92/Re
	2	62.20/Re
	3	68.36/Re
	4	72.92/Re
	6	78.80/Re
	8	82.32/Re
	∞	96.00/Re
Ellipse	a/b	
	1	64.00/Re
	2	67.28/Re
	4	72.96/Re
	8	76.60/Re
	16	78.16/Re
Isosceles triangle	θ	
	10°	50.80/Re
	30°	52.28/Re
	60°	53.32/Re
	90°	52.60/Re
	120°	50.96/Re
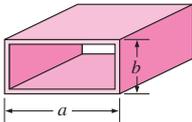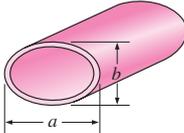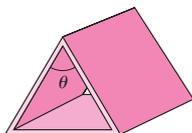
Horizontal

+15°

−15°

FIGURE 8–17
Schematic for Example 8–1.

EXAMPLE 8–1 **Flow Rates in Horizontal and Inclined Pipes**

Oil at 20°C (ρ = 888 kg/m^3 and μ = 0.800 kg/m · s) is flowing steadily through a 5-cm-diameter 40-m-long pipe (Fig. 8–17). The pressure at the pipe inlet and outlet are measured to be 745 and 97 kPa, respectively. Determine the flow rate of oil through the pipe assuming the pipe is (*a*) horizontal, (*b*) inclined 15° upward, (*c*) inclined 15° downward. Also verify that the flow through the pipe is laminar.

SOLUTION The pressure readings at the inlet and outlet of a pipe are given. The flow rates are to be determined for three different orientations, and the flow is to be shown to be laminar.
Assumptions **1** The flow is steady and incompressible. **2** The entrance effects are negligible, and thus the flow is fully developed. **3** The pipe involves no components such as bends, valves, and connectors. **4** The piping section involves no work devices such as a pump or a turbine.
Properties The density and dynamic viscosity of oil are given to be ρ = 888 kg/m^3 and μ = 0.800 kg/m · s, respectively.
Analysis The pressure drop across the pipe and the pipe cross-sectional area are

$$\Delta P = P_1 - P_2 = 745 - 97 = 648 \text{ kPa}$$

$$A_c = \pi D^2/4 = \pi(0.05 \text{ m})^2/4 = 0.001963 \text{ m}^2$$

(*a*) The flow rate for all three cases can be determined from Eq. 8–34,

$$\dot{V} = \frac{(\Delta P - \rho g L \sin \theta)\pi D^4}{128\mu L}$$

where θ is the angle the pipe makes with the horizontal. For the horizontal case, θ = 0 and thus sin θ = 0. Therefore,

$$\dot{V}_{horiz} = \frac{\Delta P\, \pi D^4}{128\mu L} = \frac{(648 \text{ kPa})\pi(0.05 \text{ m})^4}{128(0.800 \text{ kg/m · s})(40 \text{ m})}\left(\frac{1000 \text{ N/m}^2}{1 \text{ kPa}}\right)\left(\frac{1 \text{ kg · m/s}^2}{1 \text{ N}}\right)$$

$$= \textbf{0.00311 m}^3\textbf{/s}$$

(*b*) For uphill flow with an inclination of 15°, we have θ = +15°, and

$$\dot{V}_{uphill} = \frac{(\Delta P - \rho g L \sin \theta)\pi D^4}{128\mu L}$$

$$= \frac{[648,000 \text{ Pa} - (888 \text{ kg/m}^3)(9.81 \text{ m/s}^2)(40 \text{ m})\sin 15°]\pi(0.05 \text{ m})^4}{128(0.800 \text{ kg/m · s})(40 \text{ m})}\left(\frac{1 \text{ kg · m/s}^2}{1 \text{ Pa · m}^2}\right)$$

$$= \textbf{0.00267 m}^3\textbf{/s}$$

(*c*) For downhill flow with an inclination of 15°, we have θ = −15°, and

$$\dot{V}_{downhill} = \frac{(\Delta P - \rho g L \sin \theta)\pi D^4}{128\mu L}$$

$$= \frac{[648,000 \text{ Pa} - (888 \text{ kg/m}^3)(9.81 \text{ m/s}^2)(40 \text{ m})\sin(-15°)]\pi(0.05 \text{ m})^4}{128(0.800 \text{ kg/m · s})(40 \text{ m})}\left(\frac{1 \text{ kg · m/s}^2}{1 \text{ Pa · m}^2}\right)$$

$$= \textbf{0.00354 m}^3\textbf{/s}$$

The flow rate is the highest for the downhill flow case, as expected. The average fluid velocity and the Reynolds number in this case are

$$V_{avg} = \frac{\dot{V}}{A_c} = \frac{0.00354 \text{ m}^3/\text{s}}{0.001963 \text{ m}^2} = 1.80 \text{ m/s}$$

$$\text{Re} = \frac{\rho V_{avg} D}{\mu} = \frac{(888 \text{ kg/m}^3)(1.80 \text{ m/s})(0.05 \text{ m})}{0.800 \text{ kg/m} \cdot \text{s}} = 100$$

which is much less than 2300. Therefore, the flow is *laminar* for all three cases and the analysis is valid.

Discussion Note that the flow is driven by the combined effect of pressure difference and gravity. As can be seen from the flow rates we calculated, gravity opposes uphill flow, but enhances downhill flow. Gravity has no effect on the flow rate in the horizontal case. Downhill flow can occur even in the absence of an applied pressure difference. For the case of $P_1 = P_2 = 97$ kPa (i.e., no applied pressure difference), the pressure throughout the entire pipe would remain constant at 97 Pa, and the fluid would flow through the pipe at a rate of 0.00043 m³/s under the influence of gravity. The flow rate increases as the tilt angle of the pipe from the horizontal is increased in the negative direction and would reach its maximum value when the pipe is vertical.
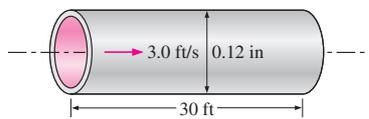
FIGURE 8–18
Schematic for Example 8–2.

EXAMPLE 8–2   **Pressure Drop and Head Loss in a Pipe**

Water at 40°F ($\rho = 62.42$ lbm/ft³ and $\mu = 1.038 \times 10^{-3}$ lbm/ft · s) is flowing through a 0.12-in- (= 0.010 ft) diameter 30-ft-long horizontal pipe steadily at an average velocity of 3.0 ft/s (Fig. 8–18). Determine (*a*) the head loss, (*b*) the pressure drop, and (*c*) the pumping power requirement to overcome this pressure drop.

SOLUTION The average flow velocity in a pipe is given. The head loss, the pressure drop, and the pumping power are to be determined.

Assumptions **1** The flow is steady and incompressible. **2** The entrance effects are negligible, and thus the flow is fully developed. **3** The pipe involves no components such as bends, valves, and connectors.

Properties The density and dynamic viscosity of water are given to be $\rho = 62.42$ lbm/ft³ and $\mu = 1.038 \times 10^{-3}$ lbm/ft · s, respectively.

Analysis (*a*) First we need to determine the flow regime. The Reynolds number is

$$\text{Re} = \frac{\rho V_{avg} D}{\mu} = \frac{(62.42 \text{ lbm/ft}^3)(3 \text{ ft/s})(0.01 \text{ ft})}{1.038 \times 10^{-3} \text{ lbm/ft} \cdot \text{s}} = 1803$$

which is less than 2300. Therefore, the flow is laminar. Then the friction factor and the head loss become

$$f = \frac{64}{\text{Re}} = \frac{64}{1803} = 0.0355$$

$$h_L = f \frac{L}{D} \frac{V_{avg}^2}{2g} = 0.0355 \frac{30 \text{ ft}}{0.01 \text{ ft}} \frac{(3 \text{ ft/s})^2}{2(32.2 \text{ ft/s}^2)} = \textbf{14.9 ft}$$

(*b*) Noting that the pipe is horizontal and its diameter is constant, the pressure drop in the pipe is due entirely to the frictional losses and is equivalent to the pressure loss,

$$\Delta P = \Delta P_L = f \frac{L}{D} \frac{\rho V_{avg}^2}{2} = 0.0355 \frac{30 \text{ ft}}{0.01 \text{ ft}} \frac{(62.42 \text{ lbm/ft}^3)(3 \text{ ft/s})^2}{2} \left(\frac{1 \text{ lbf}}{32.2 \text{ lbm} \cdot \text{ft/s}^2} \right)$$

$$= \textbf{929 lbf/ft}^2 = \textbf{6.45 psi}$$

(*c*) The volume flow rate and the pumping power requirements are

$$\dot{V} = V_{avg} A_c = V_{avg}(\pi D^2/4) = (3 \text{ ft/s})[\pi(0.01 \text{ ft})^2/4] = 0.000236 \text{ ft}^3/\text{s}$$

$$\dot{W}_{pump} = \dot{V} \Delta P = (0.000236 \text{ ft}^3/\text{s})(929 \text{ lbf/ft}^2) \left(\frac{1 \text{ W}}{0.737 \text{ lbf} \cdot \text{ft/s}} \right) = \textbf{0.30 W}$$

Therefore, power input in the amount of 0.30 W is needed to overcome the frictional losses in the flow due to viscosity.

Discussion The pressure rise provided by a pump is often listed by a pump manufacturer in units of head (Chap. 14). Thus, the pump in this flow needs to provide 14.9 ft of water head in order to overcome the irreversible head loss.

8–5 ▪ TURBULENT FLOW IN PIPES

Most flows encountered in engineering practice are turbulent, and thus it is important to understand how turbulence affects wall shear stress. However, turbulent flow is a complex mechanism dominated by fluctuations, and despite tremendous amounts of work done in this area by researchers, the theory of turbulent flow remains largely undeveloped. Therefore, we must rely on experiments and the empirical or semi-empirical correlations developed for various situations.

Turbulent flow is characterized by random and rapid fluctuations of swirling regions of fluid, called **eddies,** throughout the flow. These fluctuations provide an additional mechanism for momentum and energy transfer. In laminar flow, fluid particles flow in an orderly manner along pathlines, and momentum and energy are transferred across streamlines by molecular diffusion. In turbulent flow, the swirling eddies transport mass, momentum, and energy to other regions of flow much more rapidly than molecular diffusion, greatly enhancing mass, momentum, and heat transfer. As a result, turbulent flow is associated with much higher values of friction, heat transfer, and mass transfer coefficients (Fig. 8–19).

Even when the average flow is steady, the eddy motion in turbulent flow causes significant fluctuations in the values of velocity, temperature, pressure, and even density (in compressible flow). Figure 8–20 shows the variation of the instantaneous velocity component u with time at a specified location, as can be measured with a hot-wire anemometer probe or other sensitive device. We observe that the instantaneous values of the velocity fluctuate about an average value, which suggests that the velocity can be expressed as the sum of an *average value* $\bar{u}$ and a *fluctuating component* u',

$$u = \bar{u} + u' \tag{8–35}$$

This is also the case for other properties such as the velocity component v in the y-direction, and thus $v = \bar{v} + v'$, $P = \bar{P} + P'$, and $T = \bar{T} + T'$. The average value of a property at some location is determined by averaging it over a time interval that is sufficiently large so that the time average levels off to a constant. Therefore, the time average of fluctuating components is

(*a*) Before   (*b*) After
turbulence   turbulence
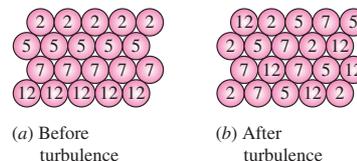
FIGURE 8–19
The intense mixing in turbulent flow brings fluid particles at different momentums into close contact and thus enhances momentum transfer.
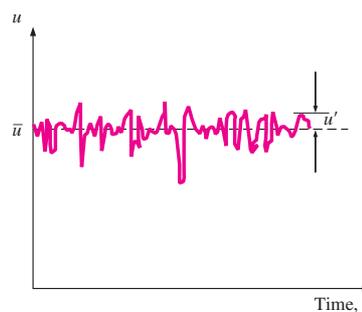
FIGURE 8–20
Fluctuations of the velocity component u with time at a specified location in turbulent flow.

FIGURE 8–21
The velocity profile and the variation of shear stress with radial distance for turbulent flow in a pipe.

FIGURE 8–22
Fluid particle moving upward through a differential area dA as a result of the velocity fluctuation v'.

zero, e.g., $\overline{u'} = 0$. The magnitude of u' is usually just a few percent of $\overline{u}$, but the high frequencies of eddies (in the order of a thousand per second) makes them very effective for the transport of momentum, thermal energy, and mass. In time-averaged *stationary* turbulent flow, the average values of properties (indicated by an overbar) are independent of time. The chaotic fluctuations of fluid particles play a dominant role in pressure drop, and these random motions must be considered in analyses together with the average velocity.

Perhaps the first thought that comes to mind is to determine the shear stress in an analogous manner to laminar flow from $\tau = -\mu \, d\overline{u}/dr$, where $\overline{u}(r)$ is the average velocity profile for turbulent flow. But the experimental studies show that this is not the case, and the shear stress is much larger due to the turbulent fluctuations. Therefore, it is convenient to think of the turbulent shear stress as consisting of two parts: the *laminar component,* which accounts for the friction between layers in the flow direction (expressed as $\tau_{\text{lam}} = -\mu \, d\overline{u}/dr$), and the *turbulent component,* which accounts for the friction between the fluctuating fluid particles and the fluid body (denoted as τ_{turb} and is related to the fluctuation components of velocity). Then the *total shear stress* in turbulent flow can be expressed as

$$\tau_{\text{total}} = \tau_{\text{lam}} + \tau_{\text{turb}} \tag{8–36}$$

The typical average velocity profile and relative magnitudes of laminar and turbulent components of shear stress for turbulent flow in a pipe are given in Fig. 8–21. Note that although the velocity profile is approximately parabolic in laminar flow, it becomes flatter or "fuller" in turbulent flow, with a sharp drop near the pipe wall. The fullness increases with the Reynolds number, and the velocity profile becomes more nearly uniform, lending support to the commonly utilized uniform velocity profile approximation for fully developed turbulent pipe flow. Keep in mind, however, that the flow speed at the wall of a stationary pipe is always zero (no-slip condition).
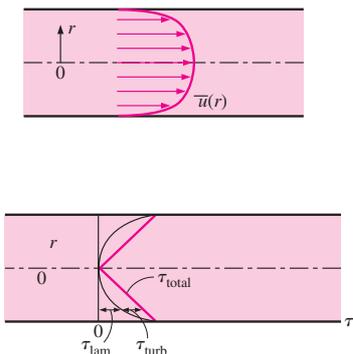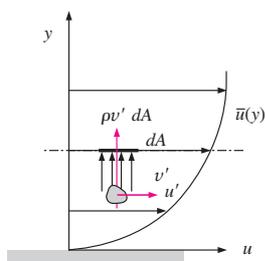
Turbulent Shear Stress

Consider turbulent flow in a horizontal pipe, and the upward eddy motion of fluid particles in a layer of lower velocity to an adjacent layer of higher velocity through a differential area dA as a result of the velocity fluctuation v', as shown in Fig. 8–22. The mass flow rate of the fluid particles rising through dA is $\rho v' dA$, and its net effect on the layer above dA is a reduction in its average flow velocity because of momentum transfer to the fluid particles with lower average flow velocity. This momentum transfer causes the horizontal velocity of the fluid particles to increase by u', and thus its momentum in the horizontal direction to increase at a rate of $(\rho v' dA)u'$, which must be equal to the decrease in the momentum of the upper fluid layer. Noting that force in a given direction is equal to the rate of change of momentum in that direction, the horizontal force acting on a fluid element above dA due to the passing of fluid particles through dA is $\delta F = (\rho v' dA)(-u') = -\rho u'v' dA$. Therefore, the shear force per unit area due to the eddy motion of fluid particles $\delta F/dA = -\rho u'v'$ can be viewed as the instantaneous turbulent shear stress. Then the **turbulent shear stress** can be expressed as

$$\tau_{\text{turb}} = -\rho \overline{u'v'} \tag{8–37}$$

where $\overline{u'v'}$ is the time average of the product of the fluctuating velocity components u' and v'. Note that $\overline{u'v'} \neq 0$ even though $\overline{u'} = 0$ and $\overline{v'} = 0$

(and thus $\overline{u'}\,\overline{v'} = 0$), and experimental results show that $\overline{u'v'}$ is usually a negative quantity. Terms such as $-\rho\overline{u'v'}$ or $-\rho\overline{u'^2}$ are called **Reynolds stresses** or **turbulent stresses.**

Many semi-empirical formulations have been developed that model the Reynolds stress in terms of average velocity gradients in order to provide mathematical *closure* to the equations of motion. Such models are called **turbulence models** and are discussed in more detail in Chap. 15.

The random eddy motion of groups of particles resembles the random motion of molecules in a gas—colliding with each other after traveling a certain distance and exchanging momentum in the process. Therefore, momentum transport by eddies in turbulent flows is analogous to the molecular momentum diffusion. In many of the simpler turbulence models, turbulent shear stress is expressed in an analogous manner as suggested by the French mathematician Joseph Boussinesq (1842–1929) in 1877 as

$$\tau_{\text{turb}} = -\rho\overline{u'v'} = \mu_t \frac{\partial \overline{u}}{\partial y} \qquad \textbf{(8–38)}$$

where μ_t is the **eddy viscosity** or **turbulent viscosity,** which accounts for momentum transport by turbulent eddies. Then the total shear stress can be expressed conveniently as

$$\tau_{\text{total}} = (\mu + \mu_t) \frac{\partial \overline{u}}{\partial y} = \rho(\nu + \nu_t) \frac{\partial \overline{u}}{\partial y} \qquad \textbf{(8–39)}$$

where $\nu_t = \mu_t/\rho$ is the **kinematic eddy viscosity** or **kinematic turbulent viscosity** (also called the *eddy diffusivity of momentum*). The concept of eddy viscosity is very appealing, but it is of no practical use unless its value can be determined. In other words, eddy viscosity must be modeled as a function of the average flow variables; we call this *eddy viscosity closure*. For example, in the early 1900s, the German engineer L. Prandtl introduced the concept of **mixing length** l_m, which is related to the average size of the eddies that are primarily responsible for mixing, and expressed the turbulent shear stress as

$$\tau_{\text{turb}} = \mu_t \frac{\partial \overline{u}}{\partial y} = \rho l_m^2 \left(\frac{\partial \overline{u}}{\partial y}\right)^2 \qquad \textbf{(8–40)}$$

But this concept is also of limited use since l_m is not a constant for a given flow (in the vicinity of the wall, for example, l_m is nearly proportional to the distance from the wall) and its determination is not easy. Final mathematical closure is obtained only when l_m is written as a function of average flow variables, distance from the wall, etc.

Eddy motion and thus eddy diffusivities are much larger than their molecular counterparts in the core region of a turbulent boundary layer. The eddy motion loses its intensity close to the wall and diminishes at the wall because of the no-slip condition (u' and v' are identically zero at a stationary wall). Therefore, the velocity profile is very slowly changing in the core region of a turbulent boundary layer, but very steep in the thin layer adjacent to the wall, resulting in large velocity gradients at the wall surface. So it is no surprise that the wall shear stress is much larger in turbulent flow than it is in laminar flow (Fig. 8–23).

Note that molecular diffusivity of momentum ν (as well as μ) is a fluid property, and its value is listed in fluid handbooks. Eddy diffusivity ν_t (as well as μ_t), however, is *not* a fluid property, and its value depends on flow

Laminar flow
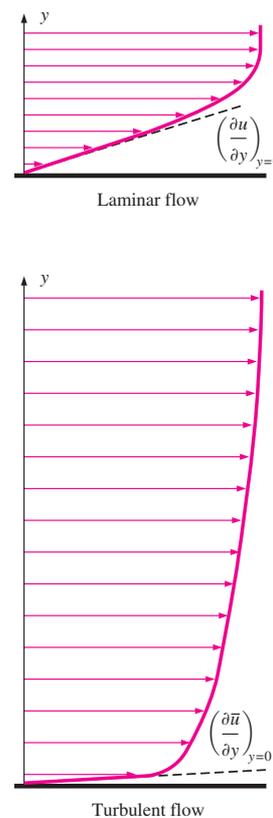
Turbulent flow

FIGURE 8–23
The velocity gradients at the wall, and thus the wall shear stress, are much larger for turbulent flow than they are for laminar flow, even though the turbulent boundary layer is thicker than the laminar one for the same value of free-stream velocity.
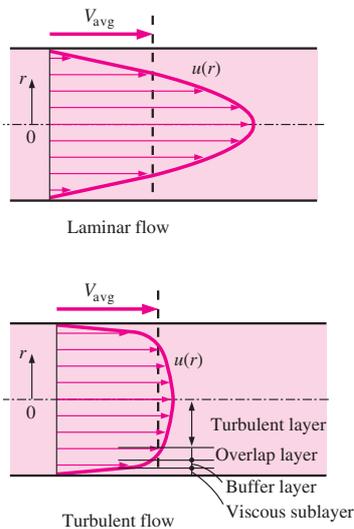
FIGURE 8–24
The velocity profile in fully developed pipe flow is parabolic in laminar flow, but much fuller in turbulent flow.

conditions. Eddy diffusivity ν_t decreases toward the wall, becoming zero at the wall. Its value ranges from zero at the wall to several thousand times the value of the molecular diffusivity in the core region.

Turbulent Velocity Profile

Unlike laminar flow, the expressions for the velocity profile in a turbulent flow are based on both analysis and measurements, and thus they are semi-empirical in nature with constants determined from experimental data. Consider fully developed turbulent flow in a pipe, and let u denote the time-averaged velocity in the axial direction (and thus drop the overbar from $\bar{u}$ for simplicity).

Typical velocity profiles for fully developed laminar and turbulent flows are given in Fig. 8–24. Note that the velocity profile is parabolic in laminar flow but is much fuller in turbulent flow, with a sharp drop near the pipe wall. Turbulent flow along a wall can be considered to consist of four regions, characterized by the distance from the wall. The very thin layer next to the wall where viscous effects are dominant is the **viscous** (or **laminar** or **linear** or **wall**) sublayer. The velocity profile in this layer is very nearly *linear*, and the flow is streamlined. Next to the viscous sublayer is the **buffer layer,** in which turbulent effects are becoming significant, but the flow is still dominated by viscous effects. Above the buffer layer is the **overlap** (or **transition**) **layer,** also called the **inertial sublayer,** in which the turbulent effects are much more significant, but still not dominant. Above that is the **outer** (or **turbulent**) **layer** in the remaining part of the flow in which turbulent effects dominate over molecular diffusion (viscous) effects.

Flow characteristics are quite different in different regions, and thus it is difficult to come up with an analytic relation for the velocity profile for the entire flow as we did for laminar flow. The best approach in the turbulent case turns out to be to identify the key variables and functional forms using dimensional analysis, and then to use experimental data to determine the numerical values of any constants.

The thickness of the viscous sublayer is very small (typically, much less than 1 percent of the pipe diameter), but this thin layer next to the wall plays a dominant role on flow characteristics because of the large velocity gradients it involves. The wall dampens any eddy motion, and thus the flow in this layer is essentially laminar and the shear stress consists of laminar shear stress which is proportional to the fluid viscosity. Considering that velocity changes from zero to nearly the core region value across a layer that is sometimes no thicker than a hair (almost like a step function), we would expect the velocity profile in this layer to be very nearly linear, and experiments confirm that. Then the velocity gradient in the viscous sublayer remains nearly constant at $du/dy = u/y$, and the wall shear stress can be expressed as

$$\tau_w = \mu \frac{u}{y} = \rho\nu\frac{u}{y} \qquad \text{or} \qquad \frac{\tau_w}{\rho} = \frac{\nu u}{y} \qquad \textbf{(8–41)}$$

where y is the distance from the wall (note that $y = R - r$ for a circular pipe). The quantity τ_w/ρ is frequently encountered in the analysis of turbulent velocity profiles. The square root of τ_w/ρ has the dimensions of velocity, and thus it is convenient to view it as a fictitious velocity called the **friction velocity** expressed as $u_* = \sqrt{\tau_w/\rho}$. Substituting this into Eq. 8–41, the velocity profile in the viscous sublayer can be expressed in dimensionless form as

Viscous sublayer:
$$\frac{u}{u_*} = \frac{yu_*}{\nu} \tag{8–42}$$

This equation is known as the **law of the wall,** and it is found to satisfactorily correlate with experimental data for smooth surfaces for $0 \le yu_*/\nu \le 5$. Therefore, the thickness of the viscous sublayer is roughly

Thickness of viscous sublayer:
$$y = \delta_{\text{sublayer}} = \frac{5\nu}{u_*} = \frac{25\nu}{u_\delta} \tag{8–43}$$

where u_δ is the flow velocity at the edge of the viscous sublayer, which is closely related to the average velocity in a pipe. Thus we conclude that *the thickness of the viscous sublayer is proportional to the kinematic viscosity and inversely proportional to the average flow velocity*. In other words, the viscous sublayer is suppressed and it gets thinner as the velocity (and thus the Reynolds number) increases. Consequently, the velocity profile becomes nearly flat and thus the velocity distribution becomes more uniform at very high Reynolds numbers.

The quantity ν/u_* has dimensions of length and is called the **viscous length;** it is used to nondimensionalize the distance y from the surface. In boundary layer analysis, it is convenient to work with nondimensionalized distance and nondimensionalized velocity defined as

Nondimensionalized variables:
$$y^+ = \frac{yu_*}{\nu} \quad \text{and} \quad u^+ = \frac{u}{u_*} \tag{8–44}$$

Then the law of the wall (Eq. 8–42) becomes simply

Normalized law of the wall:
$$u^+ = y^+ \tag{8–45}$$

Note that the friction velocity u_* is used to nondimensionalize both y and u, and y^+ resembles the Reynolds number expression.

In the overlap layer, the experimental data for velocity are observed to line up on a straight line when plotted against the logarithm of distance from the wall. Dimensional analysis indicates and the experiments confirm that the velocity in the overlap layer is proportional to the logarithm of distance, and the velocity profile can be expressed as

The logarithmic law:
$$\frac{u}{u_*} = \frac{1}{\kappa} \ln \frac{yu_*}{\nu} + B \tag{8–46}$$

where κ and B are constants whose values are determined experimentally to be about 0.40 and 5.0, respectively. Equation 8–46 is known as the **logarithmic law.** Substituting the values of the constants, the velocity profile is determined to be

Overlap layer:
$$\frac{u}{u_*} = 2.5 \ln \frac{yu_*}{\nu} + 5.0 \quad \text{or} \quad u^+ = 2.5 \ln y^+ + 5.0 \tag{8–47}$$

It turns out that the logarithmic law in Eq. 8–47 satisfactorily represents experimental data for the entire flow region except for the regions very close to the wall and near the pipe center, as shown in Fig. 8–25, and thus it is viewed as a *universal velocity profile* for turbulent flow in pipes or over surfaces. Note from the figure that the logarithmic-law velocity profile is quite accurate for $y^+ > 30$, but neither velocity profile is accurate in the buffer layer, i.e., the region $5 < y^+ < 30$. Also, the viscous sublayer appears much larger in the figure than it is since we used a logarithmic scale for distance from the wall.
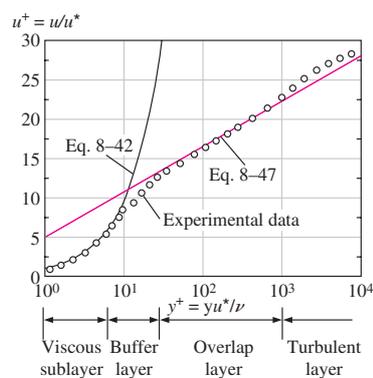
FIGURE 8–25

Comparison of the law of the wall and the logarithmic-law velocity profiles with experimental data for fully developed turbulent flow in a pipe.

A good approximation for the outer turbulent layer of pipe flow can be obtained by evaluating the constant B in Eq. 8–46 from the requirement that maximum velocity in a pipe occurs at the centerline where $r = 0$. Solving for B from Eq. 8–46 by setting $y = R - r = R$ and $u = u_{max}$, and substituting it back into Eq. 8–46 together with $\kappa = 0.4$ gives

Outer turbulent layer: $$\frac{u_{max} - u}{u_*} = 2.5 \ln \frac{R}{R - r} \qquad \text{(8–48)}$$

The deviation of velocity from the centerline value $u_{max} - u$ is called the **velocity defect,** and Eq. 8–48 is called the **velocity defect law.** This relation shows that the normalized velocity profile in the core region of turbulent flow in a pipe depends on the distance from the centerline and is independent of the viscosity of the fluid. This is not surprising since the eddy motion is dominant in this region, and the effect of fluid viscosity is negligible.

Numerous other empirical velocity profiles exist for turbulent pipe flow. Among those, the simplest and the best known is the **power-law velocity profile** expressed as

Power-law velocity profile: $$\frac{u}{u_{max}} = \left(\frac{y}{R}\right)^{1/n} \qquad \text{or} \qquad \frac{u}{u_{max}} = \left(1 - \frac{r}{R}\right)^{1/n} \qquad \text{(8–49)}$$

where the exponent n is a constant whose value depends on the Reynolds number. The value of n increases with increasing Reynolds number. The value $n = 7$ generally approximates many flows in practice, giving rise to the term *one-seventh power-law velocity profile*.

Various power-law velocity profiles are shown in Fig. 8–26 for $n = 6$, 8, and 10 together with the velocity profile for fully developed laminar flow for comparison. Note that the turbulent velocity profile is fuller than the laminar one, and it becomes more flat as n (and thus the Reynolds number) increases. Also note that the power-law profile cannot be used to calculate wall shear stress since it gives a velocity gradient of infinity there, and it fails to give zero slope at the centerline. But these regions of discrepancy constitute a small portion of flow, and the power-law profile gives highly accurate results for turbulent flow through a pipe.

Despite the small thickness of the viscous sublayer (usually much less than 1 percent of the pipe diameter), the characteristics of the flow in this layer are very important since they set the stage for flow in the rest of the pipe. Any irregularity or roughness on the surface disturbs this layer and affects the flow. Therefore, unlike laminar flow, the friction factor in turbulent flow is a strong function of surface roughness.

It should be kept in mind that roughness is a relative concept, and it has significance when its height ε is comparable to the thickness of the laminar sublayer (which is a function of the Reynolds number). All materials appear "rough" under a microscope with sufficient magnification. In fluid mechanics, a surface is characterized as being rough when the hills of roughness protrude out of the laminar sublayer. A surface is said to be smooth when the sublayer submerges the roughness elements. Glass and plastic surfaces are generally considered to be hydrodynamically smooth.

The Moody Chart

The friction factor in fully developed turbulent pipe flow depends on the Reynolds number and the **relative roughness** ε/D, which is the ratio of the
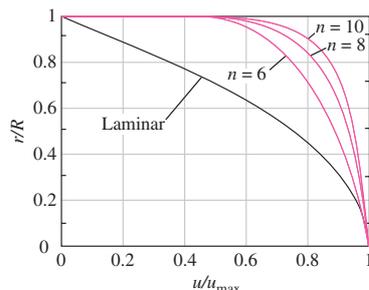
FIGURE 8–26
Power-law velocity profiles for fully developed turbulent flow in a pipe for different exponents, and its comparison with the laminar velocity profile.

mean height of roughness of the pipe to the pipe diameter. The functional form of this dependence cannot be obtained from a theoretical analysis, and all available results are obtained from painstaking experiments using artificially roughened surfaces (usually by gluing sand grains of a known size on the inner surfaces of the pipes). Most such experiments were conducted by Prandtl's student J. Nikuradse in 1933, followed by the works of others. The friction factor was calculated from the measurements of the flow rate and the pressure drop.

The experimental results obtained are presented in tabular, graphical, and functional forms obtained by curve-fitting experimental data. In 1939, Cyril F. Colebrook (1910–1997) combined the available data for transition and turbulent flow in smooth as well as rough pipes into the following implicit relation known as the **Colebrook equation:**

$$\frac{1}{\sqrt{f}} = -2.0 \log\left(\frac{\varepsilon/D}{3.7} + \frac{2.51}{\mathrm{Re}\sqrt{f}}\right) \qquad \text{(turbulent flow)} \qquad \textbf{(8–50)}$$

We note that the logarithm in Eq. 8–50 is a base 10 rather than a natural logarithm. In 1942, the American engineer Hunter Rouse (1906–1996) verified Colebrook's equation and produced a graphical plot of f as a function of Re and the product $\mathrm{Re}\sqrt{f}$. He also presented the laminar flow relation and a table of commercial pipe roughness. Two years later, Lewis F. Moody (1880–1953) redrew Rouse's diagram into the form commonly used today. The now famous **Moody chart** is given in the appendix as Fig. A–12. It presents the Darcy friction factor for pipe flow as a function of the Reynolds number and ε/D over a wide range. It is probably one of the most widely accepted and used charts in engineering. Although it is developed for circular pipes, it can also be used for noncircular pipes by replacing the diameter by the hydraulic diameter.

Commercially available pipes differ from those used in the experiments in that the roughness of pipes in the market is not uniform and it is difficult to give a precise description of it. Equivalent roughness values for some commercial pipes are given in Table 8–2 as well as on the Moody chart. But it should be kept in mind that these values are for new pipes, and the relative roughness of pipes may increase with use as a result of corrosion, scale buildup, and precipitation. As a result, the friction factor may increase by a factor of 5 to 10. Actual operating conditions must be considered in the design of piping systems. Also, the Moody chart and its equivalent Colebrook equation involve several uncertainties (the roughness size, experimental error, curve fitting of data, etc.), and thus the results obtained should not be treated as "exact." It is usually considered to be accurate to ±15 percent over the entire range in the figure.

The Colebrook equation is implicit in f, and thus the determination of the friction factor requires some iteration unless an equation solver such as EES is used. An approximate explicit relation for f was given by S. E. Haaland in 1983 as

$$\frac{1}{\sqrt{f}} \cong -1.8 \log\left[\frac{6.9}{\mathrm{Re}} + \left(\frac{\varepsilon/D}{3.7}\right)^{1.11}\right] \qquad \textbf{(8–51)}$$

The results obtained from this relation are within 2 percent of those obtained from the Colebrook equation. If more accurate results are desired, Eq. 8–51 can be used as a good *first guess* in a Newton iteration when using a programmable calculator or a spreadsheet to solve for f with Eq. 8–50.

TABLE 8–2

Equivalent roughness values for new commercial pipes*

| | Roughness, ε | |
Material	ft	mm
Glass, plastic	0 (smooth)	
Concrete	0.003–0.03	0.9–9
Wood stave	0.0016	0.5
Rubber, smoothed	0.000033	0.01
Copper or brass tubing	0.000005	0.0015
Cast iron	0.00085	0.26
Galvanized iron	0.0005	0.15
Wrought iron	0.00015	0.046
Stainless steel	0.000007	0.002
Commercial steel	0.00015	0.045

* The uncertainty in these values can be as much as ±60 percent.

Relative Roughness, ε/D	Friction Factor, f
0.0*	0.0119
0.00001	0.0119
0.0001	0.0134
0.0005	0.0172
0.001	0.0199
0.005	0.0305
0.01	0.0380
0.05	0.0716

* Smooth surface. All values are for Re = 10^6 and are calculated from the Colebrook equation.

FIGURE 8–27
The friction factor is minimum for a smooth pipe and increases with roughness.

We make the following observations from the Moody chart:

- For laminar flow, the friction factor decreases with increasing Reynolds number, and it is independent of surface roughness.

- The friction factor is a minimum for a smooth pipe (but still not zero because of the no-slip condition) and increases with roughness (Fig. 8–27). The Colebrook equation in this case ($\varepsilon = 0$) reduces to the **Prandtl equation** expressed as $1/\sqrt{f} = 2.0 \log(\text{Re}\sqrt{f}) - 0.8$.

- The transition region from the laminar to turbulent regime ($2300 < \text{Re} < 4000$) is indicated by the shaded area in the Moody chart (Figs. 8–28 and A–12). The flow in this region may be laminar or turbulent, depending on flow disturbances, or it may alternate between laminar and turbulent, and thus the friction factor may also alternate between the values for laminar and turbulent flow. The data in this range are the least reliable. At small relative roughnesses, the friction factor increases in the transition region and approaches the value for smooth pipes.

- At very large Reynolds numbers (to the right of the dashed line on the chart) the friction factor curves corresponding to specified relative roughness curves are nearly horizontal, and thus the friction factors are independent of the Reynolds number (Fig. 8–28). The flow in that region is called *fully rough turbulent flow* or just *fully rough flow* because the thickness of the viscous sublayer decreases with increasing Reynolds number, and it becomes so thin that it is negligibly small compared to the surface roughness height. The viscous effects in this case are produced in the main flow primarily by the protruding roughness elements, and the contribution of the laminar sublayer is negligible. The Colebrook equation in the *fully rough* zone (Re → ∞) reduces to the **von Kármán equation** expressed as $1/\sqrt{f} = -2.0 \log[(\varepsilon/D)/3.7]$, which is explicit in f. Some authors call this zone *completely* (or *fully*) *turbulent flow,* but this is misleading since the flow to the left of the dashed blue line in Fig. 8–28 is also fully turbulent.

In calculations, we should make sure that we use the actual internal diameter of the pipe, which may be different than the nominal diameter. For example, the internal diameter of a steel pipe whose nominal diameter is 1 in is 1.049 in (Table 8–3).
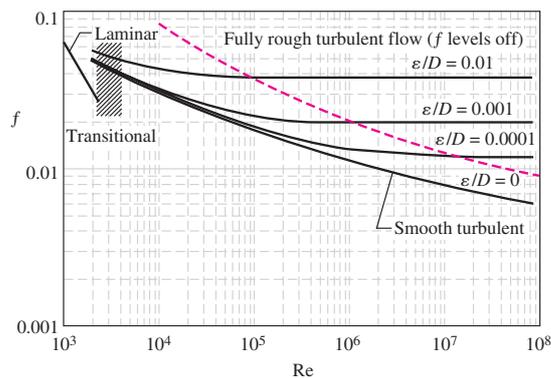
FIGURE 8–28
At very large Reynolds numbers, the friction factor curves on the Moody chart are nearly horizontal, and thus the friction factors are independent of the Reynolds number.

Types of Fluid Flow Problems

In the design and analysis of piping systems that involve the use of the Moody chart (or the Colebrook equation), we usually encounter three types of problems (the fluid and the roughness of the pipe are assumed to be specified in all cases) (Fig. 8–29):

1. Determining the **pressure drop** (or head loss) when the pipe length and diameter are given for a specified flow rate (or velocity)
2. Determining the **flow rate** when the pipe length and diameter are given for a specified pressure drop (or head loss)
3. Determining the **pipe diameter** when the pipe length and flow rate are given for a specified pressure drop (or head loss)

Problems of the *first type* are straightforward and can be solved directly by using the Moody chart. Problems of the *second type* and *third type* are commonly encountered in engineering design (in the selection of pipe diameter, for example, that minimizes the sum of the construction and pumping costs), but the use of the Moody chart with such problems requires an iterative approach unless an equation solver is used.

In problems of the *second type*, the diameter is given but the flow rate is unknown. A good guess for the friction factor in that case is obtained from the completely turbulent flow region for the given roughness. This is true for large Reynolds numbers, which is often the case in practice. Once the flow rate is obtained, the friction factor can be corrected using the Moody chart or the Colebrook equation, and the process is repeated until the solution converges. (Typically only a few iterations are required for convergence to three or four digits of precision.)

In problems of the *third type*, the diameter is not known and thus the Reynolds number and the relative roughness cannot be calculated. Therefore, we start calculations by assuming a pipe diameter. The pressure drop calculated for the assumed diameter is then compared to the specified pressure drop, and calculations are repeated with another pipe diameter in an iterative fashion until convergence.

To avoid tedious iterations in head loss, flow rate, and diameter calculations, Swamee and Jain proposed the following explicit relations in 1976 that are accurate to within 2 percent of the Moody chart:

$$h_L = 1.07 \frac{\dot{V}^2 L}{g D^5} \left\{ \ln\left[\frac{\varepsilon}{3.7D} + 4.62\left(\frac{\nu D}{\dot{V}}\right)^{0.9} \right] \right\}^{-2} \qquad \begin{array}{l} 10^{-6} < \varepsilon/D < 10^{-2} \\ 3000 < \text{Re} < 3 \times 10^8 \end{array} \qquad \text{(8–52)}$$

$$\dot{V} = -0.965\left(\frac{g D^5 h_L}{L}\right)^{0.5} \ln\left[\frac{\varepsilon}{3.7D} + \left(\frac{3.17\nu^2 L}{g D^3 h_L}\right)^{0.5} \right] \qquad \text{Re} > 2000 \qquad \text{(8–53)}$$

$$D = 0.66\left[\varepsilon^{1.25}\left(\frac{L\dot{V}^2}{g h_L}\right)^{4.75} + \nu \dot{V}^{9.4}\left(\frac{L}{g h_L}\right)^{5.2} \right]^{0.04} \qquad \begin{array}{l} 10^{-6} < \varepsilon/D < 10^{-2} \\ 5000 < \text{Re} < 3 \times 10^8 \end{array} \qquad \text{(8–54)}$$

Note that all quantities are dimensional and the units simplify to the desired unit (for example, to m or ft in the last relation) when consistent units are used. Noting that the Moody chart is accurate to within 15 percent of experimental data, we should have no reservation in using these approximate relations in the design of piping systems.

TABLE 8–3

Standard sizes for Schedule 40 steel pipes

Nominal Size, in	Actual Inside Diameter, in
$\frac{1}{8}$	0.269
$\frac{1}{4}$	0.364
$\frac{3}{8}$	0.493
$\frac{1}{2}$	0.622
$\frac{3}{4}$	0.824
1	1.049
$1\frac{1}{2}$	1.610
2	2.067
$2\frac{1}{2}$	2.469
3	3.068
5	5.047
10	10.02

Problem type	Given	Find
1	$L, D, \dot{V}$	ΔP (or h_L)
2	$L, D, \Delta P$	$\dot{V}$
3	$L, \Delta P, \dot{V}$	D

FIGURE 8–29
The three types of problems encountered in pipe flow.
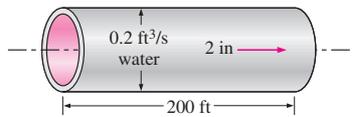
FIGURE 8–30
Schematic for Example 8–3.

EXAMPLE 8–3   **Determining the Head Loss in a Water Pipe**

Water at 60°F (ρ = 62.36 lbm/ft^3 and μ = 7.536 × 10^{-4} lbm/ft · s) is flow-ing steadily in a 2-in-diameter horizontal pipe made of stainless steel at a rate of 0.2 ft^3/s (Fig. 8–30). Determine the pressure drop, the head loss, and the required pumping power input for flow over a 200-ft-long section of the pipe.

SOLUTION   The flow rate through a specified water pipe is given. The pres-sure drop, the head loss, and the pumping power requirements are to be determined.
Assumptions   **1** The flow is steady and incompressible. **2** The entrance effects are negligible, and thus the flow is fully developed. **3** The pipe involves no components such as bends, valves, and connectors. **4** The piping section involves no work devices such as a pump or a turbine.
Properties   The density and dynamic viscosity of water are given to be ρ = 62.36 lbm/ft^3 and μ = 7.536 × 10^{-4} lbm/ft · s, respectively.
Analysis   We recognize this as a problem of the first type, since flow rate, pipe length, and pipe diameter are known. First we calculate the average velocity and the Reynolds number to determine the flow regime:

$$V = \frac{\dot{V}}{A_c} = \frac{\dot{V}}{\pi D^2/4} = \frac{0.2 \text{ ft}^3/\text{s}}{\pi (2/12 \text{ ft})^2/4} = 9.17 \text{ ft/s}$$

$$\text{Re} = \frac{\rho V D}{\mu} = \frac{(62.36 \text{ lbm/ft}^3)(9.17 \text{ ft/s})(2/12 \text{ ft})}{7.536 \times 10^{-4} \text{ lbm/ft} \cdot \text{s}} = 126{,}400$$

which is greater than 4000. Therefore, the flow is turbulent. The relative roughness of the pipe is calculated using Table 8–2

$$\varepsilon/D = \frac{0.000007 \text{ ft}}{2/12 \text{ ft}} = 0.000042$$

The friction factor corresponding to this relative roughness and the Reynolds number can simply be determined from the Moody chart. To avoid any read-ing error, we determine f from the Colebrook equation:

$$\frac{1}{\sqrt{f}} = -2.0 \log\left(\frac{\varepsilon/D}{3.7} + \frac{2.51}{\text{Re}\sqrt{f}}\right) \rightarrow \frac{1}{\sqrt{f}} = -2.0 \log\left(\frac{0.000042}{3.7} + \frac{2.51}{126{,}400\sqrt{f}}\right)$$

Using an equation solver or an iterative scheme, the friction factor is deter-mined to be f = 0.0174. Then the pressure drop (which is equivalent to pressure loss in this case), head loss, and the required power input become

$$\Delta P = \Delta P_L = f \frac{L}{D} \frac{\rho V^2}{2} = 0.0174 \frac{200 \text{ ft}}{2/12 \text{ ft}} \frac{(62.36 \text{ lbm/ft}^3)(9.17 \text{ ft/s})^2}{2} \left(\frac{1 \text{ lbf}}{32.2 \text{ lbm} \cdot \text{ft/s}^2}\right)$$

$$= \textbf{1700 lbf/ft}^2 = \textbf{11.8 psi}$$

$$h_L = \frac{\Delta P_L}{\rho g} = f \frac{L}{D} \frac{V^2}{2g} = 0.0174 \frac{200 \text{ ft}}{2/12 \text{ ft}} \frac{(9.17 \text{ ft/s})^2}{2(32.2 \text{ ft/s}^2)} = \textbf{27.3 ft}$$

$$\dot{W}_{\text{pump}} = \dot{V} \Delta P = (0.2 \text{ ft}^3/\text{s})(1700 \text{ lbf/ft}^2)\left(\frac{1 \text{ W}}{0.737 \text{ lbf} \cdot \text{ft/s}}\right) = \textbf{461 W}$$

Therefore, power input in the amount of 461 W is needed to overcome the frictional losses in the pipe.
Discussion   It is common practice to write our final answers to three signifi-cant digits, even though we know that the results are accurate to at most two significant digits because of inherent inaccuracies in the Colebrook equation,

as discussed previously. The friction factor could also be determined easily from the explicit Haaland relation (Eq. 8–51). It would give $f = 0.0172$, which is sufficiently close to 0.0174. Also, the friction factor corresponding to $\varepsilon = 0$ in this case is 0.0171, which indicates that stainless-steel pipes can be assumed to be smooth with negligible error.

EXAMPLE 8–4   Determining the Diameter of an Air Duct

Heated air at 1 atm and 35°C is to be transported in a 150-m-long circular plastic duct at a rate of 0.35 m³/s (Fig. 8–31). If the head loss in the pipe is not to exceed 20 m, determine the minimum diameter of the duct.

SOLUTION The flow rate and the head loss in an air duct are given. The diameter of the duct is to be determined.
Assumptions **1** The flow is steady and incompressible. **2** The entrance effects are negligible, and thus the flow is fully developed. **3** The duct involves no components such as bends, valves, and connectors. **4** Air is an ideal gas. **5** The duct is smooth since it is made of plastic. **6** The flow is turbulent (to be verified).
Properties The density, dynamic viscosity, and kinematic viscosity of air at 35°C are $\rho = 1.145$ kg/m³, $\mu = 1.895 \times 10^{-5}$ kg/m · s, and $\nu = 1.655 \times 10^{-5}$ m²/s.
Analysis This is a problem of the third type since it involves the determination of diameter for specified flow rate and head loss. We can solve this problem by three different approaches: (1) an iterative approach by assuming a pipe diameter, calculating the head loss, comparing the result to the specified head loss, and repeating calculations until the calculated head loss matches the specified value; (2) writing all the relevant equations (leaving the diameter as an unknown) and solving them simultaneously using an equation solver; and (3) using the third Swamee–Jain formula. We will demonstrate the use of the last two approaches.

The average velocity, the Reynolds number, the friction factor, and the head loss relations can be expressed as (D is in m, V is in m/s, and Re and f are dimensionless)

$$V = \frac{\dot{V}}{A_c} = \frac{\dot{V}}{\pi D^2/4} = \frac{0.35 \text{ m}^3/\text{s}}{\pi D^2/4}$$

$$\text{Re} = \frac{VD}{\nu} = \frac{VD}{1.655 \times 10^{-5} \text{ m}^2/\text{s}}$$

$$\frac{1}{\sqrt{f}} = -2.0 \log\left(\frac{\varepsilon/D}{3.7} + \frac{2.51}{\text{Re}\sqrt{f}}\right) = -2.0 \log\left(\frac{2.51}{\text{Re}\sqrt{f}}\right)$$

$$h_L = f\frac{L}{D}\frac{V^2}{2g} \quad \rightarrow \quad 20 = f\frac{150 \text{ m}}{D}\frac{V^2}{2(9.81 \text{ m/s}^2)}$$

The roughness is approximately zero for a plastic pipe (Table 8–2). Therefore, this is a set of four equations in four unknowns, and solving them with an equation solver such as EES gives

$$D = \textbf{0.267 m}, \quad f = 0.0180, \quad V = 6.24 \text{ m/s}, \quad \text{and} \quad \text{Re} = 100{,}800$$

Therefore, the diameter of the duct should be more than 26.7 cm if the head loss is not to exceed 20 m. Note that Re > 4000, and thus the turbulent flow assumption is verified.
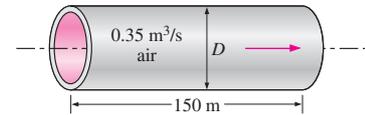
FIGURE 8–31
Schematic for Example 8–4

The diameter can also be determined directly from the third Swamee–Jain formula to be

$$
D = 0.66 \left[\varepsilon^{1.25} \left(\frac{L\dot{V}^2}{gh_L} \right)^{4.75} + \nu \dot{V}^{9.4} \left(\frac{L}{gh_L} \right)^{5.2} \right]^{0.04}
$$

$$
= 0.66 \left[0 + (1.655 \times 10^{-5} \text{ m}^2/\text{s})(0.35 \text{ m}^3/\text{s})^{9.4} \left(\frac{150 \text{ m}}{(9.81 \text{ m/s}^2)(20 \text{ m})} \right)^{5.2} \right]^{0.04}
$$

$$
= \textbf{0.271 m}
$$

Discussion Note that the difference between the two results is less than 2 percent. Therefore, the simple Swamee–Jain relation can be used with confidence. Finally, the first (iterative) approach requires an initial guess for D. If we use the Swamee–Jain result as our initial guess, the diameter converges to $D = 0.267$ m in short order.

EXAMPLE 8–5 **Determining the Flow Rate of Air in a Duct**

Reconsider Example 8–4. Now the duct length is doubled while its diameter is maintained constant. If the total head loss is to remain constant, determine the drop in the flow rate through the duct.

SOLUTION The diameter and the head loss in an air duct are given. The drop in the flow rate is to be determined.
Analysis This is a problem of the second type since it involves the determination of the flow rate for a specified pipe diameter and head loss. The solution involves an iterative approach since the flow rate (and thus the flow velocity) is not known.

The average velocity, Reynolds number, friction factor, and the head loss relations can be expressed as (D is in m, V is in m/s, and Re and f are dimensionless)

$$
V = \frac{\dot{V}}{A_c} = \frac{\dot{V}}{\pi D^2/4} \quad \rightarrow \quad V = \frac{\dot{V}}{\pi(0.267 \text{ m})^2/4}
$$

$$
\text{Re} = \frac{VD}{\nu} \quad \rightarrow \quad \text{Re} = \frac{V(0.267 \text{ m})}{1.655 \times 10^{-5} \text{ m}^2/\text{s}}
$$

$$
\frac{1}{\sqrt{f}} = -2.0 \log\left(\frac{\varepsilon/D}{3.7} + \frac{2.51}{\text{Re}\sqrt{f}} \right) \quad \rightarrow \quad \frac{1}{\sqrt{f}} = -2.0 \log\left(\frac{2.51}{\text{Re}\sqrt{f}} \right)
$$

$$
h_L = f \frac{L}{D} \frac{V^2}{2g} \quad \rightarrow \quad 20 = f \frac{300 \text{ m}}{0.267 \text{ m}} \frac{V^2}{2(9.81 \text{ m/s}^2)}
$$

This is a set of four equations in four unknowns and solving them with an equation solver such as EES gives

$$
\dot{V} = 0.24 \text{ m}^3/\text{s}, \quad f = 0.0195, \quad V = 4.23 \text{ m/s}, \quad \text{and} \quad \text{Re} = 68,300
$$

Then the drop in the flow rate becomes

$$
\dot{V}_{\text{drop}} = \dot{V}_{\text{old}} - \dot{V}_{\text{new}} = 0.35 - 0.24 = \textbf{0.11 m}^3\textbf{/s} \quad \text{(a drop of 31 percent)}
$$

Therefore, for a specified head loss (or available head or fan pumping power), the flow rate drops by about 31 percent from 0.35 to 0.24 m³/s when the duct length doubles.

Alternative Solution   If a computer is not available (as in an exam situation), another option is to set up a *manual iteration loop*. We have found that the best convergence is usually realized by first guessing the friction factor *f*, and then solving for the velocity *V*. The equation for *V* as a function of *f* is

Average velocity through the pipe: $$V = \sqrt{\frac{2gh_L}{fL/D}}$$

Now that *V* is calculated, the Reynolds number can be calculated, from which a *corrected* friction factor is obtained from the Moody chart or the Colebrook equation. We repeat the calculations with the corrected value of *f* until convergence. We guess *f* = 0.04 for illustration:

Iteration	*f* (guess)	*V*, m/s	Re	Corrected *f*
1	0.04	2.955	4.724×10^4	0.0212
2	0.0212	4.059	6.489×10^4	0.01973
3	0.01973	4.207	6.727×10^4	0.01957
4	0.01957	4.224	6.754×10^4	0.01956
5	0.01956	4.225	6.756×10^4	0.01956

Notice that the iteration has converged to three digits in only three iterations and to four digits in only four iterations. The final results are identical to those obtained with EES, yet do not require a computer.

Discussion   The new flow rate can also be determined directly from the second Swamee–Jain formula to be

$$\dot{V} = -0.965 \left(\frac{gD^5 h_L}{L}\right)^{0.5} \ln\left[\frac{\varepsilon}{3.7D} + \left(\frac{3.17\nu^2 L}{gD^3 h_L}\right)^{0.5}\right]$$

$$= -0.965 \left(\frac{(9.81 \text{ m/s}^2)(0.267 \text{ m})^5 (20 \text{ m})}{300 \text{ m}}\right)^{0.5}$$

$$\times \ln\left[0 + \left(\frac{3.17(1.655 \times 10^{-5} \text{ m}^2/\text{s})^2 (300 \text{ m})}{(9.81 \text{ m/s}^2)(0.267 \text{ m})^3 (20 \text{ m})}\right)^{0.5}\right]$$

$$= 0.24 \text{ m}^3/\text{s}$$

Note that the result from the Swamee–Jain relation is the same (to two significant digits) as that obtained with the Colebrook equation using EES or using our manual iteration technique. Therefore, the simple Swamee–Jain relation can be used with confidence.

8–6 ▪ MINOR LOSSES

The fluid in a typical piping system passes through various fittings, valves, bends, elbows, tees, inlets, exits, enlargements, and contractions in addition to the pipes. These components interrupt the smooth flow of the fluid and cause additional losses because of the flow separation and mixing they induce. In a typical system with long pipes, these losses are minor compared to the total head loss in the pipes (the **major losses**) and are called **minor losses.** Although this is generally true, in some cases the minor losses may be greater than the major losses. This is the case, for example, in systems with several turns and valves in a short distance. The head loss introduced by a completely open valve, for example, may be negligible. But a partially closed valve may cause the largest head loss in the system, as

Pipe section with valve:

$(P_1 - P_2)_{valve}$
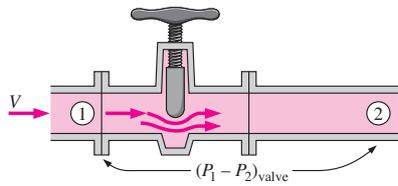
Pipe section without valve:

$(P_1 - P_2)_{pipe}$

$$\Delta P_L = (P_1 - P_2)_{valve} - (P_1 - P_2)_{pipe}$$
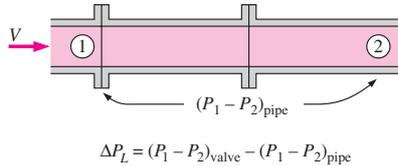
FIGURE 8–32

For a constant-diameter section of a pipe with a minor loss component, the loss coefficient of the component (such as the gate valve shown) is determined by measuring the additional pressure loss it causes and dividing it by the dynamic pressure in the pipe.

evidenced by the drop in the flow rate. Flow through valves and fittings is very complex, and a theoretical analysis is generally not plausible. Therefore, minor losses are determined experimentally, usually by the manufacturers of the components.

Minor losses are usually expressed in terms of the **loss coefficient** K_L (also called the **resistance coefficient**), defined as (Fig. 8–32)

Loss coefficient: $$K_L = \frac{h_L}{V^2/(2g)} \tag{8–55}$$

where h_L is the *additional* irreversible head loss in the piping system caused by insertion of the component, and is defined as $h_L = \Delta P_L/\rho g$. For example, imagine replacing the valve in Fig. 8–32 with a section of constant diameter pipe from location 1 to location 2. ΔP_L is defined as the pressure drop from 1 to 2 for the case *with* the valve, $(P_1 - P_2)_{valve}$, *minus* the pressure drop that would occur in the imaginary straight pipe section from 1 to 2 *without* the valve, $(P_1 - P_2)_{pipe}$ at the same flow rate. While the majority of the irreversible head loss occurs locally near the valve, some of it occurs downstream of the valve due to induced swirling turbulent eddies that are produced in the valve and continue downstream. These eddies "waste" mechanical energy because they are ultimately dissipated into heat while the flow in the downstream section of pipe eventually returns to fully developed conditions. When measuring minor losses in some minor loss components, such as *elbows,* for example, location 2 must be considerably far downstream (tens of pipe diameters) in order to fully account for the additional irreversible losses due to these decaying eddies.

When the pipe diameter downstream of the component *changes,* determination of the minor loss is even more complicated. In all cases, however, it is based on the *additional* irreversible loss of mechanical energy that would otherwise not exist if the minor loss component were not there. For simplicity, you may think of the minor loss as occurring *locally* across the minor loss component, but keep in mind that the component influences the flow for several pipe diameters downstream. By the way, this is the reason why most flow meter manufacturers recommend installing their flow meter at least 10 to 20 pipe diameters downstream of any elbows or valves—this allows the swirling turbulent eddies generated by the elbow or valve to largely disappear and the velocity profile to become fully developed before entering the flow meter. (Most flow meters are calibrated with a fully developed velocity profile at the flow meter inlet, and yield the best accuracy when such conditions also exist in the actual application.)

When the inlet diameter equals outlet diameter, the loss coefficient of a component can also be determined by measuring the pressure loss across the component and dividing it by the dynamic pressure, $K_L = \Delta P_L/(\frac{1}{2}\rho V^2)$. When the loss coefficient for a component is available, the head loss for that component is determined from

Minor loss: $$h_L = K_L \frac{V^2}{2g} \tag{8–56}$$

The loss coefficient, in general, depends on the geometry of the component and the Reynolds number, just like the friction factor. However, it is usually assumed to be independent of the Reynolds number. This is a reasonable approximation since most flows in practice have large Reynolds numbers

and the loss coefficients (including the friction factor) tend to be independent of the Reynolds number at large Reynolds numbers.

Minor losses are also expressed in terms of the **equivalent length** L_{equiv}, defined as (Fig. 8–33)

Equivalent length:
$$h_L = K_L \frac{V^2}{2g} = f\frac{L_{equiv}}{D}\frac{V^2}{2g} \rightarrow L_{equiv} = \frac{D}{f}K_L \quad (8\text{–}57)$$

where f is the friction factor and D is the diameter of the pipe that contains the component. The head loss caused by the component is equivalent to the head loss caused by a section of the pipe whose length is L_{equiv}. Therefore, the contribution of a component to the head loss can be accounted for by simply adding L_{equiv} to the total pipe length.

Both approaches are used in practice, but the use of loss coefficients is more common. Therefore, we will also use that approach in this book. Once all the loss coefficients are available, the total head loss in a piping system is determined from

Total head loss (general):
$$h_{L, total} = h_{L, major} + h_{L, minor}$$
$$= \sum_i f_i \frac{L_i}{D_i}\frac{V_i^2}{2g} + \sum_j K_{L,j}\frac{V_j^2}{2g} \quad (8\text{–}58)$$

where i represents each pipe section with constant diameter and j represents each component that causes a minor loss. If the entire piping system being analyzed has a constant diameter, Eq. 8–58 reduces to

Total head loss (D = constant):
$$h_{L, total} = \left(f\frac{L}{D} + \sum K_L\right)\frac{V^2}{2g} \quad (8\text{–}59)$$

where V is the average flow velocity through the entire system (note that V = constant since D = constant).

Representative loss coefficients K_L are given in Table 8–4 for inlets, exits, bends, sudden and gradual area changes, and valves. There is considerable uncertainty in these values since the loss coefficients, in general, vary with the pipe diameter, the surface roughness, the Reynolds number, and the details of the design. The loss coefficients of two seemingly identical valves by two different manufacturers, for example, can differ by a factor of 2 or more. Therefore, the particular manufacturer's data should be consulted in the final design of piping systems rather than relying on the representative values in handbooks.

The head loss at the inlet of a pipe is a strong function of geometry. It is almost negligible for well-rounded inlets (K_L = 0.03 for $r/D > 0.2$), but increases to about 0.50 for sharp-edged inlets (Fig. 8–34). That is, a sharp-edged inlet causes half of the velocity head to be lost as the fluid enters the pipe. This is because the fluid cannot make sharp 90° turns easily, especially at high velocities. As a result, the flow separates at the corners, and the flow is constricted into the **vena contracta** region formed in the midsection of the pipe (Fig. 8–35). Therefore, a sharp-edged inlet acts like a flow constriction. The velocity increases in the vena contracta region (and the pressure decreases) because of the reduced effective flow area and then decreases as the flow fills the entire cross section of the pipe. There would be negligible loss if the pressure were increased in accordance with Bernoulli's equation (the velocity head would simply be converted into pressure head). However, this deceleration process is far from ideal and the
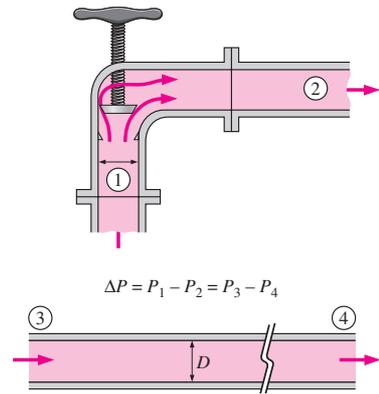
FIGURE 8–33
The head loss caused by a component (such as the angle valve shown) is equivalent to the head loss caused by a section of the pipe whose length is the equivalent length.
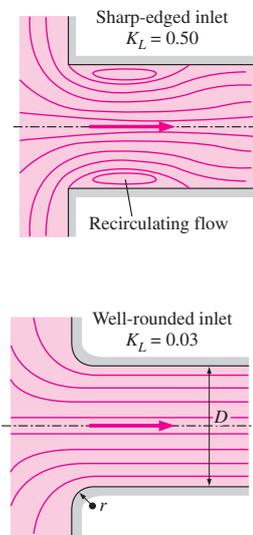
FIGURE 8–34
The head loss at the inlet of a pipe is almost negligible for well-rounded inlets (K_L = 0.03 for $r/D > 0.2$) but increases to about 0.50 for sharp-edged inlets.

TABLE 8–4

Loss coefficients K_L of various pipe components for turbulent flow (for use in the relation $h_L = K_L V^2/(2g)$, where V is the average velocity in the pipe that contains the component)*

Pipe Inlet		
Reentrant: $K_L = 0.80$ ($t \ll D$ and $l \approx 0.1D$)	Sharp-edged: $K_L = 0.50$	Well-rounded ($r/D > 0.2$): $K_L = 0.03$ Slightly rounded ($r/D = 0.1$): $K_L = 0.12$ (see Fig. 8–36)
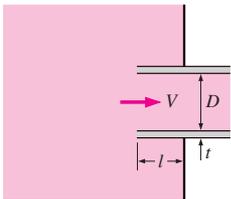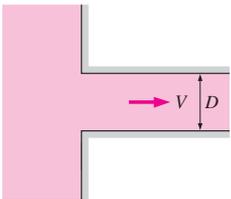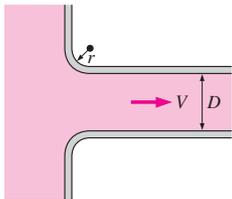
Pipe Exit		
Reentrant: $K_L = \alpha$	Sharp-edged: $K_L = \alpha$	Rounded: $K_L = \alpha$
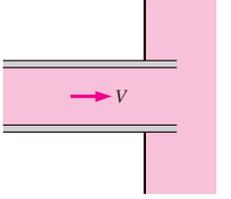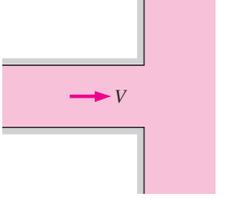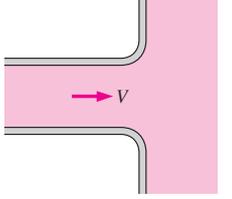
Note: The kinetic energy correction factor is $\alpha = 2$ for fully developed laminar flow, and $\alpha \approx 1$ for fully developed turbulent flow.

Sudden Expansion and Contraction (based on the velocity in the smaller-diameter pipe)

Sudden expansion: $K_L = \left(1 - \dfrac{d^2}{D^2}\right)^2$
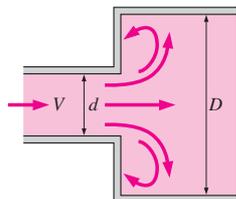
Sudden contraction: See chart.
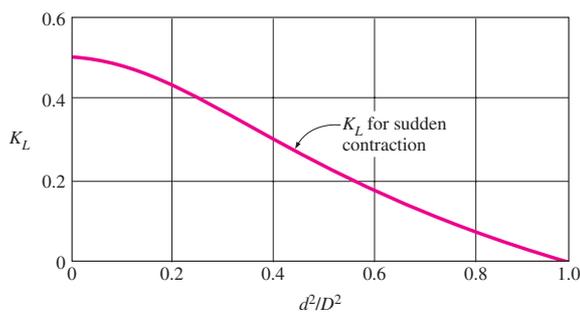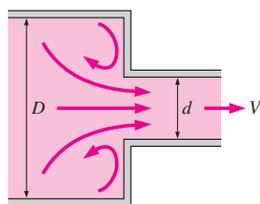
Gradual Expansion and Contraction (based on the velocity in the smaller-diameter pipe)
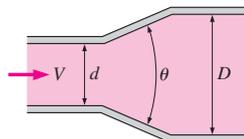
Expansion:	Contraction (for $\theta = 20°$):
$K_L = 0.02$ for $\theta = 20°$	$K_L = 0.30$ for $d/D = 0.2$
$K_L = 0.04$ for $\theta = 45°$	$K_L = 0.25$ for $d/D = 0.4$
$K_L = 0.07$ for $\theta = 60°$	$K_L = 0.15$ for $d/D = 0.6$
	$K_L = 0.10$ for $d/D = 0.8$

TABLE 8–4 (CONCLUDED)

Bends and Branches

90° smooth bend: Flanged: $K_L = 0.3$ Threaded: $K_L = 0.9$	90° miter bend (without vanes): $K_L = 1.1$	90° miter bend (with vanes): $K_L = 0.2$	45° threaded elbow: $K_L = 0.4$
V	V	V	V 45°
180° return bend: Flanged: $K_L = 0.2$ Threaded: $K_L = 1.5$	Tee (branch flow): Flanged: $K_L = 1.0$ Threaded: $K_L = 2.0$	Tee (line flow): Flanged: $K_L = 0.2$ Threaded: $K_L = 0.9$	Threaded union: $K_L = 0.08$
V	V	V	V
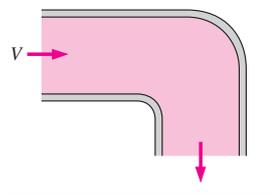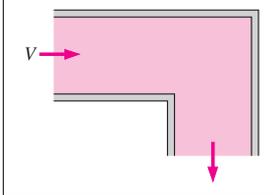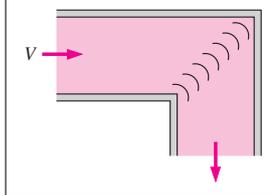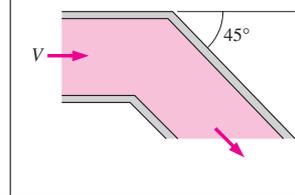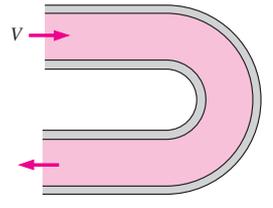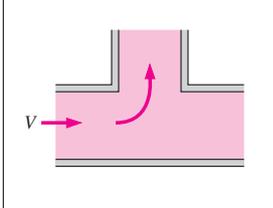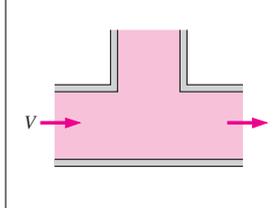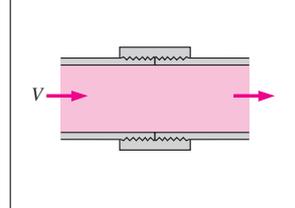
Valves

Globe valve, fully open: $K_L = 10$	Gate valve, fully open: $K_L = 0.2$
Angle valve, fully open: $K_L = 5$	$\frac{1}{4}$ closed: $K_L = 0.3$
Ball valve, fully open: $K_L = 0.05$	$\frac{1}{2}$ closed: $K_L = 2.1$
Swing check valve: $K_L = 2$	$\frac{3}{4}$ closed: $K_L = 17$

* These are representative values for loss coefficients. Actual values strongly depend on the design and manufacture of the components and may differ from the given values considerably (especially for valves). Actual manufacturer's data should be used in the final design.
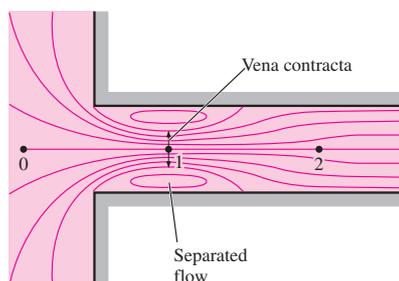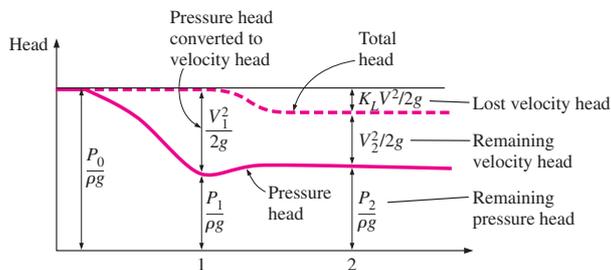
FIGURE 8–35

Graphical representation of flow contraction and the associated head loss at a sharp-edged pipe inlet.
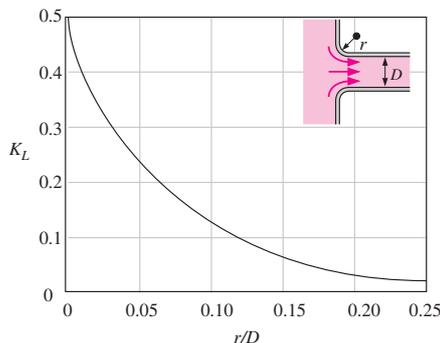
FIGURE 8–36
The effect of rounding of a pipe inlet on the loss coefficient.
From ASHRAE Handbook of Fundamentals.

FIGURE 8–37
All the kinetic energy of the flow is "lost" (turned into thermal energy) through friction as the jet decelerates and mixes with ambient fluid downstream of a submerged outlet.

viscous dissipation caused by intense mixing and the turbulent eddies convert part of the kinetic energy into frictional heating, as evidenced by a slight rise in fluid temperature. The end result is a drop in velocity without much pressure recovery, and the inlet loss is a measure of this irreversible pressure drop.

Even slight rounding of the edges can result in significant reduction of K_L, as shown in Fig. 8–36. The loss coefficient rises sharply (to about $K_L = 0.8$) when the pipe protrudes into the reservoir since some fluid near the edge in this case is forced to make a 180° turn.

The loss coefficient for a submerged pipe exit is often listed in handbooks as $K_L = 1$. More precisely, however, K_L is equal to the kinetic energy correction factor α at the exit of the pipe. Although α is indeed close to 1 for fully developed *turbulent* pipe flow, it is equal to 2 for fully developed *laminar* pipe flow. To avoid possible errors when analyzing laminar pipe flow, then, it is best to always set $K_L = \alpha$ at a submerged pipe exit. At any such exit, whether laminar or turbulent, the fluid leaving the pipe loses *all* of its kinetic energy as it mixes with the reservoir fluid and eventually comes to rest through the irreversible action of viscosity. This is true, regardless of the shape of the exit (Table 8–4 and Fig. 8–37). Therefore, there is no need to round the pipe exits.

Piping systems often involve *sudden* or *gradual* expansion or contraction sections to accommodate changes in flow rates or properties such as density and velocity. The losses are usually much greater in the case of *sudden* expansion and contraction (or wide-angle expansion) because of flow separation. By combining the conservation of mass, momentum, and energy equations, the loss coefficient for the case of **sudden expansion** is approximated as

$$K_L = \left(1 - \frac{A_{small}}{A_{large}}\right)^2 \qquad \text{(sudden expansion)} \qquad \textbf{(8–60)}$$

where A_{small} and A_{large} are the cross-sectional areas of the small and large pipes, respectively. Note that $K_L = 0$ when there is no area change ($A_{small} = A_{large}$) and $K_L = 1$ when a pipe discharges into a reservoir ($A_{large} \gg A_{small}$). No such relation exists for a sudden contraction, and the K_L values in that case can be read from the chart in Table 8–4. The losses due to expansion and contraction can be reduced significantly by installing conical gradual area changers (nozzles and diffusers) between the small and large

pipes. The K_L values for representative cases of gradual expansion and contraction are given in Table 8–4. Note that in head loss calculations, the velocity in the *small pipe* is to be used as the reference velocity in Eq. 8–56. Losses during expansion are usually much higher than the losses during contraction because of flow separation.

Piping systems also involve changes in direction without a change in diameter, and such flow sections are called *bends* or *elbows*. The losses in these devices are due to flow separation (just like a car being thrown off the road when it enters a turn too fast) on the inner side and the swirling secondary flows caused by different path lengths. The losses during changes of direction can be minimized by making the turn "easy" on the fluid by using circular arcs (like the 90° elbow) instead of sharp turns (like miter bends) (Fig. 8–38). But the use of sharp turns (and thus suffering a penalty in loss coefficient) may be necessary when the turning space is limited. In such cases, the losses can be minimized by utilizing properly placed guide vanes to help the flow turn in an orderly manner without being thrown off the course. The loss coefficients for some elbows and miter bends as well as tees are given in Table 8–4. These coefficients do not include the frictional losses along the pipe bend. Such losses should be calculated as in straight pipes (using the length of the centerline as the pipe length) and added to other losses.

Valves are commonly used in piping systems to control the flow rates by simply altering the head loss until the desired flow rate is achieved. For valves it is desirable to have a very low loss coefficient when they are fully open so that they cause minimal head loss during full-load operation. Several different valve designs, each with its own advantages and disadvantages, are in common use today. The *gate valve* slides up and down like a gate, the *globe valve* closes a hole placed in the valve, the *angle valve* is a globe valve with a 90° turn, and the *check valve* allows the fluid to flow only in one direction like a diode in an electric circuit. Table 8–4 lists the representative loss coefficients of the popular designs. Note that the loss coefficient increases drastically as a valve is closed (Fig. 8–39). Also, the deviation in the loss coefficients for different manufacturers is greatest for valves because of their complex geometries.
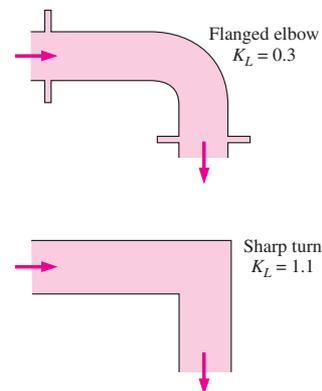
FIGURE 8–38
The losses during changes of direction can be minimized by making the turn "easy" on the fluid by using circular arcs instead of sharp turns.
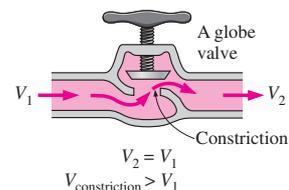
FIGURE 8–39
The large head loss in a partially closed valve is due to irreversible deceleration, flow separation, and mixing of high-velocity fluid coming from the narrow valve passage.

EXAMPLE 8–6   **Head Loss and Pressure Rise during Gradual Expansion**

A 6-cm-diameter horizontal water pipe expands gradually to a 9-cm-diameter pipe (Fig. 8–40). The walls of the expansion section are angled 30° from the horizontal. The average velocity and pressure of water before the expansion section are 7 m/s and 150 kPa, respectively. Determine the head loss in the expansion section and the pressure in the larger-diameter pipe.

SOLUTION   A horizontal water pipe expands gradually into a larger-diameter pipe. The head loss and pressure after the expansion are to be determined.
Assumptions   **1** The flow is steady and incompressible. **2** The flow at sections 1 and 2 is fully developed and turbulent with $\alpha_1 = \alpha_2 \cong 1.06$.
Properties   We take the density of water to be $\rho = 1000$ kg/m³. The loss coefficient for gradual expansion of $\theta = 60°$ total included angle is $K_L = 0.07$.
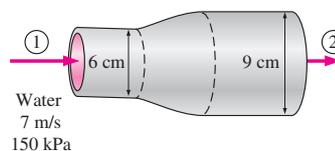
FIGURE 8–40
Schematic for Example 8–6.

Analysis Noting that the density of water remains constant, the downstream velocity of water is determined from conservation of mass to be

$$\dot{m}_1 = \dot{m}_2 \quad \rightarrow \quad \rho V_1 A_1 = \rho V_2 A_2 \quad \rightarrow \quad V_2 = \frac{A_1}{A_2} V_1 = \frac{D_1^2}{D_2^2} V_1$$

$$V_2 = \frac{(0.06 \text{ m})^2}{(0.09 \text{ m})^2} (7 \text{ m/s}) = 3.11 \text{ m/s}$$

Then the irreversible head loss in the expansion section becomes

$$h_L = K_L \frac{V_1^2}{2g} = (0.07) \frac{(7 \text{ m/s})^2}{2(9.81 \text{ m/s}^2)} = \textbf{0.175 m}$$

Noting that $z_1 = z_2$ and there are no pumps or turbines involved, the energy equation for the expansion section can be expressed in terms of heads as

$$\frac{P_1}{\rho g} + \alpha_1 \frac{V_1^2}{2g} + \cancelto{0}{z_1} + h_{\text{pump}, u} = \frac{P_2}{\rho g} + \alpha_2 \frac{V_2^2}{2g} + \cancelto{0}{z_2} + h_{\text{turbine}, e} + h_L$$

$$\rightarrow \frac{P_1}{\rho g} + \alpha_1 \frac{V_1^2}{2g} = \frac{P_2}{\rho g} + \alpha_2 \frac{V_2^2}{2g} + h_L$$

Solving for P_2 and substituting,

$$P_2 = P_1 + \rho \left\{ \frac{\alpha_1 V_1^2 - \alpha_2 V_2^2}{2} - gh_L \right\} = (150 \text{ kPa}) + (1000 \text{ kg/m}^3)$$

$$\times \left\{ \frac{1.06(7 \text{ m/s})^2 - 1.06(3.11 \text{ m/s})^2}{2} - (9.81 \text{ m/s}^2)(0.175 \text{ m}) \right\}$$

$$\times \left(\frac{1 \text{ kN}}{1000 \text{ kg} \cdot \text{m/s}} \right) \left(\frac{1 \text{ kPa}}{1 \text{ kN/m}^2} \right)$$

$$= \textbf{169 kPa}$$

Therefore, despite the head (and pressure) loss, the pressure *increases* from 150 to 169 kPa after the expansion. This is due to the conversion of dynamic pressure to static pressure when the average flow velocity is decreased in the larger pipe.

Discussion It is common knowledge that higher pressure upstream is necessary to cause flow, and it may come as a surprise to you that the downstream pressure has *increased* after the expansion, despite the loss. This is because the flow is driven by the sum of the three heads that comprise the total head (namely, the pressure head, velocity head, and elevation head). During flow expansion, the higher velocity head upstream is converted to pressure head downstream, and this increase outweighs the nonrecoverable head loss. Also, you may be tempted to solve this problem using the Bernoulli equation. Such a solution would ignore the head (and the associated pressure) loss and result in an incorrect higher pressure for the fluid downstream.

8–7 ▪ PIPING NETWORKS AND PUMP SELECTION

Most piping systems encountered in practice such as the water distribution systems in cities or commercial or residential establishments involve numerous parallel and series connections as well as several sources (supply of fluid into the system) and loads (discharges of fluid from the system) (Fig. 8–41). A piping project may involve the design of a new system or the

FIGURE 8–41
A piping network in an industrial facility.
Courtesy UMDE Engineering, Contracting, and Trading. Used by permission.

expansion of an existing system. The engineering objective in such projects is to design a piping system that will deliver the specified flow rates at specified pressures reliably at minimum total (initial plus operating and maintenance) cost. Once the layout of the system is prepared, the determination of the pipe diameters and the pressures throughout the system, while remaining within the budget constraints, typically requires solving the system repeatedly until the optimal solution is reached. Computer modeling and analysis of such systems make this tedious task a simple chore.

Piping systems typically involve several pipes connected to each other in series and/or in parallel, as shown in Figs. 8–42 and 8–43. When the pipes are connected **in series,** the flow rate through the entire system remains constant regardless of the diameters of the individual pipes in the system. This is a natural consequence of the conservation of mass principle for steady incompressible flow. The total head loss in this case is equal to the sum of the head losses in individual pipes in the system, including the minor losses. The expansion or contraction losses at connections are considered to belong to the smaller-diameter pipe since the expansion and contraction loss coefficients are defined on the basis of the average velocity in the smaller-diameter pipe.

For a pipe that branches out into two (or more) **parallel pipes** and then rejoins at a junction downstream, the total flow rate is the sum of the flow rates in the individual pipes. The pressure drop (or head loss) in each individual pipe connected in parallel must be the same since $\Delta P = P_A - P_B$ and the junction pressures P_A and P_B are the same for all the individual pipes. For a system of two parallel pipes 1 and 2 between junctions A and B with negligible minor losses, this can be expressed as

$$h_{L, 1} = h_{L, 2} \quad \rightarrow \quad f_1 \frac{L_1}{D_1} \frac{V_1^2}{2g} = f_2 \frac{L_2}{D_2} \frac{V_2^2}{2g}$$

Then the ratio of the average velocities and the flow rates in the two parallel pipes become

$$\frac{V_1}{V_2} = \left(\frac{f_2 L_2 D_1}{f_1 L_1 D_2} \right)^{1/2} \quad \text{and} \quad \frac{\dot{V}_1}{\dot{V}_2} = \frac{A_{c, 1} V_1}{A_{c, 2} V_2} = \frac{D_1^2}{D_2^2} \left(\frac{f_2 L_2 D_1}{f_1 L_1 D_2} \right)^{1/2}$$

Therefore, the relative flow rates in parallel pipes are established from the requirement that the head loss in each pipe be the same. This result can be extended to any number of pipes connected in parallel. The result is also valid for pipes for which the minor losses are significant if the equivalent lengths for components that contribute to minor losses are added to the pipe
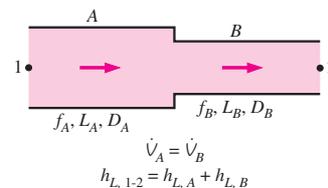
FIGURE 8–42

For pipes *in series*, the flow rate is the same in each pipe, and the total head loss is the sum of the head losses in individual pipes.
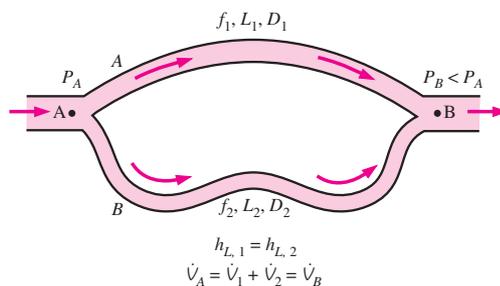
FIGURE 8–43

For pipes *in parallel*, the head loss is the same in each pipe, and the total flow rate is the sum of the flow rates in individual pipes.

length. Note that the flow rate in one of the parallel branches is proportional to its diameter to the power 5/2 and is inversely proportional to the square root of its length and friction factor.

The analysis of piping networks, no matter how complex they are, is based on two simple principles:

1. *Conservation of mass throughout the system must be satisfied.* This is done by requiring the total flow into a junction to be equal to the total flow out of the junction for all junctions in the system. Also, the flow rate must remain constant in pipes connected in series regardless of the changes in diameters.

2. *Pressure drop (and thus head loss) between two junctions must be the same for all paths between the two junctions.* This is because pressure is a point function and it cannot have two values at a specified point. In practice this rule is used by requiring that the algebraic sum of head losses in a loop (for all loops) be equal to zero. (A head loss is taken to be positive for flow in the clockwise direction and negative for flow in the counterclockwise direction.)

Therefore, the analysis of piping networks is very similar to the analysis of electric circuits, with flow rate corresponding to electric current and pressure corresponding to electric potential. However, the situation is much more complex here since, unlike the electrical resistance, the "flow resistance" is a highly nonlinear function. Therefore, the analysis of piping networks requires the simultaneous solution of a system of nonlinear equations. The analysis of such systems is beyond the scope of this introductory text.

Piping Systems with Pumps and Turbines

When a piping system involves a pump and/or turbine, the steady-flow energy equation on a unit-mass basis can be expressed as (see Section 5–7)

$$\frac{P_1}{\rho} + \alpha_1 \frac{V_1^2}{2} + gz_1 + w_{\text{pump, }u} = \frac{P_2}{\rho} + \alpha_2 \frac{V_2^2}{2} + gz_2 + w_{\text{turbine, }e} + gh_L \quad \textbf{(8–61)}$$

It can also be expressed in terms of heads as

$$\frac{P_1}{\rho g} + \alpha_1 \frac{V_1^2}{2g} + z_1 + h_{\text{pump, }u} = \frac{P_2}{\rho g} + \alpha_2 \frac{V_2^2}{2g} + z_2 + h_{\text{turbine, }e} + h_L \quad \textbf{(8–62)}$$

where $h_{\text{pump, }u} = w_{\text{pump, }u}/g$ is the useful pump head delivered to the fluid, $h_{\text{turbine, }e} = w_{\text{turbine, }e}/g$ is the turbine head extracted from the fluid, α is the kinetic energy correction factor whose value is nearly 1 for most (turbulent) flows encountered in practice, and h_L is the total head loss in piping (including the minor losses if they are significant) between points 1 and 2. The pump head is zero if the piping system does not involve a pump or a fan, the turbine head is zero if the system does not involve a turbine, and both are zero if the system does not involve any mechanical work-producing or work-consuming devices.

Many practical piping systems involve a pump to move a fluid from one reservoir to another. Taking points 1 and 2 to be at the *free surfaces* of the reservoirs, the energy equation in this case reduces for the useful pump head required to (Fig. 8–44)

$$h_{\text{pump, }u} = (z_2 - z_1) + h_L \quad \textbf{(8–63)}$$
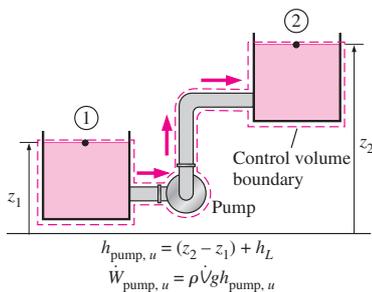
FIGURE 8–44
When a pump moves a fluid from one reservoir to another, the useful pump head requirement is equal to the elevation difference between the two reservoirs plus the head loss.

$h_{pump, u} = (z_2 - z_1) + h_L$
$\dot{W}_{pump, u} = \rho \dot{V} g h_{pump, u}$

since the velocities at free surfaces are negligible and the pressures are at atmospheric pressure. Therefore, the useful pump head is equal to the elevation difference between the two reservoirs plus the head loss. If the head loss is negligible compared to $z_2 - z_1$, the useful pump head is simply equal to the elevation difference between the two reservoirs. In the case of $z_1 > z_2$ (the first reservoir being at a higher elevation than the second one) with no pump, the flow is driven by gravity at a flow rate that causes a head loss equal to the elevation difference. A similar argument can be given for the turbine head for a hydroelectric power plant by replacing $h_{pump, u}$ in Eq. 8–63 by $-h_{turbine, e}$.

Once the useful pump head is known, the *mechanical power that needs to be delivered by the pump to the fluid* and the *electric power consumed by the motor of the pump* for a specified flow rate are determined from

$$\dot{W}_{pump, shaft} = \frac{\rho \dot{V} g h_{pump, u}}{\eta_{pump}} \quad \text{and} \quad \dot{W}_{elect} = \frac{\rho \dot{V} g h_{pump, u}}{\eta_{pump-motor}} \quad \text{(8–64)}$$

where $\eta_{pump-motor}$ is the *efficiency of the pump–motor combination,* which is the product of the pump and the motor efficiencies (Fig. 8–45). The pump–motor efficiency is defined as the ratio of the net mechanical energy delivered to the fluid by the pump to the electric energy consumed by the motor of the pump, and it usually ranges between 50 and 85 percent.

The head loss of a piping system increases (usually quadratically) with the flow rate. A plot of required useful pump head $h_{pump, u}$ as a function of flow rate is called the **system (or demand) curve.** The head produced by a pump is not a constant either. Both the pump head and the pump efficiency vary with the flow rate, and pump manufacturers supply this variation in tabular or graphical form, as shown in Fig. 8–46. These experimentally determined $h_{pump, u}$ and $\eta_{pump, u}$ versus $\dot{V}$ curves are called **characteristic (or supply or performance) curves.** Note that the flow rate of a pump increases as the required head decreases. The intersection point of the pump head curve with the vertical axis typically represents the *maximum head* the pump can provide, while the intersection point with the horizontal axis indicates the *maximum flow rate* (called the **free delivery**) that the pump can supply.

The *efficiency* of a pump is sufficiently high for a certain range of head and flow rate combination. Therefore, a pump that can supply the required head and flow rate is not necessarily a good choice for a piping system unless the efficiency of the pump at those conditions is sufficiently high. The pump installed in a piping system will operate at the point where the *system curve* and the *characteristic curve* intersect. This point of intersection is called the **operating point,** as shown in Fig. 8–46. The useful head

$\eta_{pump-motor} = \eta_{pump}\eta_{motor}$
$= 0.70 \times 0.90 = 0.63$
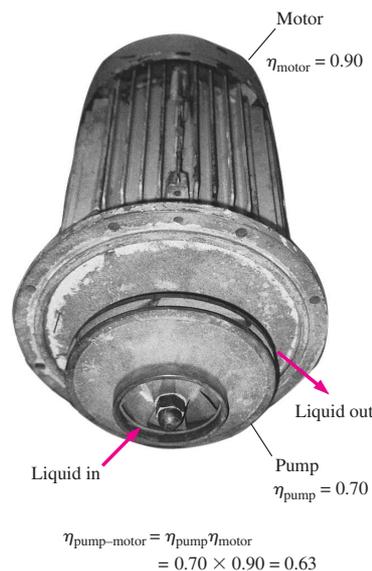
FIGURE 8–45
The efficiency of the pump–motor combination is the product of the pump and the motor efficiencies.
Courtesy Yunus Çengel
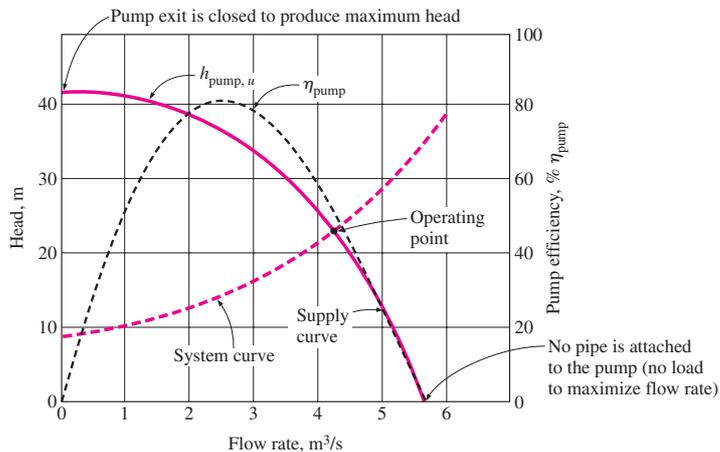
FIGURE 8–46
Characteristic pump curves for centrifugal pumps, the system curve for a piping system, and the operating point.

produced by the pump at this point matches the head requirements of the system at that flow rate. Also, the efficiency of the pump during operation is the value corresponding to that flow rate.

EXAMPLE 8–7 **Pumping Water through Two Parallel Pipes**

Water at 20°C is to be pumped from a reservoir ($z_A = 5$ m) to another reservoir at a higher elevation ($z_B = 13$ m) through two 36-m-long pipes connected in parallel, as shown in Fig. 8–47. The pipes are made of commercial steel, and the diameters of the two pipes are 4 and 8 cm. Water is to be pumped by a 70 percent efficient motor–pump combination that draws 8 kW of electric power during operation. The minor losses and the head loss in pipes that connect the parallel pipes to the two reservoirs are considered to be negligible. Determine the total flow rate between the reservoirs and the flow rate through each of the parallel pipes.

SOLUTION The pumping power input to a piping system with two parallel pipes is given. The flow rates are to be determined.
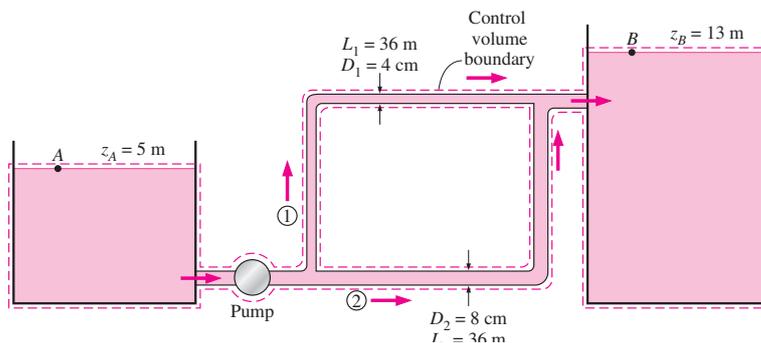
FIGURE 8–47
The piping system discussed in Example 8–7.

Assumptions **1** The flow is steady and incompressible. **2** The entrance effects are negligible, and thus the flow is fully developed. **3** The elevations of the reservoirs remain constant. **4** The minor losses and the head loss in pipes other than the parallel pipes are said to be negligible. **5** Flows through both pipes are turbulent (to be verified).

Properties The density and dynamic viscosity of water at 20°C are $\rho = 998$ kg/m³ and $\mu = 1.002 \times 10^{-3}$ kg/m · s. The roughness of commercial steel pipe is $\varepsilon = 0.000045$ m.

Analysis This problem cannot be solved directly since the velocities (or flow rates) in the pipes are not known. Therefore, we would normally use a trial-and-error approach here. However, nowadays equation solvers such as EES are widely available, and thus we will simply set up the equations to be solved by an equation solver. The useful head supplied by the pump to the fluid is determined from

$$\dot{W}_{elect} = \frac{\rho \dot{V} g h_{pump,u}}{\eta_{pump-motor}} \quad \rightarrow \quad 8000\ \text{W} = \frac{(998\ \text{kg/m}^3)\dot{V}(9.81\ \text{m/s}^2)h_{pump,u}}{0.70} \quad (1)$$

We choose points A and B at the free surfaces of the two reservoirs. Noting that the fluid at both points is open to the atmosphere (and thus $P_A = P_B = P_{atm}$) and that the fluid velocities at both points are zero ($V_A = V_B = 0$), the energy equation for a control volume between these two points simplifies to

$$\frac{\cancel{P_A}}{\rho g} + \alpha_A \cancel{\frac{V_A^2}{2g}}^0 + z_A + h_{pump,u} = \frac{\cancel{P_B}}{\rho g} + \alpha_B \cancel{\frac{V_B^2}{2g}}^0 + z_B + h_L \rightarrow h_{pump,u}$$

$$= (z_B - z_A) + h_L$$

or

$$h_{pump,u} = (13 - 5) + h_L \quad (2)$$

where

$$h_L = h_{L,1} = h_{L,2} \quad (3)(4)$$

We designate the 4-cm-diameter pipe by 1 and the 8-cm-diameter pipe by 2. The average velocity, the Reynolds number, the friction factor, and the head loss in each pipe are expressed as

$$V_1 = \frac{\dot{V}_1}{A_{c,1}} = \frac{\dot{V}_1}{\pi D_1^2/4} \quad \rightarrow \quad V_1 = \frac{\dot{V}_1}{\pi(0.04\ \text{m})^2/4} \quad (5)$$

$$V_2 = \frac{\dot{V}_2}{A_{c,2}} = \frac{\dot{V}_2}{\pi D_2^2/4} \quad \rightarrow \quad V_2 = \frac{\dot{V}_2}{\pi(0.08\ \text{m})^2/4} \quad (6)$$

$$Re_1 = \frac{\rho V_1 D_1}{\mu} \quad \rightarrow \quad Re_1 = \frac{(998\ \text{kg/m}^3)V_1(0.04\ \text{m})}{1.002 \times 10^{-3}\ \text{kg/m} \cdot \text{s}} \quad (7)$$

$$Re_2 = \frac{\rho V_2 D_2}{\mu} \quad \rightarrow \quad Re_2 = \frac{(998\ \text{kg/m}^3)V_2(0.08\ \text{m})}{1.002 \times 10^{-3}\ \text{kg/m} \cdot \text{s}} \quad (8)$$

$$\frac{1}{\sqrt{f_1}} = -2.0 \log\left(\frac{\varepsilon/D_1}{3.7} + \frac{2.51}{Re_1\sqrt{f_1}}\right)$$

$$\rightarrow \quad \frac{1}{\sqrt{f_1}} = -2.0 \log\left(\frac{0.000045}{3.7 \times 0.04} + \frac{2.51}{Re_1\sqrt{f_1}}\right) \quad (9)$$

$$\frac{1}{\sqrt{f_2}} = -2.0 \log\left(\frac{\varepsilon/D_2}{3.7} + \frac{2.51}{Re_2\sqrt{f_2}}\right)$$

$$\rightarrow \quad \frac{1}{\sqrt{f_2}} = -2.0 \log\left(\frac{0.000045}{3.7 \times 0.08} + \frac{2.51}{Re_2\sqrt{f_2}}\right) \quad \textbf{(10)}$$

$$h_{L,1} = f_1 \frac{L_1}{D_1} \frac{V_1^2}{2g} \quad \rightarrow \quad h_{L,1} = f_1 \frac{36\ m}{0.04\ m} \frac{V_1^2}{2(9.81\ m/s^2)} \quad \textbf{(11)}$$

$$h_{L,2} = f_2 \frac{L_2}{D_2} \frac{V_2^2}{2g} \quad \rightarrow \quad h_{L,2} = f_2 \frac{36\ m}{0.08\ m} \frac{V_2^2}{2(9.81\ m/s^2)} \quad \textbf{(12)}$$

$$\dot{V} = \dot{V}_1 + \dot{V}_2 \quad \textbf{(13)}$$

This is a system of 13 equations in 13 unknowns, and their simultaneous solution by an equation solver gives

$$\dot{V} = \textbf{0.0300 m}^3\textbf{/s}, \quad \dot{V}_1 = \textbf{0.00415 m}^3\textbf{/s}, \quad \dot{V}_2 = \textbf{0.0259 m}^3\textbf{/s}$$

$$V_1 = 3.30\ m/s, \quad V_2 = 5.15\ m/s, \quad h_L = h_{L,1} = h_{L,2} = 11.1\ m, \quad h_{pump} = 19.1\ m$$

$$Re_1 = 131,600, \quad Re_2 = 410,000, \quad f_1 = 0.0221, \quad f_2 = 0.0182$$

Note that Re > 4000 for both pipes, and thus the assumption of turbulent flow is verified.

Discussion The two parallel pipes are identical, except the diameter of the first pipe is half the diameter of the second one. But only 14 percent of the water flows through the first pipe. This shows the strong dependence of the flow rate (and the head loss) on diameter. Also, it can be shown that if the free surfaces of the two reservoirs were at the same elevation (and thus $z_A = z_B$), the flow rate would increase by 20 percent from 0.0300 to 0.0361 m³/s. Alternately, if the reservoirs were as given but the irreversible head losses were negligible, the flow rate would become 0.0715 m³/s (an increase of 138 percent).

EXAMPLE 8–8 **Gravity-Driven Water Flow in a Pipe**

Water at 10°C flows from a large reservoir to a smaller one through a 5-cm-diameter cast iron piping system, as shown in Fig. 8–48. Determine the elevation z_1 for a flow rate of 6 L/s.
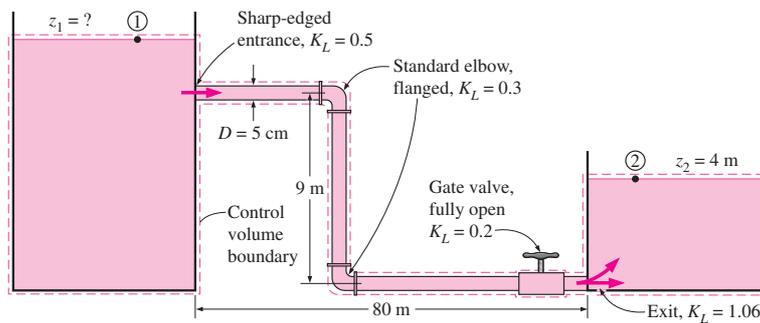
FIGURE 8–48
The piping system discussed in Example 8–8.

SOLUTION The flow rate through a piping system connecting two reservoirs is given. The elevation of the source is to be determined.

Assumptions **1** The flow is steady and incompressible. **2** The elevations of the reservoirs remain constant. **3** There are no pumps or turbines in the line.

Properties The density and dynamic viscosity of water at 10°C are $\rho = 999.7$ kg/m³ and $\mu = 1.307 \times 10^{-3}$ kg/m · s. The roughness of cast iron pipe is $\varepsilon = 0.00026$ m.

Analysis The piping system involves 89 m of piping, a sharp-edged entrance ($K_L = 0.5$), two standard flanged elbows ($K_L = 0.3$ each), a fully open gate valve ($K_L = 0.2$), and a submerged exit ($K_L = 1.06$). We choose points 1 and 2 at the free surfaces of the two reservoirs. Noting that the fluid at both points is open to the atmosphere (and thus $P_1 = P_2 = P_{atm}$) and that the fluid velocities at both points are zero ($V_1 = V_2 = 0$), the energy equation for a control volume between these two points simplifies to

$$\frac{\cancel{P_1}}{\rho g} + \alpha_1 \cancel{\frac{V_1^2}{2g}}^{0} + z_1 = \frac{\cancel{P_2}}{\rho g} + \alpha_2 \cancel{\frac{V_2^2}{2g}}^{0} + z_2 + h_L \qquad \rightarrow \qquad z_1 = z_2 + h_L$$

where

$$h_L = h_{L,\,total} = h_{L,\,major} + h_{L,\,minor} = \left(f\frac{L}{D} + \sum K_L\right)\frac{V^2}{2g}$$

since the diameter of the piping system is constant. The average velocity in the pipe and the Reynolds number are

$$V = \frac{\dot{V}}{A_c} = \frac{\dot{V}}{\pi D^2/4} = \frac{0.006 \text{ m}^3/\text{s}}{\pi(0.05 \text{ m})^2/4} = 3.06 \text{ m/s}$$

$$\text{Re} = \frac{\rho V D}{\mu} = \frac{(999.7 \text{ kg/m}^3)(3.06 \text{ m/s})(0.05 \text{ m})}{1.307 \times 10^{-3} \text{ kg/m} \cdot \text{s}} = 117,000$$

The flow is turbulent since Re > 4000. Noting that $\varepsilon/D = 0.00026/0.05 = 0.0052$, the friction factor can be determined from the Colebrook equation (or the Moody chart),

$$\frac{1}{\sqrt{f}} = -2.0 \log\left(\frac{\varepsilon/D}{3.7} + \frac{2.51}{\text{Re}\sqrt{f}}\right) \quad \rightarrow \quad \frac{1}{\sqrt{f}} = -2.0 \log\left(\frac{0.0052}{3.7} + \frac{2.51}{117,000\sqrt{f}}\right)$$

It gives $f = 0.0315$. The sum of the loss coefficients is

$$\sum K_L = K_{L,\,entrance} + 2K_{L,\,elbow} + K_{L,\,valve} + K_{L,\,exit}$$
$$= 0.5 + 2 \times 0.3 + 0.2 + 1.06 = 2.36$$

Then the total head loss and the elevation of the source become

$$h_L = \left(f\frac{L}{D} + \sum K_L\right)\frac{V^2}{2g} = \left(0.0315\frac{89 \text{ m}}{0.05 \text{ m}} + 2.36\right)\frac{(3.06 \text{ m/s})^2}{2(9.81 \text{ m/s}^2)} = 27.9 \text{ m}$$

$$z_1 = z_2 + h_L = 4 + 27.9 = \mathbf{31.9 \text{ m}}$$

Therefore, the free surface of the first reservoir must be 31.9 m above the ground level to ensure water flow between the two reservoirs at the specified rate.

Discussion Note that $fL/D = 56.1$ in this case, which is about 24 times the total minor loss coefficient. Therefore, ignoring the sources of minor losses in this case would result in about 4 percent error.

It can be shown that the total head loss would be 35.9 m (instead of 27.9 m) if the valve were three-fourths closed, and it would drop to 24.8 m if the pipe between the two reservoirs were straight at the ground level (thus

eliminating the elbows and the vertical section of the pipe). The head loss could be reduced further (from 24.8 to 24.6 m) by rounding the entrance. The head loss can be reduced significantly (from 27.9 to 16.0 m) by replacing the cast iron pipes by smooth pipes such as those made of plastic.

EXAMPLE 8–9   **Effect of Flushing on Flow Rate from a Shower**

The bathroom plumbing of a building consists of 1.5-cm-diameter copper pipes with threaded connectors, as shown in Fig. 8–49. (*a*) If the gage pressure at the inlet of the system is 200 kPa during a shower and the toilet reservoir is full (no flow in that branch), determine the flow rate of water through the shower head. (*b*) Determine the effect of flushing of the toilet on the flow rate through the shower head. Take the loss coefficients of the shower head and the reservoir to be 12 and 14, respectively.

SOLUTION   The cold-water plumbing system of a bathroom is given. The flow rate through the shower and the effect of flushing the toilet on the flow rate are to be determined.
Assumptions   **1** The flow is steady and incompressible. **2** The flow is turbulent and fully developed. **3** The reservoir is open to the atmosphere. **4** The velocity heads are negligible.
Properties   The properties of water at 20°C are $\rho = 998$ kg/m^3, $\mu = 1.002 \times 10^{-3}$ kg/m · s, and $\nu = \mu/\rho = 1.004 \times 10^{-6}$ m^2/s. The roughness of copper pipes is $\varepsilon = 1.5 \times 10^{-6}$ m.
Analysis   This is a problem of the second type since it involves the determination of the flow rate for a specified pipe diameter and pressure drop. The solution involves an iterative approach since the flow rate (and thus the flow velocity) is not known.
(*a*) The piping system of the shower alone involves 11 m of piping, a tee with line flow ($K_L = 0.9$), two standard elbows ($K_L = 0.9$ each), a fully open globe valve ($K_L = 10$), and a shower head ($K_L = 12$). Therefore, $\Sigma K_L = 0.9 + 2 \times 0.9 + 10 + 12 = 24.7$. Noting that the shower head is open to the atmosphere, and the velocity heads are negligible, the energy equation for a control volume between points 1 and 2 simplifies to

$$\frac{P_1}{\rho g} + \alpha_1 \frac{V_1^2}{2g} + z_1 + h_{\text{pump}, u} = \frac{P_2}{\rho g} + \alpha_2 \frac{V_2^2}{2g} + z_2 + h_{\text{turbine}, e} + h_L$$

$$\rightarrow \quad \frac{P_{1, \text{gage}}}{\rho g} = (z_2 - z_1) + h_L$$
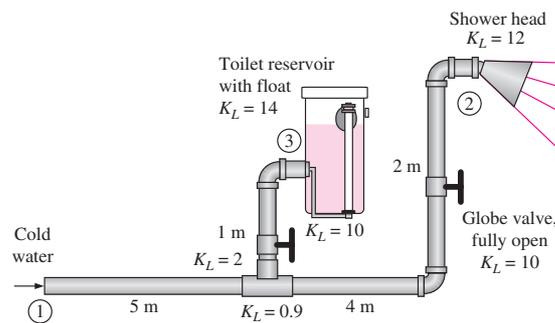
FIGURE 8–49
Schematic for Example 8–9.

Shower head $K_L = 12$

Toilet reservoir with float $K_L = 14$

③

②

2 m

Globe valve, fully open $K_L = 10$

Cold water

1 m $K_L = 2$

$K_L = 10$

① 5 m $K_L = 0.9$ 4 m

Therefore, the head loss is

$$h_L = \frac{200{,}000 \text{ N/m}^2}{(998 \text{ kg/m}^3)(9.81 \text{ m/s}^2)} - 2 \text{ m} = 18.4 \text{ m}$$

Also,

$$h_L = \left(f\frac{L}{D} + \sum K_L\right)\frac{V^2}{2g} \quad \rightarrow \quad 18.4 = \left(f\frac{11 \text{ m}}{0.015 \text{ m}} + 24.7\right)\frac{V^2}{2(9.81 \text{ m/s}^2)}$$

since the diameter of the piping system is constant. The average velocity in the pipe, the Reynolds number, and the friction factor are

$$V = \frac{\dot{V}}{A_c} = \frac{\dot{V}}{\pi D^2/4} \quad \rightarrow \quad V = \frac{\dot{V}}{\pi(0.015 \text{ m})^2/4}$$

$$\text{Re} = \frac{VD}{\nu} \quad \rightarrow \quad \text{Re} = \frac{V(0.015 \text{ m})}{1.004 \times 10^{-6} \text{ m}^2/\text{s}}$$

$$\frac{1}{\sqrt{f}} = -2.0 \log\left(\frac{\varepsilon/D}{3.7} + \frac{2.51}{\text{Re}\sqrt{f}}\right)$$

$$\rightarrow \quad \frac{1}{\sqrt{f}} = -2.0 \log\left(\frac{1.5 \times 10^{-6} \text{ m}}{3.7(0.015 \text{ m})} + \frac{2.51}{\text{Re}\sqrt{f}}\right)$$

This is a set of four equations with four unknowns, and solving them with an equation solver such as EES gives

$$\dot{V} = 0.00053 \text{ m}^3/\text{s}, \quad f = 0.0218, \quad V = 2.98 \text{ m/s}, \quad \text{and} \quad \text{Re} = 44{,}550$$

Therefore, the flow rate of water through the shower head is **0.53 L/s.**

(*b*) When the toilet is flushed, the float moves and opens the valve. The discharged water starts to refill the reservoir, resulting in parallel flow after the tee connection. The head loss and minor loss coefficients for the shower branch were determined in (*a*) to be $h_{L,2} = 18.4$ m and $\sum K_{L,2} = 24.7$, respectively. The corresponding quantities for the reservoir branch can be determined similarly to be

$$h_{L,3} = \frac{200{,}000 \text{ N/m}^2}{(998 \text{ kg/m}^3)(9.81 \text{ m/s}^2)} - 1 \text{ m} = 19.4 \text{ m}$$

$$\sum K_{L,3} = 2 + 10 + 0.9 + 14 = 26.9$$

The relevant equations in this case are

$$\dot{V}_1 = \dot{V}_2 + \dot{V}_3$$

$$h_{L,2} = f_1\frac{5 \text{ m}}{0.015 \text{ m}}\frac{V_1^2}{2(9.81 \text{ m/s}^2)} + \left(f_2\frac{6 \text{ m}}{0.015 \text{ m}} + 24.7\right)\frac{V_2^2}{2(9.81 \text{ m/s}^2)} = 18.4$$

$$h_{L,3} = f_1\frac{5 \text{ m}}{0.015 \text{ m}}\frac{V_1^2}{2(9.81 \text{ m/s}^2)} + \left(f_3\frac{1 \text{ m}}{0.015 \text{ m}} + 26.9\right)\frac{V_3^2}{2(9.81 \text{ m/s}^2)} = 19.4$$

$$V_1 = \frac{\dot{V}_1}{\pi(0.015 \text{ m})^2/4}, \quad V_2 = \frac{\dot{V}_2}{\pi(0.015 \text{ m})^2/4}, \quad V_3 = \frac{\dot{V}_3}{\pi(0.015 \text{ m})^2/4}$$

$$\text{Re}_1 = \frac{V_1(0.015 \text{ m})}{1.004 \times 10^{-6} \text{m}^2/\text{s}}, \quad \text{Re}_2 = \frac{V_2(0.015 \text{ m})}{1.004 \times 10^{-6} \text{m}^2/\text{s}}, \quad \text{Re}_3 = \frac{V_3(0.015 \text{ m})}{1.004 \times 10^{-6} \text{m}^2/\text{s}}$$

Ouch!

FIGURE 8–50
Flow rate of cold water through a shower may be affected significantly by the flushing of a nearby toilet.

$$\frac{1}{\sqrt{f_1}} = -2.0 \log\left(\frac{1.5 \times 10^{-6}\,\text{m}}{3.7(0.015\,\text{m})} + \frac{2.51}{\text{Re}_1\sqrt{f_1}}\right)$$

$$\frac{1}{\sqrt{f_2}} = -2.0 \log\left(\frac{1.5 \times 10^{-6}\,\text{m}}{3.7(0.015\,\text{m})} + \frac{2.51}{\text{Re}_2\sqrt{f_2}}\right)$$

$$\frac{1}{\sqrt{f_3}} = -2.0 \log\left(\frac{1.5 \times 10^{-6}\,\text{m}}{3.7(0.015\,\text{m})} + \frac{2.51}{\text{Re}_3\sqrt{f_3}}\right)$$

Solving these 12 equations in 12 unknowns simultaneously using an equation solver, the flow rates are determined to be

$$\dot{V}_1 = 0.00090\,\text{m}^3/\text{s}, \quad \dot{V}_2 = 0.00042\,\text{m}^3/\text{s}, \quad \text{and} \quad \dot{V}_3 = 0.00048\,\text{m}^3/\text{s}$$

Therefore, the flushing of the toilet **reduces the flow rate of cold water through the shower by 21 percent** from 0.53 to 0.42 L/s, causing the shower water to suddenly get very hot (Fig. 8–50).

Discussion   If the velocity heads were considered, the flow rate through the shower would be 0.43 instead of 0.42 L/s. Therefore, the assumption of negligible velocity heads is reasonable in this case

Note that a leak in a piping system will cause the same effect, and thus an unexplained drop in flow rate at an end point may signal a leak in the system.

8–8 ▪ FLOW RATE AND VELOCITY MEASUREMENT

A major application area of fluid mechanics is the determination of the flow rate of fluids, and numerous devices have been developed over the years for the purpose of flow metering. Flowmeters range widely in their level of sophistication, size, cost, accuracy, versatility, capacity, pressure drop, and the operating principle. We give an overview of the meters commonly used to measure the flow rate of liquids and gases flowing through pipes or ducts. We limit our consideration to incompressible flow.

Some flowmeters measure the flow rate directly by discharging and recharging a measuring chamber of known volume continuously and keeping track of the number of discharges per unit time. But most flowmeters measure the flow rate indirectly—they measure the average velocity V or a quantity that is related to average velocity such as pressure and drag, and determine the volume flow rate $\dot{V}$ from

$$\dot{V} = VA_c \tag{8–65}$$

where A_c is the cross-sectional area of flow. Therefore, measuring the flow rate is usually done by measuring flow velocity, and most flowmeters are simply velocimeters used for the purpose of metering flow.

The velocity in a pipe varies from zero at the wall to a maximum at the center, and it is important to keep this in mind when taking velocity measurements. For laminar flow, for example, the average velocity is half the centerline velocity. But this is not the case in turbulent flow, and it may be necessary to take the weighted average of several local velocity measurements to determine the average velocity.

Printed from PDF by LPS

The flow rate measurement techniques range from very crude to very elegant. The flow rate of water through a garden hose, for example, can be measured simply by collecting the water in a bucket of known volume and dividing the amount collected by the collection time (Fig. 8–51). A crude way of estimating the flow velocity of a river is to drop a float on the river and measure the drift time between two specified locations. At the other extreme, some flowmeters use the propagation of sound in flowing fluids while others use the electromotive force generated when a fluid passes through a magnetic field. In this section we discuss devices that are commonly used to measure velocity and flow rate, starting with the Pitot-static probe introduced in Chap. 5.

FIGURE 8–51
A primitive (but fairly accurate) way of measuring the flow rate of water through a garden hose involves collecting water in a bucket and recording the collection time.

Pitot and Pitot-Static Probes

Pitot probes (also called *Pitot tubes*) and **Pitot-static probes,** named after the French engineer Henri de Pitot (1695–1771), are widely used for flow rate measurement. A Pitot probe is just a tube with a pressure tap at the stagnation point that measures stagnation pressure, while a Pitot-static probe has both a stagnation pressure tap and several circumferential static pressure taps and it measures both stagnation and static pressures (Figs. 8–52 and 8–53). Pitot was the first person to measure velocity with the upstream pointed tube, while French engineer Henry Darcy (1803–1858) developed most of the features of the instruments we use today, including the use of small openings and the placement of the static tube on the same assembly. Therefore, it is more appropriate to call the Pitot-static probes **Pitot–Darcy probes.**

The Pitot-static probe measures local velocity by measuring the pressure difference in conjunction with the Bernoulli equation. It consists of a slender double-tube aligned with the flow and connected to a differential pressure meter. The inner tube is fully open to flow at the nose, and thus it measures the stagnation pressure at that location (point 1). The outer tube is sealed at the nose, but it has holes on the side of the outer wall (point 2) and thus it measures the static pressure. For incompressible flow with sufficiently high velocities (so that the frictional effects between points 1 and 2 are negligible), the Bernoulli equation is applicable and can be expressed as

$$\frac{P_1}{\rho g} + \frac{V_1^2}{2g} + z_1 = \frac{P_2}{\rho g} + \frac{V_2^2}{2g} + z_2 \qquad \textbf{(8–66)}$$

FIGURE 8–52
(*a*) A Pitot probe measures stagnation pressure at the nose of the probe, while (*b*) a Pitot-static probe measures both stagnation pressure and static pressure, from which the flow speed can be calculated.
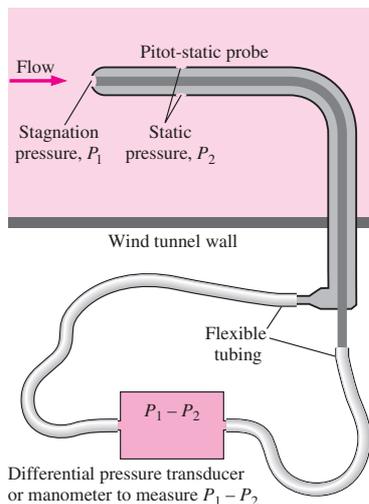
FIGURE 8–53
Measuring flow velocity with a Pitot-static probe. (A manometer may also be used in place of the differential pressure transducer.)
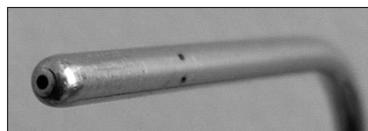
FIGURE 8–54
Close-up of a Pitot-static probe, showing the stagnation pressure hole and two of the five static circumferential pressure holes.
Photo by Po-Ya Abel Chuang.
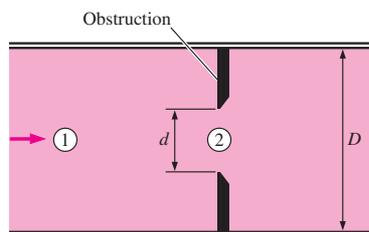
FIGURE 8–55
Flow through a constriction in a pipe.

Noting that $z_1 \cong z_2$ since the static pressure holes of the Pitot-static probe are arranged circumferentially around the tube and $V_1 = 0$ because of the stagnation conditions, the flow velocity $V = V_2$ becomes

Pitot formula:
$$V = \sqrt{\frac{2(P_1 - P_2)}{\rho}} \qquad \text{(8–67)}$$

which is known as the **Pitot formula.** If the velocity is measured at a location where the local velocity is equal to the average flow velocity, the volume flow rate can be determined from $\dot{V} = V A_c$.

The Pitot-static probe is a simple, inexpensive, and highly reliable device since it has no moving parts (Fig. 8–54). It also causes very small pressure drop and usually does not disturb the flow appreciably. However, it is important that it be properly aligned with the flow to avoid significant errors that may be caused by misalignment. Also, the difference between the static and stagnation pressures (which is the dynamic pressure) is proportional to the density of the fluid and the square of the flow velocity. It can be used to measure velocity in both liquids and gases. Noting that gases have low densities, the flow velocity should be sufficiently high when the Pitot-static probe is used for gas flow such that a measurable dynamic pressure develops.

Obstruction Flowmeters: Orifice, Venturi, and Nozzle Meters

Consider incompressible steady flow of a fluid in a horizontal pipe of diameter D that is constricted to a flow area of diameter d, as shown in Fig. 8–55. The mass balance and the Bernoulli equations between a location before the constriction (point 1) and the location where constriction occurs (point 2) can be written as

Mass balance:
$$\dot{V} = A_1 V_1 = A_2 V_2 \quad \rightarrow \quad V_1 = (A_2/A_1) V_2 = (d/D)^2 V_2 \qquad \text{(8–68)}$$

Bernoulli equation ($z_1 = z_2$):
$$\frac{P_1}{\rho g} + \frac{V_1^2}{2g} = \frac{P_2}{\rho g} + \frac{V_2^2}{2g} \qquad \text{(8–69)}$$

Combining Eqs. 8–68 and 8–69 and solving for velocity V_2 gives

Obstruction (with no loss):
$$V_2 = \sqrt{\frac{2(P_1 - P_2)}{\rho(1 - \beta^4)}} \qquad \text{(8–70)}$$

where $\beta = d/D$ is the diameter ratio. Once V_2 is known, the flow rate can be determined from $\dot{V} = A_2 V_2 = (\pi d^2/4) V_2$.

This simple analysis shows that the flow rate through a pipe can be determined by constricting the flow and measuring the decrease in pressure due to the increase in velocity at the constriction site. Noting that the pressure drop between two points along the flow can be measured easily by a differential pressure transducer or manometer, it appears that a simple flow rate measurement device can be built by obstructing the flow. Flowmeters based on this principle are called **obstruction flowmeters** and are widely used to measure flow rates of gases and liquids.

The velocity in Eq. 8–70 is obtained by assuming no loss, and thus it is the maximum velocity that can occur at the constriction site. In reality, some pressure losses due to frictional effects are inevitable, and thus the velocity will be less. Also, the fluid stream will continue to contract past the

obstruction, and the vena contracta area is less than the flow area of the obstruction. Both losses can be accounted for by incorporating a correction factor called the **discharge coefficient** C_d whose value (which is less than 1) is determined experimentally. Then the flow rate for obstruction flowmeters can be expressed as

Obstruction flowmeters:
$$\dot{V} = A_0 C_d \sqrt{\frac{2(P_1 - P_2)}{\rho(1 - \beta^4)}}$$
(8–71)

where $A_0 = A_2 = \pi d^2/4$ is the cross-sectional area of the hole and $\beta = d/D$ is the ratio of hole diameter to pipe diameter. The value of C_d depends on both β and the Reynolds number $\text{Re} = V_1 D/\nu$, and charts and curve-fit correlations for C_d are available for various types of obstruction meters.

Of the numerous types of obstruction meters available, those most widely used are orifice meters, flow nozzles, and Venturi meters (Fig. 8–56). The experimentally determined data for discharge coefficients are expressed as (Miller, 1997)

Orifice meters:
$$C_d = 0.5959 + 0.0312\beta^{2.1} - 0.184\beta^8 + \frac{91.71\beta^{2.5}}{\text{Re}^{0.75}}$$
(8–72)

Nozzle meters:
$$C_d = 0.9975 - \frac{6.53\beta^{0.5}}{\text{Re}^{0.5}}$$
(8–73)

These relations are valid for $0.25 < \beta < 0.75$ and $10^4 < \text{Re} < 10^7$. Precise values of C_d depend on the particular design of the obstruction, and thus the manufacturer's data should be consulted when available. For flows with high Reynolds numbers ($\text{Re} > 30,000$), the value of C_d can be taken to be 0.96 for flow nozzles and 0.61 for orifices.

Owing to its streamlined design, the discharge coefficients of Venturi meters are very high, ranging between 0.95 and 0.99 (the higher values are for the higher Reynolds numbers) for most flows. In the absence of specific data, we can take $C_d = 0.98$ for Venturi meters. Also, the Reynolds number depends on the flow velocity, which is not known a priori. Therefore, the solution is iterative in nature when curve-fit correlations are used for C_d.

The orifice meter has the simplest design and it occupies minimal space as it consists of a plate with a hole in the middle, but there are considerable variations in design (Fig. 8–57). Some orifice meters are sharp-edged, while
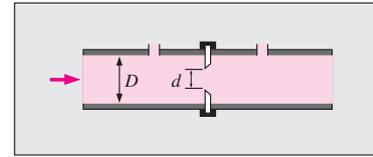
(a) Orifice meter
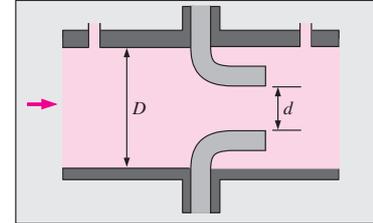
(b) Flow nozzle
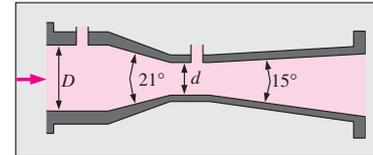
(c) Venturi meter

FIGURE 8–56
Common types of obstruction meters.
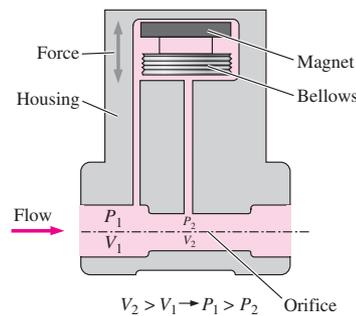
FIGURE 8–57
An orifice meter and schematic showing its built-in pressure transducer and digital readout.
Courtesy KOBOLD Instruments, Pittsburgh, PA. www.koboldusa.com. Used by permission.
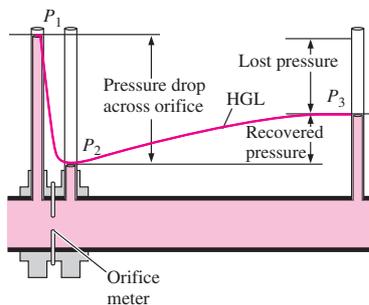
FIGURE 8–58
The variation of pressure along a flow section with an orifice meter as measured with piezometer tubes; the lost pressure and the pressure recovery are shown.

others are beveled or rounded. The sudden change in the flow area in orifice meters causes considerable swirl and thus significant head loss or permanent pressure loss, as shown in Fig. 8–58. In nozzle meters, the plate is replaced by a nozzle, and thus the flow in the nozzle is streamlined. As a result, the vena contracta is practically eliminated and the head loss is small. However, flow nozzle meters are more expensive than orifice meters.

The Venturi meter, invented by the American engineer Clemans Herschel (1842–1930) and named by him after the Italian Giovanni Venturi (1746–1822) for his pioneering work on conical flow sections, is the most accurate flowmeter in this group, but it is also the most expensive. Its gradual contraction and expansion prevent flow separation and swirling, and it suffers only frictional losses on the inner wall surfaces. Venturi meters cause very low head losses, as shown in Fig. 8–59, and thus they should be preferred for applications that cannot allow large pressure drops. The irreversible head loss for Venturi meters due to friction is only about 10 percent.

EXAMPLE 8–10   **Measuring Flow Rate with an Orifice Meter**

The flow rate of methanol at 20°C (ρ = 788.4 kg/m^3 and μ = 5.857 $\times$ 10^{-4} kg/m · s) through a 4-cm-diameter pipe is to be measured with a 3-cm-diameter orifice meter equipped with a mercury manometer across the orifice place, as shown in Fig. 8–60. If the differential height of the manometer is read to be 11 cm, determine the flow rate of methanol through the pipe and the average flow velocity.

SOLUTION   The flow rate of methanol is to be measured with an orifice meter. For a given pressure drop across the orifice plate, the flow rate and the average flow velocity are to be determined.
Assumptions   **1** The flow is steady and incompressible. **2** The discharge coefficient of the orifice meter is C_d = 0.61.

FIGURE 8–59
The fraction of pressure (or head) loss for various obstruction meters.
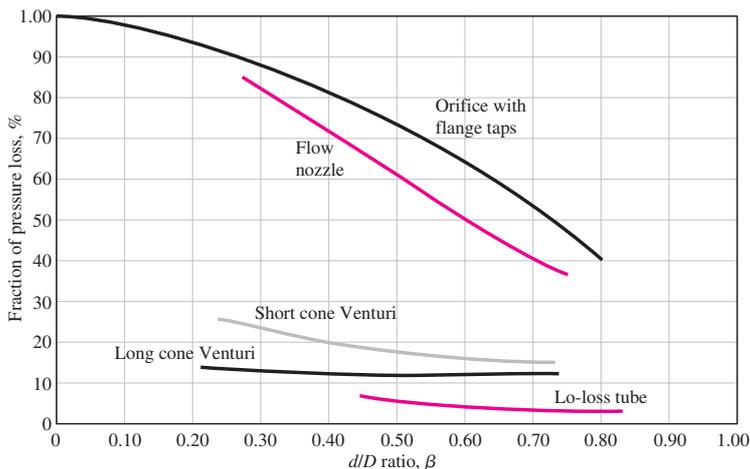
Properties The density and dynamic viscosity of methanol are given to be $\rho = 788.4$ kg/m^3 and $\mu = 5.857 \times 10^{-4}$ kg/m · s, respectively. We take the density of mercury to be 13,600 kg/m^3.

Analysis The diameter ratio and the throat area of the orifice are

$$\beta = \frac{d}{D} = \frac{3}{4} = 0.75$$

$$A_0 = \frac{\pi d^2}{4} = \frac{\pi(0.03 \text{ m})^2}{4} = 7.069 \times 10^{-4} \text{ m}^2$$

The pressure drop across the orifice plate can be expressed as

$$\Delta P = P_1 - P_2 = (\rho_{Hg} - \rho_{met})gh$$

Then the flow rate relation for obstruction meters becomes

$$\dot{V} = A_0 C_d \sqrt{\frac{2(P_1 - P_2)}{\rho(1 - \beta^4)}} = A_0 C_d \sqrt{\frac{2(\rho_{Hg} - \rho_{met})gh}{\rho_{met}(1 - \beta^4)}} = A_0 C_d \sqrt{\frac{2(\rho_{Hg}/\rho_{met} - 1)gh}{1 - \beta^4}}$$

Substituting, the flow rate is determined to be

$$\dot{V} = (7.069 \times 10^{-4} \text{ m}^2)(0.61)\sqrt{\frac{2(13,600/788.4 - 1)(9.81 \text{ m/s}^2)(0.11 \text{ m})}{1 - 0.75^4}}$$

$$= \textbf{3.09} \times \textbf{10}^{-3} \textbf{ m}^3\textbf{/s}$$

which is equivalent to 3.09 L/s. The average flow velocity in the pipe is determined by dividing the flow rate by the cross-sectional area of the pipe,

$$V = \frac{\dot{V}}{A_c} = \frac{\dot{V}}{\pi D^2/4} = \frac{3.09 \times 10^{-3} \text{ m}^3/\text{s}}{\pi(0.04 \text{ m})^2/4} = \textbf{2.46 m/s}$$

Discussion The Reynolds number of flow through the pipe is

$$\text{Re} = \frac{\rho V D}{\mu} = \frac{(788.4 \text{ kg/m}^3)(2.46 \text{ m/s})(0.04 \text{ m})}{5.857 \times 10^{-4} \text{ kg/m} \cdot \text{s}} = 1.32 \times 10^5$$

Substituting $\beta = 0.75$ and Re $= 1.32 \times 10^5$ into the orifice discharge coefficient relation

$$C_d = 0.5959 + 0.0312\beta^{2.1} - 0.184\beta^8 + \frac{91.71\beta^{2.5}}{\text{Re}^{0.75}}$$

gives $C_d = 0.601$, which is very close to the assumed value of 0.61. Using this refined value of C_d, the flow rate becomes 3.04 L/s, which differs from our original result by only 1.6 percent. Therefore, it is convenient to analyze orifice meters using the recommended value of $C_d = 0.61$ for the discharge coefficient, and then to verify the assumed value. If the problem is solved using an equation solver such as EES, then the problem can be formulated using the curve-fit formula for C_d (which depends on the Reynolds number), and all equations can be solved simultaneously by letting the equation solver perform the iterations as necessary.
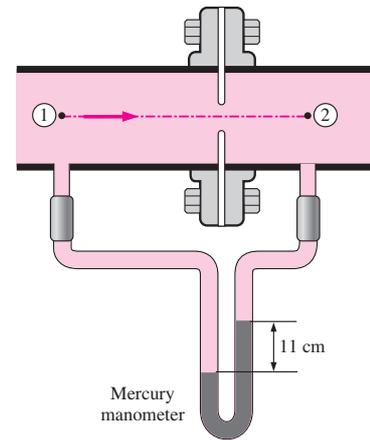
FIGURE 8–60
Schematic for the orifice meter considered in Example 8–10.

Positive Displacement Flowmeters

When we buy gasoline for the car, we are interested in the total amount of gasoline that flows through the nozzle during the period we fill the tank rather than the flow rate of gasoline. Likewise, we care about the total

FIGURE 8–61

A positive displacement flowmeter with double helical three-lobe impeller design.

Courtesy Flow Technology, Inc.
Source: www.ftimeters.com.

amount of water or natural gas we use in our homes during a billing period. In these and many other applications, the quantity of interest is the total amount of mass or volume of a fluid that passes through a cross section of a pipe over a certain period of time rather than the instantaneous value of flow rate, and **positive displacement flowmeters** are well suited for such applications. There are numerous types of displacement meters, and they are based on continuous filling and discharging of the measuring chamber. They operate by trapping a certain amount of incoming fluid, displacing it to the discharge side of the meter, and counting the number of such discharge–recharge cycles to determine the total amount of fluid displaced. The clearance between the impeller and its casing must be controlled carefully to prevent leakage and thus to avoid error.

Figure 8–61 shows a positive displacement flowmeter with two rotating impellers driven by the flowing liquid. Each impeller has three gear lobes, and a pulsed output signal is generated each time a lobe passes by a nonintrusive sensor. Each pulse represents a known volume of liquid that is captured in between the lobes of the impellers, and an electronic controller converts the pulses to volume units. This particular meter has a quoted accuracy of 0.1 percent, has a low pressure drop, and can be used with high- or low-viscosity liquids at temperatures up to 230°C and pressures up to 7 MPa for flow rates of up to 700 gal/min (or 50 L/s).

The most widely used flowmeters to measure liquid volumes are **nutating disk flowmeters,** shown in Fig. 8–62. They are commonly used as water and gasoline meters. The liquid enters the nutating disk meter through the chamber (A). This causes the disk (B) to nutate or wobble and results in the rotation of a spindle (C) and the excitation of a magnet (D). This signal is transmitted through the casing of the meter to a second magnet (E). The total volume is obtained by counting the number of these signals during a discharge process.

Quantities of gas flows, such as the amount of natural gas used in buildings, are commonly metered by using bellows flowmeters that displace a certain amount of gas volume during each revolution.

Turbine Flowmeters

We all know from experience that a propeller held against the wind rotates, and the rate of rotation increases as the wind velocity increases. You may

FIGURE 8–62

A nutating disk flowmeter.

(a) Courtesy Badger Meter, Inc.
Source: www.badgermeter.com.
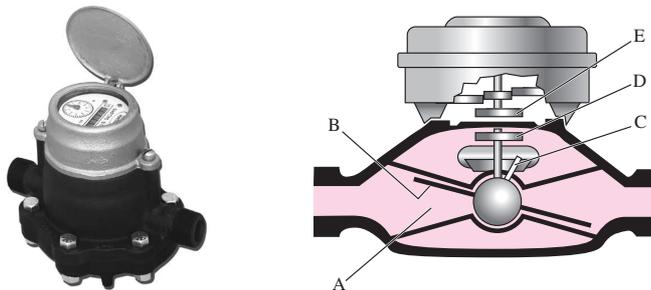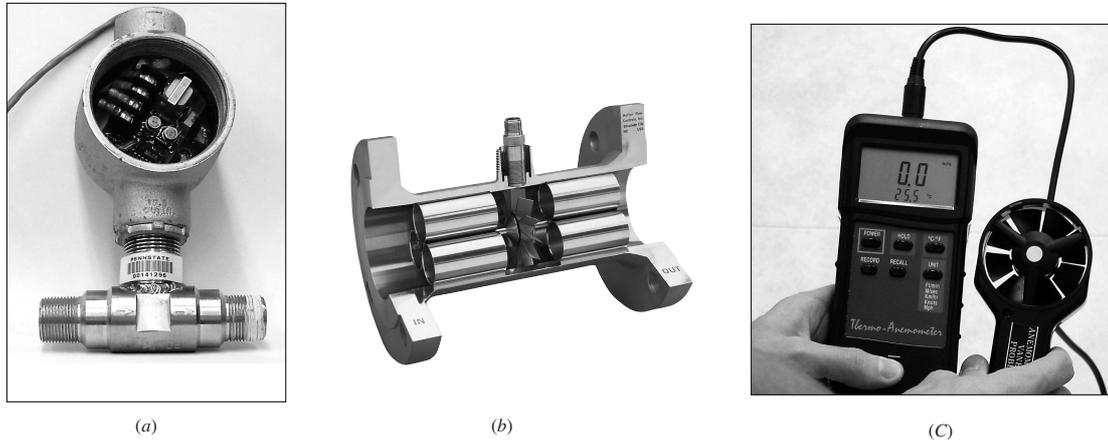
(*a*) (*b*) (*C*)

also have seen that the turbine blades of wind turbines rotate rather slowly
at low winds, but quite fast at high winds. These observations suggest that
the flow velocity in a pipe can be measured by placing a freely rotating
propeller inside a pipe section and doing the necessary calibration. Flow
measurement devices that work on this principle are called **turbine flowme-
ters** or sometimes **propeller flowmeters,** although the latter is a misnomer
since, by definition, propellers add energy to a fluid, while turbines extract
energy from a fluid.

A turbine flowmeter consists of a cylindrical flow section that houses a
turbine (a vaned rotor) that is free to rotate, additional stationary vanes at
the inlet to straighten the flow, and a sensor that generates a pulse each time
a marked point on the turbine passes by to determine the rate of rotation.
The rotational speed of the turbine is nearly proportional to the flow rate of
the fluid. Turbine flowmeters give highly accurate results (as accurate as
0.25 percent) over a wide range of flow rates when calibrated properly for
the anticipated flow conditions. Turbine flowmeters have very few blades
(sometimes just two blades) when used to measure liquid flow, but several
blades when used to measure gas flow to ensure adequate torque generation.
The head loss caused by the turbine is very small.

Turbine flowmeters have been used extensively for flow measurement
since the 1940s because of their simplicity, low cost, and accuracy over a
wide range of flow conditions. They are made commercially available for
both liquids and gases and for pipes of practically all sizes. Turbine flowme-
ters are also commonly used to measure flow velocities in unconfined flows
such as winds, rivers, and ocean currents. The handheld device shown in
Fig. 8–63*b* is used to measure wind velocity.

Paddlewheel Flowmeters

Paddlewheel flowmeters are low-cost alternatives to turbine flowmeters for
flows where very high accuracy is not required. In paddlewheel flowmeters,
the paddlewheel (the rotor and the blades) is perpendicular to the flow, as
shown in Fig. 8–64, rather than parallel as was the case with turbine

FIGURE 8–64

Paddlewheel flowmeter to measure liquid flow, with flow from left to right, and a schematic diagram of its operation.

Photo by John M. Cimbala.
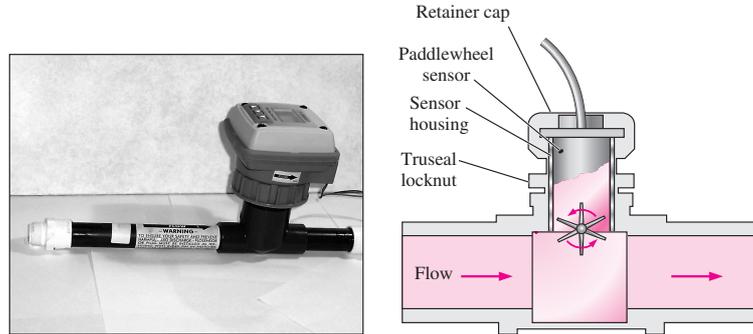
flowmeters. The paddles cover only a portion of the flow cross section (typically, less than half), and thus the head loss is much smaller compared to that of turbine flowmeters, but the depth of insertion of the paddlewheel into the flow is of critical importance for accuracy. Also, no strainers are required since the paddlewheels are not susceptible to fouling. A sensor detects the passage of each of the paddlewheel blades and transmits a signal. A microprocessor then converts this rotational speed information to flow rate or integrated flow quantity.

Variable-Area Flowmeters (Rotameters)

A simple, reliable, inexpensive, and easy-to-install flowmeter with low pressure drop and no electrical connections that gives a direct reading of flow rate for a wide range of liquids and gases is the **variable-area flowmeter,** also called a **rotameter** or **floatmeter.** A variable-area flowmeter consists of a vertical tapered conical transparent tube made of glass or plastic with a float inside that is free to move, as shown in Fig. 8–65. As fluid flows through the tapered tube, the float rises within the tube to a location where the float weight, drag force, and buoyancy force balance each other and the net force acting on the float is zero. The flow rate is determined by simply matching the position of the float against the graduated flow scale outside the tapered transparent tube.

We know from experience that high winds knock down trees, break power lines, and blow away hats or umbrellas. This is because the drag force increases with flow velocity. The weight and the buoyancy force acting on the float are constant, but the drag force changes with flow velocity. Also, the velocity along the tapered tube decreases in the flow direction because of the increase in the cross-sectional area. There is a certain velocity that generates enough drag to balance the float weight and the buoyancy force, and the location at which this velocity occurs around the float is the location where the float settles. The degree of tapering of the tube can be made such that the vertical rise changes linearly with flow rate, and thus the tube can be calibrated linearly for flow rates. The transparent tube also allows the fluid to be seen during flow.

There are numerous kinds of variable-area flowmeters. The gravity-based flowmeter discussed previously must be positioned vertically, with fluid entering from the bottom and leaving from the top. In spring-opposed

(b)

(a)

FIGURE 8–65

Two types of variable-area flowmeters: (*a*) an ordinary gravity-based meter and (*b*) a spring-opposed meter.

(a) Photo by John M. Cimbala and (b) Courtesy Insite, Universal Flow Monitors, Inc. Used by permission. Sources: www.omega.com and www.flowmeters.com.

flowmeters, the drag force is balanced by the spring force, and such flowmeters can be installed horizontally. Another type of flowmeter uses a loose-fitting piston instead of a float.

The accuracy of variable-area flowmeters is typically ±5 percent. Therefore, these flowmeters are not appropriate for applications that require precision measurements. However, some manufacturers quote accuracies of the order of 1 percent. Also, these meters depend on visual checking of the location of the float, and thus they cannot be used to measure the flow rate of fluids that are opaque or dirty, or fluids that coat the float since such fluids block visual access. Finally, glass tubes are prone to breakage and thus they pose a safety hazard if toxic fluids are handled. In such applications, variable-area flowmeters should be installed at locations with minimum traffic.

Ultrasonic Flowmeters

It is a common observation that when a stone is dropped into calm water, the waves that are generated spread out as concentric circles uniformly in all directions. But when a stone is thrown into flowing water such as a river, the waves move much faster in the flow direction (the wave and flow velocities are added since they are in the same direction) compared to the waves moving in the upstream direction (the wave and flow velocities are subtracted since they are in opposite directions). As a result, the waves appear spread out downstream while they appear tightly packed upstream. The difference between the number of waves in the upstream and downstream parts of the flow per unit length is proportional to the flow velocity, and this suggests that flow velocity can be measured by comparing the propagation of waves in the forward and backward directions to flow. **Ultrasonic flowmeters** operate on this principle, using sound waves in the ultrasonic range (typically at a frequency of 1 MHz).

Ultrasonic (or acoustic) flowmeters operate by generating sound waves with a transducer and measuring the propagation of those waves through a flowing fluid. There are two basic kinds of ultrasonic flowmeters: *transit time* and *Doppler-effect* (or *frequency shift*) flowmeters. The transit time flowmeter transmits sound waves in the upstream and downstream directions and measures the difference in travel time. A typical transit time ultrasonic meter is shown schematically in Fig. 8–66. It involves two transducers that alternately transmit and receive ultrasonic waves, one in the direction of flow and the other in the opposite direction. The travel time for each direction can be measured accurately, and the difference in the travel time can be calculated. The average flow velocity V in the pipe is proportional to this travel time difference Δt, and can be determined from

$$V = KL\,\Delta t \tag{8–74}$$

where L is the distance between the transducers and K is a constant.

Doppler-Effect Ultrasonic Flowmeters

You have probably noticed that when a fast-moving car approaches with its horn blowing, the tone of the high-pitched sound of the horn drops to a lower pitch as the car passes by. This is due to the sonic waves being compressed in front of the car and being spread out behind it. This shift in frequency is called the **Doppler effect,** and it forms the basis for the operation of most ultrasonic flowmeters.
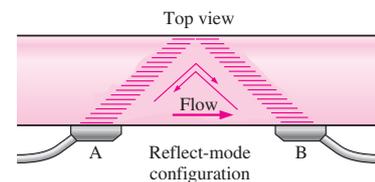
FIGURE 8–66
The operation of a transit time ultrasonic flowmeter equipped with two transducers, www.flocat.com.
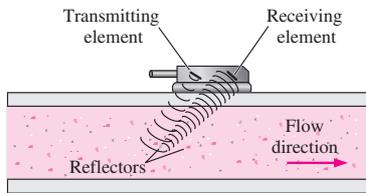
FIGURE 8–67
The operation of a Doppler-effect ultrasonic flowmeter equipped with a transducer pressed on the outer surface of a pipe.

Doppler-effect ultrasonic flowmeters measure the average flow velocity along the sonic path. This is done by clamping a piezoelectric transducer on the outside surface of a pipe (or pressing the transducer against the pipe for handheld units). The transducer transmits a sound wave at a fixed frequency through the pipe wall and into the flowing liquid. The waves reflected by impurities, such as suspended solid particles or entrained gas bubbles, are relayed to a receiving transducer. The change in the frequency of the reflected waves is proportional to the flow velocity, and a microprocessor determines the flow velocity by comparing the frequency shift between the transmitted and reflected signals (Figs. 8–67 and 8–68). The flow rate and the total amount of flow can also be determined using the measured velocity by properly configuring the flowmeter for the given pipe and flow conditions.

The operation of ultrasonic flowmeters depends on the ultrasound waves being reflected off discontinuities in density. Ordinary ultrasonic flowmeters require the liquid to contain impurities in concentrations greater than 25 parts per million (ppm) in sizes greater than at least 30 μm. But advanced ultrasonic units can also measure the velocity of clean liquids by sensing the waves reflected off turbulent swirls and eddies in the flow stream, provided that they are installed at locations where such disturbances are nonsymmetrical and at a high level, such as a flow section just downstream of a 90° elbow.

Ultrasonic flowmeters have the following advantages:

• They are easy and quick to install by clamping them on the outside of pipes of 0.6 cm to over 3 m in diameter, and even on open channels.

• They are nonintrusive. Since the meters clamp on, there is no need to stop operation and drill holes into piping, and no production downtime.

• There is no pressure drop since the meters do not interfere with the flow.
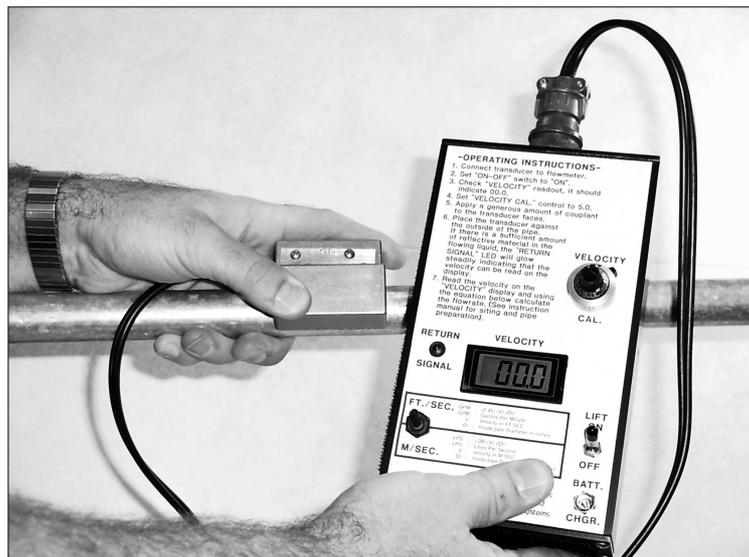
FIGURE 8–68
Ultrasonic flowmeters enable one to measure flow velocity without even contacting the fluid by simply pressing a transducer on the outer surface of the pipe.
Photo by John M. Cimbala.

- Since there is no direct contact with the fluid, there is no danger of corrosion or clogging.
- They are suitable for a wide range of fluids from toxic chemicals to slurries to clean liquids, for permanent or temporary flow measurement.
- There are no moving parts, and thus the meters provide reliable and maintenance-free operation.
- They can also measure flow quantities in reverse flow.
- The quoted accuracies are 1 to 2 percent.

Ultrasonic flowmeters are noninvasive devices, and the ultrasonic transducers can effectively transmit signals through polyvinyl chloride (PVC), steel, iron, and glass pipe walls. However, coated pipes and concrete pipes are not suitable for this measurement technique since they absorb ultrasonic waves.

Electromagnetic Flowmeters

It has been known since Faraday's experiments in the 1830s that when a conductor is moved in a magnetic field, an electromotive force develops across that conductor as a result of magnetic induction. Faraday's law states that the voltage induced across any conductor as it moves at right angles through a magnetic field is proportional to the velocity of that conductor. This suggests that we may be able to determine flow velocity by replacing the solid conductor by a conducting fluid, and **electromagnetic flowmeters** do just that. Electromagnetic flowmeters have been in use since the mid-1950s, and they come in various designs such as full-flow and insertion types.

A *full-flow electromagnetic flowmeter* is a nonintrusive device that consists of a magnetic coil that encircles the pipe, and two electrodes drilled into the pipe along a diameter flush with the inner surface of the pipe so that the electrodes are in contact with the fluid but do not interfere with the flow and thus do not cause any head loss (Fig. 8–69a). The electrodes are connected to a voltmeter. The coils generate a magnetic field when subjected to electric current, and the voltmeter measures the electric potential

(a) Full-flow electromagnetic flowmeter

(b) Insertion electromagnetic flowmeter
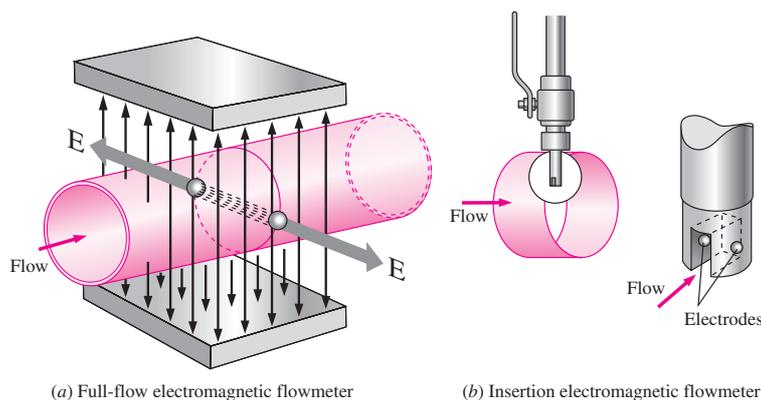
FIGURE 8–69
(*a*) Full-flow and (*b*) insertion electromagnetic flowmeters, www.flocat.com.

difference between the electrodes. This potential difference is proportional to the flow velocity of the conducting fluid, and thus the flow velocity can be calculated by relating it to the voltage generated.

Insertion electromagnetic flowmeters operate similarly, but the magnetic field is confined within a flow channel at the tip of a rod inserted into the flow, as shown in Fig. 8–69*b*.

Electromagnetic flowmeters are well-suited for measuring flow velocities of liquid metals such as mercury, sodium, and potassium that are used in some nuclear reactors. They can also be used for liquids that are poor conductors, such as water, provided that they contain an adequate amount of charged particles. Blood and seawater, for example, contain sufficient amounts of ions, and thus electromagnetic flowmeters can be used to measure their flow rates. Electromagnetic flowmeters can also be used to measure the flow rates of chemicals, pharmaceuticals, cosmetics, corrosive liquids, beverages, fertilizers, and numerous slurries and sludges, provided that the substances have high enough electrical conductivities. Electromagnetic flowmeters are not suitable for use with distilled or deionized water.

Electromagnetic flowmeters measure flow velocity indirectly, and thus careful calibration is important during installation. Their use is limited by their relatively high cost, power consumption, and the restrictions on the types of suitable fluids with which they can be used.

Vortex Flowmeters

You have probably noticed that when a flow stream such as a river encounters an obstruction such as a rock, the fluid separates and moves around the rock. But the presence of the rock is felt for some distance downstream via the swirls generated by it.

Most flows encountered in practice are turbulent, and a disk or a short cylinder placed in the flow coaxially sheds vortices (see also Chap. 4). It is observed that these vortices are shed periodically, and the shedding frequency is proportional to the average flow velocity. This suggests that the flow rate can be determined by generating vortices in the flow by placing an obstruction along the flow and measuring the shedding frequency. The flow measurement devices that work on this principle are called **vortex flowmeters.** The *Strouhal number*, defined as $St = fd/V$, where f is the vortex shedding frequency, d is the characteristic diameter or width of the obstruction, and V is the velocity of the flow impinging on the obstruction, also remains constant in this case, provided that the flow velocity is high enough.

A vortex flowmeter consists of a sharp-edged bluff body (strut) placed in the flow that serves as the vortex generator, and a detector (such as a pressure transducer that records the oscillation in pressure) placed a short distance downstream on the inner surface of the casing to measure the shedding frequency. The detector can be an ultrasonic, electronic, or fiber-optic sensor that monitors the changes in the vortex pattern and transmits a pulsating output signal (Fig. 8–70). A microprocessor then uses the frequency information to calculate and display the flow velocity or flow rate. The frequency of vortex shedding is proportional to the average velocity over a wide range of Reynolds numbers, and vortex flowmeters operate reliably and accurately at Reynolds numbers from 10^4 to 10^7.
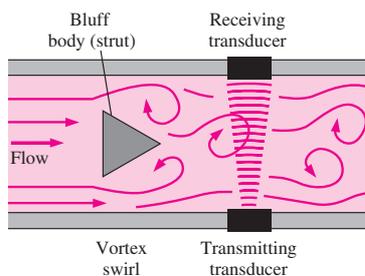
FIGURE 8–70
The operation of a vortex flowmeter, www.flocat.com.

The vortex flowmeter has the advantage that it has no moving parts and thus is inherently reliable, versatile, and very accurate (usually ± 1 percent over a wide range of flow rates), but it obstructs flow and thus causes considerable head loss.

Thermal (Hot-Wire and Hot-Film) Anemometers

Thermal anemometers were introduced in the late 1950s and have been in common use since then in fluid research facilities and labs. As the name implies, thermal anemometers involve an electrically heated sensor, as shown in Fig. 8–71, and utilize a thermal effect to measure flow velocity. Thermal anemometers have extremely small sensors, and thus they can be used to measure the instantaneous velocity at any point in the flow without appreciably disturbing the flow. They can take thousands of velocity measurements per second with excellent spatial and temporal resolution, and thus they can be used to study the details of fluctuations in turbulent flow. They can measure velocities in liquids and gases accurately over a wide range—from a few centimeters to over a hundred meters per second.

A thermal anemometer is called a **hot-wire anemometer** if the sensing element is a wire, and a **hot-film anemometer** if the sensor is a thin metallic film (less than 0.1 μm thick) mounted usually on a relatively thick ceramic support having a diameter of about 50 μm. The hot-wire anemometer is characterized by its very small sensor wire—usually a few microns in diameter and a couple of millimeters in length. The sensor is usually made of platinum, tungsten, or platinum–iridium alloys, and it is attached to the probe through holders. The fine wire sensor of a hot-wire anemometer is very fragile because of its small size and can easily break if the liquid or gas contains excessive amounts of contaminants or particulate matter. This is especially of consequence at high velocities. In such cases, the more rugged hot-film probes should be used. But the sensor of the hot-film probe is larger, has significantly lower frequency response, and interferes more with the flow; thus it is not always suitable for studying the fine details of turbulent flow.

The operating principle of a constant-temperature anemometer (CTA), which is the most common type and is shown schematically in Fig. 8–72, is as follows: the sensor is electrically heated to a specified temperature (typically about 200°C). The sensor tends to cool as it loses heat to the surrounding flowing fluid, but electronic controls maintain the sensor at a constant
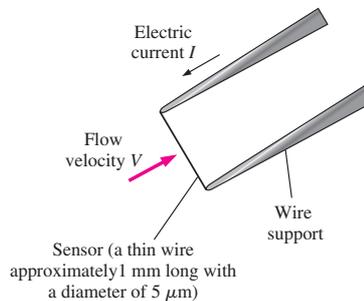
FIGURE 8–71
The electrically heated sensor and its support of a hot-wire probe.
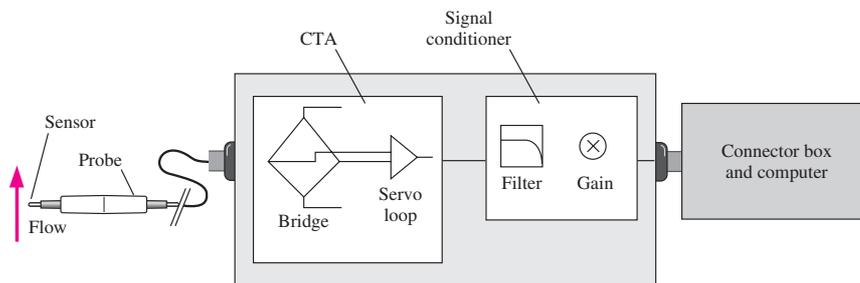
FIGURE 8–72
Schematic of a thermal anemometer system.

FIGURE 8–73
Thermal anemometer probes with single, double, and triple sensors to measure (*a*) one-, (*b*) two-, and (*c*) three-dimensional velocity components simultaneously.
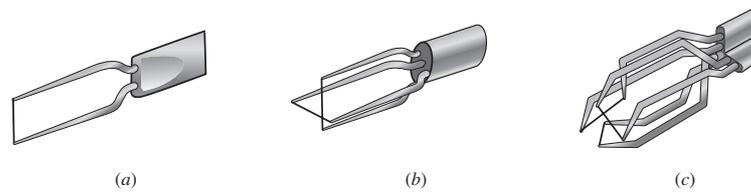
temperature by varying the electric current (which is done by varying the voltage) as needed. The higher the flow velocity, the higher the rate of heat transfer from the sensor, and thus the larger the voltage that needs to be applied across the sensor to maintain it at constant temperature. There is a close correlation between the flow velocity and voltage, and the flow velocity can be determined by measuring the voltage applied by an amplifier or the electric current passing through the sensor.

The sensor is maintained at a constant temperature during operation, and thus its thermal energy content remains constant. The conservation of energy principle requires that the electrical Joule heating $\dot{W}_{elect} = I^2 R_w = E^2/R_w$ of the sensor must be equal to the total rate of heat loss from the sensor $\dot{Q}_{total}$, which consists of convection heat transfer since conduction to the wire supports and radiation to the surrounding surfaces are small and can be disregarded. Using proper relations for forced convection, the energy balance can be expressed by **King's law** as

$$E^2 = a + bV^n \tag{8–75}$$

where E is the voltage, and the values of the constants a, b, and n are calibrated for a given probe. Once the voltage is measured, this relation gives the flow velocity V directly.

Most hot-wire sensors have a diameter of 5 μm and a length of approximately 1 mm and are made of tungsten. The wire is spot-welded to needle-shaped prongs embedded in a probe body, which is connected to the anemometer electronics. Thermal anemometers can be used to measure two- or three-dimensional velocity components simultaneously by using probes with two or three sensors, respectively (Fig. 8–73). When selecting probes, consideration should be given to the type and the contamination level of the fluid, the number of velocity components to be measured, the required spatial and temporal resolution, and the location of measurement.

Laser Doppler Velocimetry

Laser Doppler velocimetry (LDV), also called **laser velocimetry (LV)** or **laser Doppler anemometry (LDA),** is an optical technique to measure flow velocity at any desired point without disturbing the flow. Unlike thermal anemometry, LDV involves no probes or wires inserted into the flow, and thus it is a nonintrusive method. Like thermal anemometry, it can accurately measure velocity at a very small volume, and thus it can also be used to study the details of flow at a locality, including turbulent fluctuations, and it can be traversed through the entire flow field without intrusion.

The LDV technique was developed in the mid-1960s and has found widespread acceptance because of the high accuracy it provides for both gas and

liquid flows; the high spatial resolution it offers; and, in recent years, its ability to measure all three velocity components. Its drawbacks are the relatively high cost; the requirement for sufficient transparency between the laser source, the target location in the flow, and the photodetector; and the requirement for careful alignment of emitted and reflected beams for accuracy. The latter drawback is eliminated for the case of a fiber-optic LDV system, since it is aligned at the factory.

The operating principle of LDV is based on sending a highly coherent monochromatic (all waves are in phase and at the same wavelength) light beam toward the target, collecting the light reflected by small particles in the target area, determining the change in frequency of the reflected radiation due to the Doppler effect, and relating this frequency shift to the flow velocity of the fluid at the target area.

LDV systems are available in many different configurations. A basic dual-beam LDV system to measure a single velocity component is shown in Fig. 8–74. In the heart of all LDV systems is a laser power source, which is usually a helium–neon or argon-ion laser with a power output of 10 mW to 20 W. Lasers are preferred over other light sources since laser beams are highly coherent and highly focused. The helium–neon laser, for example, emits radiation at a wavelength of 0.6328 μm, which is in the reddish-orange color range. The laser beam is first split into two parallel beams of equal intensity by a half-silvered mirror called a *beam splitter*. Both beams then pass through a converging lens that focuses the beams at a point in the flow (the *target*). The small fluid volume where the two beams intersect is the region where the velocity is measured and is called the *measurement volume* or the *focal volume*. The measurement volume resembles an ellipsoid, typically of 0.1 mm diameter and 0.5 mm in length. The laser light is scattered by particles passing through this measurement volume, and the light scattered in a certain direction is collected by a receiving lens and is passed through a photodetector that converts the fluctuations in light intensity into fluctuations in a voltage signal. Finally, a signal processor determines the frequency of the voltage signal and thus the velocity of the flow.

The waves of the two laser beams that cross in the measurement volume are shown schematically in Fig. 8–75. The waves of the two beams interfere in the measurement volume, creating a bright fringe where they are in phase and thus support each other, and creating a dark fringe where they are out of phase and thus cancel each other. The bright and dark fringes form lines
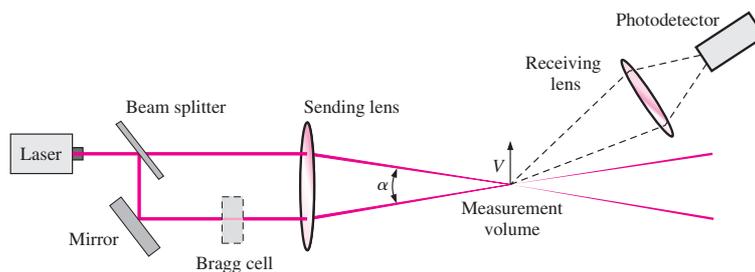
FIGURE 8–74
A dual-beam LDV system in forward scatter mode.
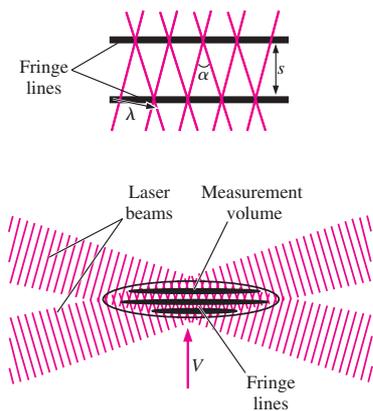
FIGURE 8–75
Fringes that form as a result of the interference at the intersection of two laser beams of an LDV system (lines represent peaks of waves). The top diagram is a close-up view of two fringes.
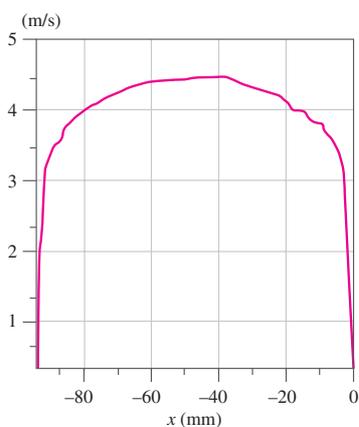
FIGURE 8–76
A time-averaged velocity profile in turbulent pipe flow obtained by an LDV system.
*Courtesy Dantec Dynamics, Inc.
www.dantecmt.com. Used by permission.*

parallel to the midplane between the two incident laser beams. Using trigonometry, the spacing s between the fringe lines, which can be viewed as the wavelength of fringes, can be shown to be $s = \lambda/[2 \sin(\alpha/2)]$, where λ is the wavelength of the laser beam and α is the angle between the two laser beams. When a particle traverses these fringe lines at velocity V, the frequency of the scattered fringe lines is

$$f = \frac{V}{s} = \frac{2V \sin(\alpha/2)}{\lambda} \tag{8–76}$$

This fundamental relation shows the flow velocity to be proportional to the frequency and is known as the LDV equation. As a particle passes through the measurement volume, the reflected light is bright, then dark, then bright, etc., because of the fringe pattern, and the flow velocity is determined by measuring the frequency of the reflected light. The velocity profile at a cross section of a pipe can be obtained by mapping the flow across the pipe (Fig. 8–76).

The LDV method obviously depends on the presence of scattered fringe lines, and thus the flow must contain a sufficient amount of small particles called *seeds* or *seeding particles.* These particles must be small enough to follow the flow closely so that the particle velocity is equal to the flow velocity, but large enough (relative to the wavelength of the laser light) to scatter an adequate amount of light. Particles with a diameter of 1 μm usually serve the purpose well. Some fluids such as tap water naturally contain an adequate amount of such particles, and no seeding is necessary. Gases such as air are commonly seeded with smoke or with particles made of latex, oil, or other materials. By using three laser beam pairs at different wavelengths, the LDV system is also used to obtain all three velocity components at any point in the flow.

Particle Image Velocimetry

Particle image velocimetry (PIV) is a double-pulsed laser technique used to measure the instantaneous velocity distribution in a plane of flow by photographically determining the displacement of particles in the plane during a very short time interval. Unlike methods like hot-wire anemometry and LDV that measure velocity at a point, PIV provides velocity values simultaneously throughout an entire cross section, and thus it is a whole-field technique. PIV combines the accuracy of LDV with the capability of flow visualization and provides instantaneous flow field mapping. The entire instantaneous velocity profile at a cross section of pipe, for example, can be obtained with a single PIV measurement. A PIV system can be viewed as a camera that can take a snapshot of velocity distribution at any desired plane in a flow. Ordinary flow visualization gives a qualitative picture of the details of flow. PIV also provides an accurate *quantitative* description of various flow quantities such as the velocity field, and thus the capability to analyze the flow numerically using the velocity data provided. Because of its whole-field capability, PIV is also used to validate computational fluid dynamics (CFD) codes (Chap. 15).

The PIV technique has been used since the mid-1980s, and its use and capabilities have grown in recent years with improvements in frame grabber

and charge-coupled device (CCD) camera technologies. The accuracy, flexibility, and versatility of PIV systems with their ability to capture whole-field images with submicrosecond exposure time have made them extremely valuable tools in the study of supersonic flows, explosions, flame propagation, bubble growth and collapse, turbulence, and unsteady flow.

The PIV technique for velocity measurement consists of two main steps: visualization and image processing. The first step is to seed the flow with suitable particles in order to trace the fluid motion. Then a pulse of laser light sheet illuminates a thin slice of the flow field at the desired plane, and the positions of particles in that plane are determined by detecting the light scattered by particles on a digital video or photographic camera positioned at right angles to the light sheet (Fig. 8–77). After a very short time period Δt (typically in μs), the particles are illuminated again by a second pulse of laser light sheet, and their new positions are recorded. Using the information on these two superimposed camera images, the particle displacements Δs are determined for all particles, and the magnitude of velocity of the particles in the plane of the laser light sheet is determined from $\Delta s/\Delta t$. The direction of motion of the particles is also determined from the two positions, so that two components of velocity in the plane are calculated. The built-in algorithms of PIV systems determine the velocities at thousands of area elements called *interrogation regions* throughout the entire plane and display the velocity field on the computer monitor in any desired form (Fig. 8–78).

The PIV technique relies on the laser light scattered by particles, and thus the flow must be seeded if necessary with particles, also called *markers,* in order to obtain an adequate reflected signal. Seed particles must be able to follow the pathlines in the flow for their motion to be representative of the
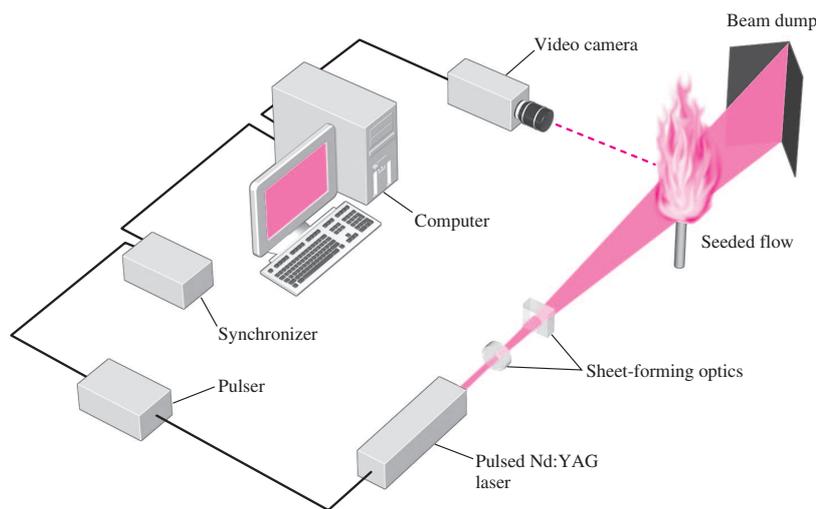
FIGURE 8–77
A PIV system to study flame stabilization.
Courtesy of TSI Incorporated (www.tsi.com).
Used by permission.

FIGURE 8–78

Instantaneous velocity field in the wake region of a car as measured by a PIV system in a wind tunnel. The velocity vectors are superimposed on a contour plot of pressure. The interface between two adjacent gray-scale levels is an isobar.

Courtesy Dantec Dynamics, Inc.
www.dantecmt.com.
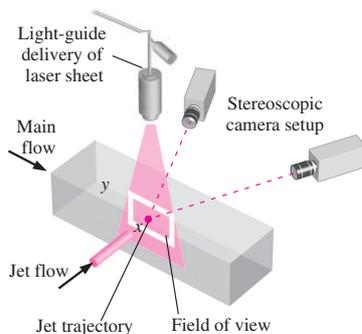
FIGURE 8–79

A three-dimensional PIV system set up to study the mixing of an air jet with cross duct flow.

Courtesy TSI Incorporated (www.tsi.com).
Used by permission.

flow, and this requires the particle density to be equal to the fluid density (so that they are neutrally buoyant) or the particles to be so small (typically μm-sized) that their movement relative to the fluid is insignificant. A variety of such particles is available to seed gas or liquid flow. Very small particles must be used in high-speed flows. Silicon carbide particles (mean diameter of 1.5 μm) are suitable for both liquid and gas flow, titanium dioxide particles (mean diameter of 0.2 μm) are usually used for gas flow and are suitable for high-temperature applications, and polystyrene latex particles (nominal diameter of 1.0 μm) are suitable for low-temperature applications. Metallic-coated particles (mean diameter of 9.0 μm) are also used to seed water flows for LDV measurements because of their high reflectivity. Gas bubbles as well as droplets of some liquids such as olive oil or silicon oil are also used as seeding particles after they are atomized to μm-sized spheres.

A variety of laser light sources such as argon, copper vapor, and Nd:YAG can be used with PIV systems, depending on the requirements for pulse duration, power, and time between pulses. Nd:YAG lasers are commonly used in PIV systems over a wide range of applications. A beam delivery system such as a light arm or a fiber-optic system is used to generate and deliver a high-energy pulsed laser sheet at a specified thickness.

With PIV, other flow properties such as vorticity and strain rates can also be obtained, and the details of turbulence can be studied. Recent advances in PIV technology have made it possible to obtain three-dimensional velocity profiles at a cross section of a flow using two cameras (Fig. 8–79). This is done by recording the images of the target plane simultaneously by both cameras at different angles, processing the information to produce two separate two-dimensional velocity maps, and combining these two maps to generate the instantaneous three-dimensional velocity field.

APPLICATION SPOTLIGHT ■ How Orifice Plate Flowmeters Work, or Do Not Work

Guest Author: Lorenz Sigurdson, Vortex Fluid Dynamics Lab, University of Alberta

The Bernoulli equation is the most beloved of all fluid mechanical equations because it is a scalar equation and has a vast range of applications. One very valuable use is in the development of Bernoulli obstruction theory. This theory allows an estimate of the flow velocity from the measured pressure drop between locations upstream and downstream of an obstruction in a pipe flow. The volume flow rate can be calculated by using the Bernoulli equation, conservation of mass, and the obstruction geometry. The cheapest obstruction to produce is a plate with a circular orifice in it. There are hundreds of thousands of orifice plate flowmeters in use in North America. It is the accepted international standard of measurement of volume flow rates. The accuracy can become very important in industries such as natural gas pipelining where the commodity is bought and sold based on measurements from these meters. Some pipes carry more than a million dollars per hour of natural gas.

For practical purposes, meter calibration is required because, although the pipe and orifice diameter may be known, the flow separates from the lip of the orifice and creates a flow tube narrower than the orifice diameter. The flow is accelerated through this vena contracta. Figure 8–80 shows the flow downstream of the orifice visualized by using a smoke-wire to introduce streaklines in a transparent flowmeter. The calibration assumes that there is no pulsation in the pipe flow. However, this is not the case in practice if there is a reciprocating compressor in the pipeline, or a loose flapping valve. Figure 8–81 shows what can happen to the vena contracta in this circumstance, if the frequency of the pulsation is near a resonance frequency of the turbulent flow structures. The vena contracta diameter is reduced. Stop reading and ask yourself, "Will this cause a flow rate underprediction or overprediction?"

Conservation of mass and the narrower vena contracta mean a higher average velocity there than without pulsation. The Bernoulli equation says that the pressure will be lower there as a result, meaning a larger pressure drop and an overprediction. Errors as high as 40 percent have been found at high pulsation levels. For the natural gas pipeline mentioned, that could mean paying (or earning) $400,000 too much per hour! Characteristic instabilities that have previously been found in shear flows, jet flows, and reattaching flows (Sigurdson, 1995; Sigurdson and Chapple, 1997) also exist downstream of the orifice plate. Thankfully, meter installation designers can now avoid the dangerously resonant pulsation frequencies associated with these instabilities, thereby minimizing flowmeter error.

References

Sigurdson, L. W., "The Structure and Control of a Turbulent Reattaching Flow," *J. Fluid Mechanics*, 298, pp. 139–165, 1995.

Sigurdson, L. W., and Chapple, D., "Visualization of Acoustically Pulsated Flow through an Orifice Plate Flow Meter," *Proc. 1st Pacific Image Processing and Flow Visualization Conf.*, Honolulu, HI, February 23–26, 1997.

Sigurdson, L. W., and Chapple, D., "A Turbulent Mechanism for Pulsation—Induced Orifice Plate Flow Meter Error," *Proc. 13th Australasian Fluid Mechanics Conf.*, December 13–18, 1998, Monash U., Melbourne, Australia, Thompson, M.C., and Hourigan, K., eds., 1, pp. 67–70, 1998.
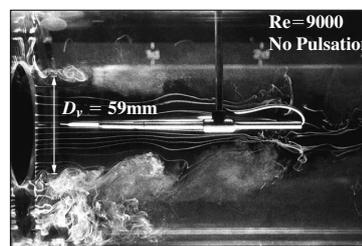
FIGURE 8–80

Smoke-wire streakline photograph of orifice plate flowmeter with no pulsation present, Reynolds number = 9000. D_v indicates the estimated vena contracta diameter. A hot-wire probe can be seen along the pipe centerline.

From Sigurdson and Chapple (1998).
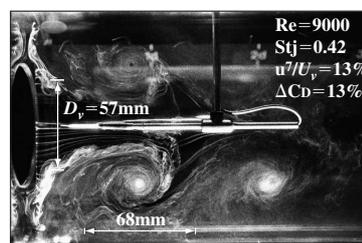
FIGURE 8–81

Smoke-wire streakline photograph of orifice plate flowmeter with pulsation present, showing a large effect. The meter is in error by 13%. Reynolds number = 9000. The vena contracta diameter D_v is reduced from the no pulsation case of Fig. 8–80.

From Sigurdson and Chapple (1998).

SUMMARY

In *internal flow*, a pipe is completely filled with a fluid. *Laminar flow* is characterized by smooth streamlines and highly ordered motion, and *turbulent flow* is characterized by velocity fluctuations and highly disordered motion. The *Reynolds number* is defined as

$$\text{Re} = \frac{\text{Inertial forces}}{\text{Viscous forces}} = \frac{V_{avg}D}{\nu} = \frac{\rho V_{avg}D}{\mu}$$

Under most practical conditions, the flow in a pipe is laminar at $\text{Re} < 2300$, turbulent at $\text{Re} > 4000$, and transitional in between.

The region of the flow in which the effects of the viscous shearing forces are felt is called the *velocity boundary layer*. The region from the pipe inlet to the point at which the boundary layer merges at the centerline is called the *hydrodynamic entrance region*, and the length of this region is called the *hydrodynamic entry length* L_h. It is given by

$$L_{h,\,laminar} \cong 0.05\ \text{Re}\ D \quad \text{and} \quad L_{h,\,turbulent} \cong 10D$$

The friction coefficient in the fully developed flow region remains constant. The *maximum* and *average* velocities in fully developed laminar flow in a circular pipe are

$$u_{max} = 2V_{avg} \quad \text{and} \quad V_{avg} = \frac{\Delta P D^2}{32\mu L}$$

The *volume flow rate* and the *pressure drop* for laminar flow in a horizontal pipe are

$$\dot{V} = V_{avg} A_c = \frac{\Delta P \pi D^4}{128\mu L} \quad \text{and} \quad \Delta P = \frac{32\mu L V_{avg}}{D^2}$$

These results for horizontal pipes can also be used for inclined pipes provided that ΔP is replaced by $\Delta P - \rho g L \sin\theta$,

$$V_{avg} = \frac{(\Delta P - \rho g L \sin\theta)D^2}{32\mu L} \quad \text{and}$$

$$\dot{V} = \frac{(\Delta P - \rho g L \sin\theta)\pi D^4}{128\mu L}$$

The *pressure loss* and *head loss* for all types of internal flows (laminar or turbulent, in circular or noncircular pipes, smooth or rough surfaces) are expressed as

$$\Delta P_L = f\frac{L}{D}\frac{\rho V^2}{2} \quad \text{and} \quad h_L = \frac{\Delta P_L}{\rho g} = f\frac{L}{D}\frac{V^2}{2g}$$

where $\rho V^2/2$ is the *dynamic pressure* and the dimensionless quantity f is the *friction factor*. For fully developed laminar flow in a circular pipe, the friction factor is $f = 64/\text{Re}$.

For noncircular pipes, the diameter in the previous relations is replaced by the *hydraulic diameter* defined as $D_h = 4A_c/p$, where A_c is the cross-sectional area of the pipe and p is its wetted perimeter.

In fully developed turbulent flow, the friction factor depends on the Reynolds number and the *relative roughness* ε/D. The friction factor in turbulent flow is given by the *Colebrook equation*, expressed as

$$\frac{1}{\sqrt{f}} = -2.0\log\left(\frac{\varepsilon/D}{3.7} + \frac{2.51}{\text{Re}\sqrt{f}}\right)$$

The plot of this formula is known as the Moody chart. The design and analysis of piping systems involve the determination of the head loss, flow rate, or the pipe diameter. Tedious iterations in these calculations can be avoided by the approximate Swamee–Jain formulas expressed as

$$h_L = 1.07\frac{\dot{V}^2 L}{gD^5}\left\{\ln\left[\frac{\varepsilon}{3.7D} + 4.62\left(\frac{\nu D}{\dot{V}}\right)^{0.9}\right]\right\}^{-2}$$

$$10^{-6} < \varepsilon/D < 10^{-2}$$
$$3000 < \text{Re} < 3\times 10^8$$

$$\dot{V} = -0.965\left(\frac{gD^5 h_L}{L}\right)^{0.5}\ln\left[\frac{\varepsilon}{3.7D} + \left(\frac{3.17\nu^2 L}{gD^3 h_L}\right)^{0.5}\right]$$

$$\text{Re} > 2000$$

$$D = 0.66\left[\varepsilon^{1.25}\left(\frac{L\dot{V}^2}{gh_L}\right)^{4.75} + \nu\dot{V}^{9.4}\left(\frac{L}{gh_L}\right)^{5.2}\right]^{0.04}$$

$$10^{-6} < \varepsilon/D < 10^{-2}$$
$$5000 < \text{Re} < 3\times 10^8$$

The losses that occur in piping components such as fittings, valves, bends, elbows, tees, inlets, exits, enlargements, and contractions are called *minor losses*. The minor losses are usually expressed in terms of the *loss coefficient* K_L. The head loss for a component is determined from

$$h_L = K_L\frac{V^2}{2g}$$

When all the loss coefficients are available, the total head loss in a piping system is determined from

$$h_{L,\,total} = h_{L,\,major} + h_{L,\,minor} = \sum_i f_i\frac{L_i}{D_i}\frac{V_i^2}{2g} + \sum_j K_{L,j}\frac{V_j^2}{2g}$$

If the entire piping system has a constant diameter, the total head loss reduces to

$$h_{L,\,total} = \left(f\frac{L}{D} + \sum K_L\right)\frac{V^2}{2g}$$

The analysis of a piping system is based on two simple principles: (1) The conservation of mass throughout the system must be satisfied and (2) the pressure drop between two points must be the same for all paths between the two points.

When the pipes are connected *in series*, the flow rate through the entire system remains constant regardless of the diameters of the individual pipes. For a pipe that branches out into two (or more) *parallel pipes* and then rejoins at a junction downstream, the total flow rate is the sum of the flow rates in the individual pipes but the head loss in each branch is the same.

When a piping system involves a pump and/or turbine, the steady-flow energy equation is expressed as

$$\frac{P_1}{\rho g} + \alpha_1 \frac{V_1^2}{2g} + z_1 + h_{pump,\, u}$$

$$= \frac{P_2}{\rho g} + \alpha_2 \frac{V_2^2}{2g} + z_2 + h_{turbine,\, e} + h_L$$

When the useful pump head $h_{pump,\, u}$ is known, the mechanical power that needs to be supplied by the pump to the fluid and the electric power consumed by the motor of the pump for a specified flow rate are determined from

$$\dot{W}_{pump,\, shaft} = \frac{\rho \dot{V} g h_{pump,\, u}}{\eta_{pump}} \quad \text{and} \quad \dot{W}_{elect} = \frac{\rho \dot{V} g h_{pump,\, u}}{\eta_{pump-motor}}$$

where $\eta_{pump-motor}$ is the *efficiency of the pump–motor combination,* which is the product of the pump and the motor efficiencies.

The plot of the head loss versus the flow rate $\dot{V}$ is called the *system curve.* The head produced by a pump is not a constant, and the curves of $h_{pump,\, u}$ and η_{pump} versus $\dot{V}$ are called the *characteristic curves.* A pump installed in a piping system operates at the *operating point*, which is the point of intersection of the system curve and the characteristic curve.

Flow measurement techniques and devices can be considered in three major categories: (1) volume (or mass) flow rate measurement techniques and devices such as obstruction flowmeters, turbine meters, positive displacement flowmeters, rotameters, and ultrasonic meters; (2) point velocity measurement techniques such as the Pitot-static probes, hot-wires, and LDV; and (3) whole-field velocity measurement techniques such as PIV.

The emphasis in this chapter has been on flow through pipes. A detailed treatment of numerous types of pumps and turbines, including their operation principles and performance parameters, is given in Chap. 14.

REFERENCES AND SUGGESTED READING

1. H. S. Bean (ed.). *Fluid Meters: Their Theory and Applications*, 6th ed. New York: American Society of Mechanical Engineers, 1971.

2. M. S. Bhatti and R. K. Shah. "Turbulent and Transition Flow Convective Heat Transfer in Ducts." In *Handbook of Single-Phase Convective Heat Transfer*, ed. S. Kakaç, R. K. Shah, and W. Aung. New York: Wiley Interscience, 1987.

3. C. F. Colebrook. "Turbulent Flow in Pipes, with Particular Reference to the Transition between the Smooth and Rough Pipe Laws," *Journal of the Institute of Civil Engineers London.* 11 (1939), pp. 133–156.

4. C. T. Crowe, J. A. Roberson, and D. F. Elger. *Engineering Fluid Mechanics*, 7th ed. New York: Wiley, 2001.

5. F. Durst, A. Melling, and J. H. Whitelaw. *Principles and Practice of Laser-Doppler Anemometry*, 2nd ed. New York: Academic, 1981.

6. R. W. Fox and A. T. McDonald. *Introduction to Fluid Mechanics*, 5th ed. New York: Wiley, 1999.

7. *Fundamentals of Orifice Meter Measurement*. Houston, TX: Daniel Measurement and Control, 1997.

8. S. E. Haaland. "Simple and Explicit Formulas for the Friction Factor in Turbulent Pipe Flow," *Journal of Fluids Engineering*, March 1983, pp. 89–90.

9. I. E. Idelchik. *Handbook of Hydraulic Resistance*, 3rd ed. Boca Raton, FL: CRC Press, 1993.

10. W. M. Kays and M. E. Crawford. *Convective Heat and Mass Transfer*, 3rd ed. New York: McGraw-Hill, 1993.

11. R. W. Miller. *Flow Measurement Engineering Handbook,* 3rd ed. New York: McGraw-Hill, 1997.

12. L. F. Moody. "Friction Factors for Pipe Flows," *Transactions of the ASME* 66 (1944), pp. 671–684.

13. B. R. Munson, D. F. Young, and T. Okiishi. *Fundamentals of Fluid Mechanics*, 4th ed. New York: Wiley, 2002.

14. O. Reynolds. "On the Experimental Investigation of the Circumstances Which Determine Whether the Motion of Water Shall Be Direct or Sinuous, and the Law of Resistance in Parallel Channels." *Philosophical Transactions of the Royal Society of London*, 174 (1883), pp. 935–982.

15. H. Schlichting. *Boundary Layer Theory*, 7th ed. New York: McGraw-Hill, 1979.

16. R. K. Shah and M. S. Bhatti. "Laminar Convective Heat Transfer in Ducts." In *Handbook of Single-Phase Convective Heat Transfer*, ed. S. Kakaç, R. K. Shah, and W. Aung. New York: Wiley Interscience, 1987.

17. P. L. Skousen. *Valve Handbook*. New York: McGraw-Hill, 1998.

18. P. K. Swamee and A. K. Jain. "Explicit Equations for Pipe-Flow Problems," *Journal of the Hydraulics Division. ASCE* 102, no. HY5 (May 1976), pp. 657–664.

19. G. Vass. "Ultrasonic Flowmeter Basics," *Sensors*, 14, no. 10 (1997).

20. A. J. Wheeler and A. R. Ganji. *Introduction to Engineering Experimentation*. Englewood Cliffs, NJ: Prentice-Hall, 1996.

21. F. M. White. *Fluid Mechanics*, 5th ed. New York: McGraw-Hill, 2003.

22. W. Zhi-qing. "Study on Correction Coefficients of Laminar and Turbulent Entrance Region Effects in Round Pipes," *Applied Mathematical Mechanics*, 3 (1982), p. 433.

PROBLEMS*

Laminar and Turbulent Flow

8–1C Why are liquids usually transported in circular pipes?

8–2C What is the physical significance of the Reynolds number? How is it defined for (*a*) flow in a circular pipe of inner diameter D and (*b*) flow in a rectangular duct of cross section $a \times b$?
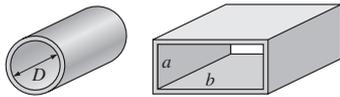
FIGURE P8–2C

8–3C Consider a person walking first in air and then in water at the same speed. For which motion will the Reynolds number be higher?

8–4C Show that the Reynolds number for flow in a circular pipe of diameter D can be expressed as Re = $4\dot{m}/(\pi D\mu)$.

8–5C Which fluid at room temperature requires a larger pump to flow at a specified velocity in a given pipe: water or engine oil? Why?

8–6C What is the generally accepted value of the Reynolds number above which the flow in smooth pipes is turbulent?

8–7C Consider the flow of air and water in pipes of the same diameter, at the same temperature, and at the same mean velocity. Which flow is more likely to be turbulent? Why?

8–8C What is hydraulic diameter? How is it defined? What is it equal to for a circular pipe of diameter D?

8–9C How is the hydrodynamic entry length defined for flow in a pipe? Is the entry length longer in laminar or turbulent flow?

---

* Problems designated by a "C" are concept questions, and students are encouraged to answer them all. Problems designated by an "E" are in English units, and the SI users can ignore them. Problems with the ⊛ icon are solved using EES, and complete solutions together with parametric studies are included on the enclosed DVD. Problems with the 🖳 icon are comprehensive in nature and are intended to be solved with a computer, preferably using the EES software that accompanies this text.

8–10C Consider laminar flow in a circular pipe. Will the wall shear stress τ_w be higher near the inlet of the pipe or near the exit? Why? What would your response be if the flow were turbulent?

8–11C How does surface roughness affect the pressure drop in a pipe if the flow is turbulent? What would your response be if the flow were laminar?

Fully Developed Flow in Pipes

8–12C How does the wall shear stress τ_w vary along the flow direction in the fully developed region in (*a*) laminar flow and (*b*) turbulent flow?

8–13C What fluid property is responsible for the development of the velocity boundary layer? For what kinds of fluids will there be no velocity boundary layer in a pipe?

8–14C In the fully developed region of flow in a circular pipe, will the velocity profile change in the flow direction?

8–15C How is the friction factor for flow in a pipe related to the pressure loss? How is the pressure loss related to the pumping power requirement for a given mass flow rate?

8–16C Someone claims that the shear stress at the center of a circular pipe during fully developed laminar flow is zero. Do you agree with this claim? Explain.

8–17C Someone claims that in fully developed turbulent flow in a pipe, the shear stress is a maximum at the pipe surface. Do you agree with this claim? Explain.

8–18C Consider fully developed flow in a circular pipe with negligible entrance effects. If the length of the pipe is doubled, the head loss will (*a*) double, (*b*) more than double, (*c*) less than double, (*d*) reduce by half, or (*e*) remain constant.

8–19C Someone claims that the volume flow rate in a circular pipe with laminar flow can be determined by measuring the velocity at the centerline in the fully developed region, multiplying it by the cross-sectional area, and dividing the result by 2. Do you agree? Explain.

8–20C Someone claims that the average velocity in a circular pipe in fully developed laminar flow can be determined by simply measuring the velocity at $R/2$ (midway between the wall surface and the centerline). Do you agree? Explain.

8–21C Consider fully developed laminar flow in a circular pipe. If the diameter of the pipe is reduced by half while the flow rate and the pipe length are held constant, the head loss will (a) double, (b) triple, (c) quadruple, (d) increase by a factor of 8, or (e) increase by a factor of 16.

8–22C What is the physical mechanism that causes the friction factor to be higher in turbulent flow?

8–23C What is turbulent viscosity? What is it caused by?

8–24C The head loss for a certain circular pipe is given by $h_L = 0.0826fL(\dot{V}^2/D^5)$, where f is the friction factor (dimensionless), L is the pipe length, $\dot{V}$ is the volumetric flow rate, and D is the pipe diameter. Determine if the 0.0826 is a dimensional or dimensionless constant. Is this equation dimensionally homogeneous as it stands?

8–25C Consider fully developed laminar flow in a circular pipe. If the viscosity of the fluid is reduced by half by heating while the flow rate is held constant, how will the head loss change?

8–26C How is head loss related to pressure loss? For a given fluid, explain how you would convert head loss to pressure loss.

8–27C Consider laminar flow of air in a circular pipe with perfectly smooth surfaces. Do you think the friction factor for this flow will be zero? Explain.

8–28C Explain why the friction factor is independent of the Reynolds number at very large Reynolds numbers.

8–29E Oil at 80°F ($\rho = 56.8$ lbm/ft^3 and $\mu = 0.0278$ lbm/ft · s) is flowing steadily in a 0.5-in-diameter, 120-ft-long pipe. During the flow, the pressure at the pipe inlet and exit is measured to be 120 psi and 14 psi, respectively. Determine the flow rate of oil through the pipe assuming the pipe is (a) horizontal, (b) inclined 20° upward, and (c) inclined 20° downward.

8–30 Oil with a density of 850 kg/m^3 and kinematic viscosity of 0.00062 m^2/s is being discharged by a 5-mm-diameter, 40-m-long horizontal pipe from a storage tank open to the atmosphere. The height of the liquid level above the center of the pipe is 3 m. Disregarding the minor losses, determine the flow rate of oil through the pipe.
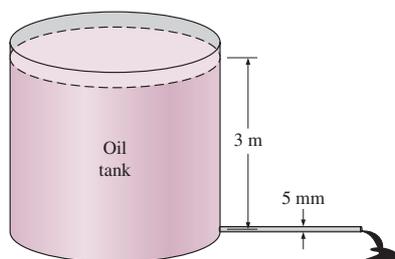
FIGURE P8–30

8–31 Water at 10°C ($\rho = 999.7$ kg/m^3 and $\mu = 1.307 \times 10^{-3}$ kg/m · s) is flowing steadily in a 0.20-cm-diameter, 15-m-long pipe at an average velocity of 1.2 m/s. Determine (a) the pressure drop, (b) the head loss, and (c) the pumping power requirement to overcome this pressure drop. *Answers: (a) 188 kPa, (b) 19.2 m, (c) 0.71 W*

8–32 Water at 15°C ($\rho = 999.1$ kg/m^3 and $\mu = 1.138 \times 10^{-3}$ kg/m · s) is flowing steadily in a 30-m-long and 4-cm-diameter horizontal pipe made of stainless steel at a rate of 8 L/s. Determine (a) the pressure drop, (b) the head loss, and (c) the pumping power requirement to overcome this pressure drop.
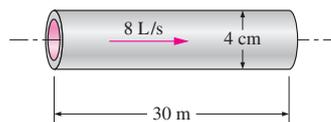
FIGURE P8–32

8–33E Heated air at 1 atm and 100°F is to be transported in a 400-ft-long circular plastic duct at a rate of 12 ft^3/s. If the head loss in the pipe is not to exceed 50 ft, determine the minimum diameter of the duct.

8–34 In fully developed laminar flow in a circular pipe, the velocity at $R/2$ (midway between the wall surface and the centerline) is measured to be 6 m/s. Determine the velocity at the center of the pipe. *Answer: 8 m/s*

8–35 The velocity profile in fully developed laminar flow in a circular pipe of inner radius $R = 2$ cm, in m/s, is given by $u(r) = 4(1 - r^2/R^2)$. Determine the average and maximum velocities in the pipe and the volume flow rate.
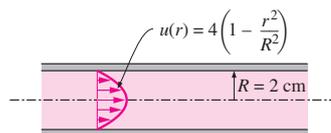
FIGURE P8–35

8–36 Repeat Prob. 8–35 for a pipe of inner radius 7 cm.

8–37 Consider an air solar collector that is 1 m wide and 5 m long and has a constant spacing of 3 cm between the glass cover and the collector plate. Air flows at an average temperature of 45°C at a rate of 0.15 m^3/s through the 1-m-wide edge of the collector along the 5-m-long passageway. Disregarding the entrance and roughness effects, determine the pressure drop in the collector. *Answer: 29 Pa*
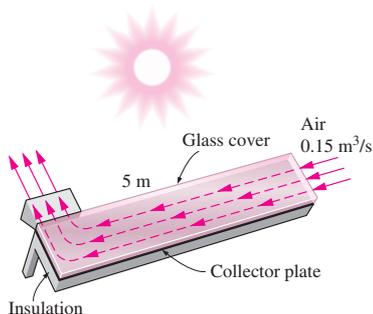
FIGURE P8–37

8–38 Consider the flow of oil with $\rho = 894$ kg/m^3 and $\mu = 2.33$ kg/m · s in a 40-cm-diameter pipeline at an average velocity of 0.5 m/s. A 300-m-long section of the pipeline passes through the icy waters of a lake. Disregarding the entrance effects, determine the pumping power required to overcome the pressure losses and to maintain the flow of oil in the pipe.

8–39 Consider laminar flow of a fluid through a square channel with smooth surfaces. Now the average velocity of the fluid is doubled. Determine the change in the head loss of the fluid. Assume the flow regime remains unchanged.

8–40 Repeat Prob. 8–39 for turbulent flow in smooth pipes for which the friction factor is given as $f = 0.184\text{Re}^{-0.2}$. What would your answer be for fully turbulent flow in a rough pipe?

8–41 Air enters a 7-m-long section of a rectangular duct of cross section 15 cm × 20 cm made of commercial steel at 1 atm and 35°C at an average velocity of 7 m/s. Disregarding the entrance effects, determine the fan power needed to overcome the pressure losses in this section of the duct. *Answer:* 4.9 W
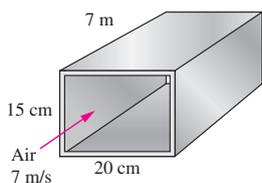
FIGURE P8–41

8–42E Water at 60°F passes through 0.75-in-internal-diameter copper tubes at a rate of 1.2 lbm/s. Determine the pumping power per ft of pipe length required to maintain this flow at the specified rate.

8–43 Oil with $\rho = 876$ kg/m^3 and $\mu = 0.24$ kg/m · s is flowing through a 1.5-cm-diameter pipe that discharges into the

atmosphere at 88 kPa. The absolute pressure 15 m before the exit is measured to be 135 kPa. Determine the flow rate of oil through the pipe if the pipe is (*a*) horizontal, (*b*) inclined 8° upward from the horizontal, and (*c*) inclined 8° downward from the horizontal.
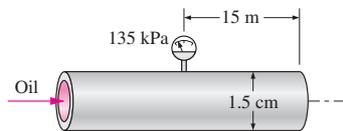
FIGURE P8–43

8–44 Glycerin at 40°C with $\rho = 1252$ kg/m^3 and $\mu = 0.27$ kg/m · s is flowing through a 2-cm-diameter, 25-m-long pipe that discharges into the atmosphere at 100 kPa. The flow rate through the pipe is 0.035 L/s. (*a*) Determine the absolute pressure 25 m before the pipe exit. (*b*) At what angle θ must the pipe be inclined downward from the horizontal for the pressure in the entire pipe to be atmospheric pressure and the flow rate to be maintained the same?

8–45 In an air heating system, heated air at 40°C and 105 kPa absolute is distributed through a 0.2 m × 0.3 m rectangular duct made of commercial steel at a rate of 0.5 m^3/s. Determine the pressure drop and head loss through a 40-m-long section of the duct. *Answers:* 128 Pa, 93.8 m

8–46 Glycerin at 40°C with $\rho = 1252$ kg/m^3 and $\mu = 0.27$ kg/m · s is flowing through a 5-cm-diameter horizontal smooth pipe with an average velocity of 3.5 m/s. Determine the pressure drop per 10 m of the pipe.

8–47 Reconsider Prob. 8–46. Using EES (or other) software, investigate the effect of the pipe diameter on the pressure drop for the same constant flow rate. Let the pipe diameter vary from 1 to 10 cm in increments of 1 cm. Tabulate and plot the results, and draw conclusions.

8–48E Air at 1 atm and 60°F is flowing through a 1 ft × 1 ft square duct made of commercial steel at a rate of 1200 cfm. Determine the pressure drop and head loss per ft of the duct.
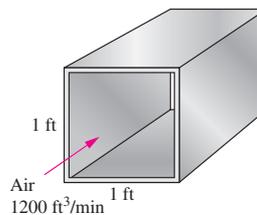
FIGURE P8–48E

8–49 Liquid ammonia at −20°C is flowing through a 30-m-long section of a 5-mm-diameter copper tube at a rate of

0.15 kg/s. Determine the pressure drop, the head loss, and the pumping power required to overcome the frictional losses in the tube. *Answers: 4792 kPa, 743 m, 1.08 kW*

8–50 Shell-and-tube heat exchangers with hundreds of tubes housed in a shell are commonly used in practice for heat transfer between two fluids. Such a heat exchanger used in an active solar hot-water system transfers heat from a water-antifreeze solution flowing through the shell and the solar collector to fresh water flowing through the tubes at an average temperature of 60°C at a rate of 15 L/s. The heat exchanger contains 80 brass tubes 1 cm in inner diameter and 1.5 m in length. Disregarding inlet, exit, and header losses, determine the pressure drop across a single tube and the pumping power required by the tube-side fluid of the heat exchanger.

After operating a long time, 1-mm-thick scale builds up on the inner surfaces with an equivalent roughness of 0.4 mm. For the same pumping power input, determine the percent reduction in the flow rate of water through the tubes.
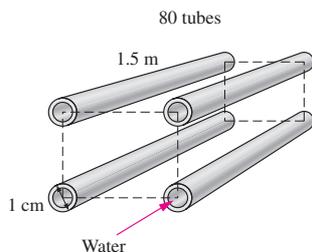
FIGURE P8–50

Minor Losses

8–51C What is minor loss in pipe flow? How is the minor loss coefficient K_L defined?

8–52C Define equivalent length for minor loss in pipe flow. How is it related to the minor loss coefficient?

8–53C The effect of rounding of a pipe inlet on the loss coefficient is (*a*) negligible, (*b*) somewhat significant, or (*c*) very significant.

8–54C The effect of rounding of a pipe exit on the loss coefficient is (*a*) negligible, (*b*) somewhat significant, or (*c*) very significant.

8–55C Which has a greater minor loss coefficient during pipe flow: gradual expansion or gradual contraction? Why?

8–56C A piping system involves sharp turns, and thus large minor head losses. One way of reducing the head loss is to replace the sharp turns by circular elbows. What is another way?

8–57C During a retrofitting project of a fluid flow system to reduce the pumping power, it is proposed to install vanes into the miter elbows or to replace the sharp turns in 90° miter elbows by smooth curved bends. Which approach will result in a greater reduction in pumping power requirements?

8–58 Water is to be withdrawn from a 3-m-high water reservoir by drilling a 1.5-cm-diameter hole at the bottom surface. Disregarding the effect of the kinetic energy correction factor, determine the flow rate of water through the hole if (*a*) the entrance of the hole is well-rounded and (*b*) the entrance is sharp-edged.

8–59 Consider flow from a water reservoir through a circular hole of diameter D at the side wall at a vertical distance H from the free surface. The flow rate through an actual hole with a sharp-edged entrance ($K_L = 0.5$) will be considerably less than the flow rate calculated assuming "frictionless" flow and thus zero loss for the hole. Disregarding the effect of the kinetic energy correction factor, obtain a relation for the "equivalent diameter" of the sharp-edged hole for use in frictionless flow relations.
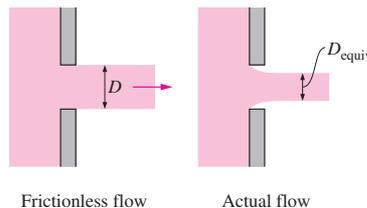
FIGURE P8–59

8–60 Repeat Prob. 8–59 for a slightly rounded entrance ($K_L = 0.12$).

8–61 A horizontal pipe has an abrupt expansion from $D_1 = 8$ cm to $D_2 = 16$ cm. The water velocity in the smaller section is 10 m/s and the flow is turbulent. The pressure in the smaller section is $P_1 = 300$ kPa. Taking the kinetic energy correction factor to be 1.06 at both the inlet and the outlet, determine the downstream pressure P_2, and estimate the error that would have occurred if Bernoulli's equation had been used. *Answers: 321 kPa, 28 kPa*
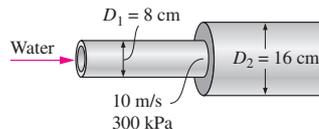
FIGURE P8–61

Piping Systems and Pump Selection

8–62C A piping system involves two pipes of different diameters (but of identical length, material, and roughness) connected in series. How would you compare the (*a*) flow rates and (*b*) pressure drops in these two pipes?

8–63C A piping system involves two pipes of different diameters (but of identical length, material, and roughness) connected in parallel. How would you compare the (*a*) flow rates and (*b*) pressure drops in these two pipes?

8–64C A piping system involves two pipes of identical diameters but of different lengths connected in parallel. How would you compare the pressure drops in these two pipes?

8–65C Water is pumped from a large lower reservoir to a higher reservoir. Someone claims that if the head loss is negligible, the required pump head is equal to the elevation difference between the free surfaces of the two reservoirs. Do you agree?

8–66C A piping system equipped with a pump is operating steadily. Explain how the operating point (the flow rate and the head loss) is established.

8–67C For a piping system, define the system curve, the characteristic curve, and the operating point on a head versus flow rate chart.

8–68 Water at 20°C is to be pumped from a reservoir ($z_A = 2$ m) to another reservoir at a higher elevation ($z_B = 9$ m) through two 25-m-long plastic pipes connected in parallel. The diameters of the two pipes are 3 cm and 5 cm. Water is to be pumped by a 68 percent efficient motor–pump unit that draws 7 kW of electric power during operation. The minor losses and the head loss in the pipes that connect the parallel pipes to the two reservoirs are considered to be negligible. Determine the total flow rate between the reservoirs and the flow rates through each of the parallel pipes.
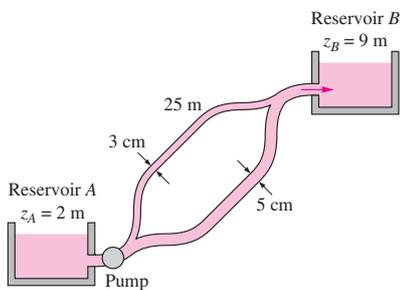
FIGURE P8–68

8–69E Water at 70°F flows by gravity from a large reservoir at a high elevation to a smaller one through a 120-ft-long, 2-in-diameter cast iron piping system that includes four standard flanged elbows, a well-rounded entrance, a sharp-edged exit, and a fully open gate valve. Taking the free surface of the lower reservoir as the reference level, determine the elevation z_1 of the higher reservoir for a flow rate of 10 ft³/min.
Answer: 23.1 ft

8–70 A 3-m-diameter tank is initially filled with water 2 m above the center of a sharp-edged 10-cm-diameter orifice. The tank water surface is open to the atmosphere, and the orifice drains to the atmosphere. Neglecting the effect of the kinetic energy correction factor, calculate (*a*) the initial velocity from the tank and (*b*) the time required to empty the tank. Does the loss coefficient of the orifice cause a significant increase in the draining time of the tank?
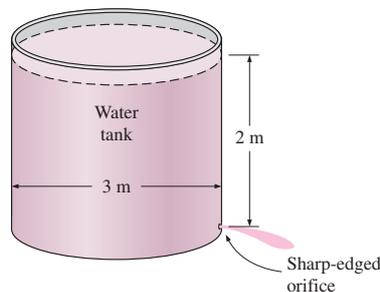
FIGURE P8–70

8–71 A 3-m-diameter tank is initially filled with water 2 m above the center of a sharp-edged 10-cm-diameter orifice. The tank water surface is open to the atmosphere, and the orifice drains to the atmosphere through a 100-m-long pipe. The friction coefficient of the pipe can be taken to be 0.015 and the effect of the kinetic energy correction factor can be neglected. Determine (*a*) the initial velocity from the tank and (*b*) the time required to empty the tank.

8–72 Reconsider Prob. 8–71. In order to drain the tank faster, a pump is installed near the tank exit. Determine how much pump power input is necessary to establish an average water velocity of 4 m/s when the tank is full at $z = 2$ m. Also, assuming the discharge velocity to remain constant, estimate the time required to drain the tank.

Someone suggests that it makes no difference whether the pump is located at the beginning or at the end of the pipe, and that the performance will be the same in either case, but
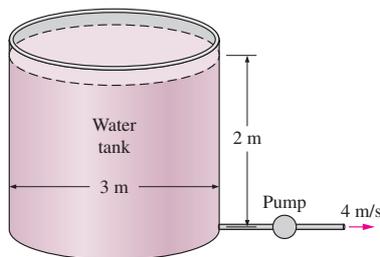
FIGURE P8–72

another person argues that placing the pump near the end of the pipe may cause cavitation. The water temperature is 30°C, so the water vapor pressure is $P_v = 4.246$ kPa $= 0.43$ m-H_2O, and the system is located at sea level. Investigate if there is the possibility of cavitation and if we should be concerned about the location of the pump.

8–73 Oil at 20°C is flowing through a vertical glass funnel that consists of a 15-cm-high cylindrical reservoir and a 1-cm-diameter, 25-cm-high pipe. The funnel is always maintained full by the addition of oil from a tank. Assuming the entrance effects to be negligible, determine the flow rate of oil through the funnel and calculate the "funnel effectiveness," which can be defined as the ratio of the actual flow rate through the funnel to the maximum flow rate for the "frictionless" case. *Answers:* 4.09×10^{-6} m³/s, 1.86 percent
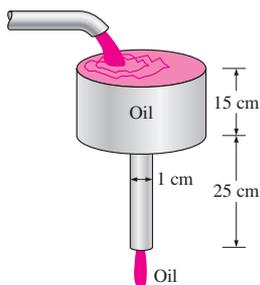
FIGURE P8–73

8–74 Repeat Prob. 8–73 assuming (*a*) the diameter of the pipe is doubled and (*b*) the length of the pipe is doubled.

8–75 Water at 15°C is drained from a large reservoir using two horizontal plastic pipes connected in series. The first pipe is 20 m long and has a 10-cm diameter, while the second pipe is 35 m long and has a 4-cm diameter. The water level in the reservoir is 18 m above the centerline of the pipe. The pipe entrance is sharp-edged, and the contraction between the two pipes is sudden. Neglecting the effect of the kinetic energy correction factor, determine the discharge rate of water from the reservoir.
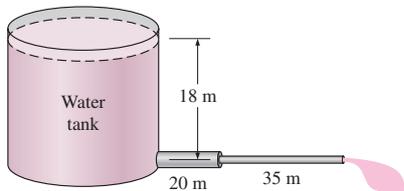
FIGURE P8–75

8–76E A farmer is to pump water at 70°F from a river to a water storage tank nearby using a 125-ft-long, 5-in-diameter plastic pipe with three flanged 90° smooth bends. The water velocity near the river surface is 6 ft/s, and the pipe inlet is placed in the river normal to the flow direction of water to take advantage of the dynamic pressure. The elevation difference between the river and the free surface of the tank is 12 ft. For a flow rate of 1.5 ft³/s and an overall pump efficiency of 70 percent, determine the required electric power input to the pump.

8–77E Reconsider Prob. 8–76E. Using EES (or other) software, investigate the effect of the pipe diameter on the required electric power input to the pump. Let the pipe diameter vary from 1 to 10 in, in increments of 1 in. Tabulate and plot the results, and draw conclusions.

8–78 A water tank filled with solar-heated water at 40°C is to be used for showers in a field using gravity-driven flow. The system includes 20 m of 1.5-cm-diameter galvanized iron piping with four miter bends (90°) without vanes and a wide-open globe valve. If water is to flow at a rate of 0.7 L/s through the shower head, determine how high the water level in the tank must be from the exit level of the shower. Disregard the losses at the entrance and at the shower head, and neglect the effect of the kinetic energy correction factor.

8–79 Two water reservoirs *A* and *B* are connected to each other through a 40-m-long, 2-cm-diameter cast iron pipe with a sharp-edged entrance. The pipe also involves a swing check valve and a fully open gate valve. The water level in both reservoirs is the same, but reservoir *A* is pressurized by compressed air while reservoir *B* is open to the atmosphere at 88 kPa. If the initial flow rate through the pipe is 1.2 L/s, determine the absolute air pressure on top of reservoir *A*. Take the water temperature to be 10°C. *Answer:* 733 kPa
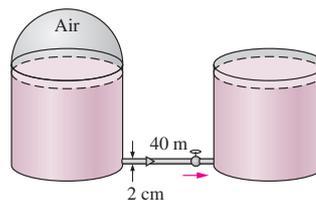
FIGURE P8–79

8–80 A vented tanker is to be filled with fuel oil with $\rho = 920$ kg/m³ and $\mu = 0.045$ kg/m · s from an underground reservoir using a 20-m-long, 5-cm-diameter plastic hose with a slightly rounded entrance and two 90° smooth bends. The elevation difference between the oil level in the reservoir and the top of the tanker where the hose is discharged is 5 m. The capacity of the tanker is 18 m³ and the filling time is 30 min. Taking the kinetic energy correction factor at hose discharge

to be 1.05 and assuming an overall pump efficiency of 82 percent, determine the required power input to the pump.

Tanker
18 m³

20 m

5 m

5 cm→

Pump
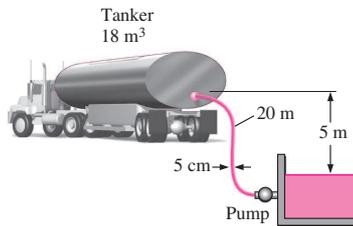
FIGURE P8–80

8–81 Two pipes of identical length and material are connected in parallel. The diameter of pipe A is twice the diameter of pipe B. Assuming the friction factor to be the same in both cases and disregarding minor losses, determine the ratio of the flow rates in the two pipes.

8–82 A certain part of cast iron piping of a water distribution system involves a parallel section. Both parallel pipes have a diameter of 30 cm, and the flow is fully turbulent. One of the branches (pipe A) is 1000 m long while the other branch (pipe B) is 3000 m long. If the flow rate through pipe A is 0.4 m³/s, determine the flow rate through pipe B. Disregard minor losses and assume the water temperature to be 15°C. Show that the flow is fully turbulent, and thus the friction factor is independent of Reynolds number. *Answer: 0.231 m³/s*

1000 m

A

30 cm

0.4 m³/s

B

30 cm

3000 m
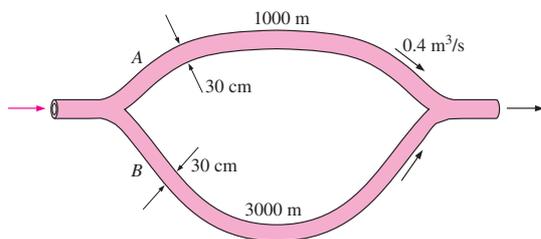
FIGURE P8–82

8–83 Repeat Prob. 8–82 assuming pipe A has a halfway-closed gate valve ($K_L = 2.1$) while pipe B has a fully open globe valve ($K_L = 10$), and the other minor losses are negligible. Assume the flow to be fully turbulent.

8–84 A geothermal district heating system involves the transport of geothermal water at 110°C from a geothermal well to a city at about the same elevation for a distance of 12 km at a rate of 1.5 m³/s in 60-cm-diameter stainless-steel pipes. The fluid pressures at the wellhead and the arrival point in the city are to be the same. The minor losses are neg-

ligible because of the large length-to-diameter ratio and the relatively small number of components that cause minor losses. (*a*) Assuming the pump–motor efficiency to be 74 percent, determine the electric power consumption of the system for pumping. Would you recommend the use of a single large pump or several smaller pumps of the same total pumping power scattered along the pipeline? Explain. (*b*) Determine the daily cost of power consumption of the system if the unit cost of electricity is $0.06/kWh. (*c*) The temperature of geothermal water is estimated to drop 0.5°C during this long flow. Determine if the frictional heating during flow can make up for this drop in temperature.

8–85 Repeat Prob. 8–84 for cast iron pipes of the same diameter.

8–86E A clothes dryer discharges air at 1 atm and 120°F at a rate of 1.2 ft³/s when its 5-in-diameter, well-rounded vent with negligible loss is not connected to any duct. Determine the flow rate when the vent is connected to a 15-ft-long, 5-in-diameter duct made of galvanized iron, with three 90° flanged smooth bends. Take the friction factor of the duct to be 0.019, and assume the fan power input to remain constant.

Hot air

Clothes drier

15 ft

5 in
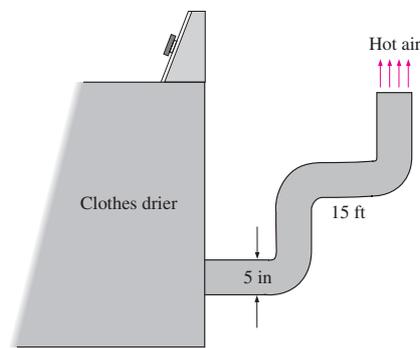
FIGURE P8–86E

8–87 In large buildings, hot water in a water tank is circulated through a loop so that the user doesn't have to wait for all the water in long piping to drain before hot water starts coming out. A certain recirculating loop involves 40-m-long, 1.2-cm-diameter cast iron pipes with six 90° threaded smooth bends and two fully open gate valves. If the average flow velocity through the loop is 2.5 m/s, determine the required power input for the recirculating pump. Take the average water temperature to be 60°C and the efficiency of the pump to be 70 percent. *Answer: 0.217 kW*

8–88 Reconsider Prob. 8–87. Using EES (or other) software, investigate the effect of the average flow velocity on the power input to the recirculating pump.

Let the velocity vary from 0 to 3 m/s in increments of 0.3 m/s. Tabulate and plot the results.

8–89 Repeat Prob. 8–87 for plastic pipes.

Flow Rate and Velocity Measurements

8–90C What are the primary considerations when selecting a flowmeter to measure the flow rate of a fluid?

8–91C Explain how flow rate is measured with a Pitot-static tube, and discuss its advantages and disadvantages with respect to cost, pressure drop, reliability, and accuracy.

8–92C Explain how flow rate is measured with obstruction-type flowmeters. Compare orifice meters, flow nozzles, and Venturi meters with respect to cost, size, head loss, and accuracy.

8–93C How do positive displacement flowmeters operate? Why are they commonly used to meter gasoline, water, and natural gas?

8–94C Explain how flow rate is measured with a turbine flowmeter, and discuss how they compare to other types of flowmeters with respect to cost, head loss, and accuracy.

8–95C What is the operating principle of variable-area flowmeters (rotameters)? How do they compare to other types of flowmeters with respect to cost, head loss, and reliability?

8–96C What is the difference between the operating principles of thermal and laser Doppler anemometers?

8–97C What is the difference between laser Doppler velocimetry (LDV) and particle image velocimetry (PIV)?

8–98 The flow rate of ammonia at 10°C ($\rho = 624.6$ kg/m^3 and $\mu = 1.697 \times 10^{-4}$ kg/m · s) through a 3-cm-diameter pipe is to be measured with a 1.5-cm-diameter flow nozzle equipped with a differential pressure gage. If the gage reads a pressure differential of 4 kPa, determine the flow rate of ammonia through the pipe, and the average flow velocity.

8–99 The flow rate of water through a 10-cm-diameter pipe is to be determined by measuring the water velocity at several locations along a cross section. For the set of measurements given in the table, determine the flow rate.

r, cm	V, m/s
0	6.4
1	6.1
2	5.2
3	4.4
4	2.0
5	0.0

8–100E An orifice with a 2-in-diameter opening is used to measure the mass flow rate of water at 60°F ($\rho = 62.36$ lbm/ft^3 and $\mu = 7.536 \times 10^{-4}$ lbm/ft · s) through a horizontal 4-in-diameter pipe. A mercury manometer is used to measure the pressure difference across the orifice. If the differential height of the manometer is read to be 6 in, determine the volume flow rate of water through the pipe, the average velocity, and the head loss caused by the orifice meter.
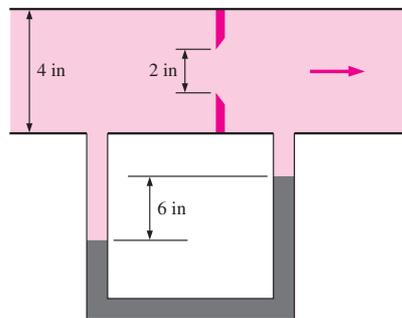
FIGURE P8–100E

8–101E Repeat Prob. 8–100E for a differential height of 9 in.

8–102 The flow rate of water at 20°C ($\rho = 998$ kg/m^3 and $\mu = 1.002 \times 10^{-3}$ kg/m · s) through a 50-cm-diameter pipe is measured with an orifice meter with a 30-cm-diameter opening to be 250 L/s. Determine the pressure difference indicated by the orifice meter and the head loss.

8–103 A Venturi meter equipped with a differential pressure gage is used to measure the flow rate of water at 15°C ($\rho = 999.1$ kg/m^3) through a 5-cm-diameter horizontal pipe. The diameter of the Venturi neck is 3 cm, and the measured pressure drop is 5 kPa. Taking the discharge coefficient to be 0.98, determine the volume flow rate of water and the average velocity through the pipe. *Answers:* 2.35 L/s and 1.20 m/s
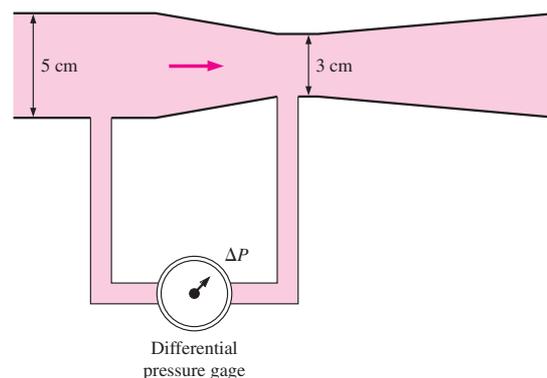
FIGURE P8–103

8–104 Reconsider Prob. 8–103. Letting the pressure drop vary from 1 kPa to 10 kPa, evaluate the flow rate at intervals of 1 kPa, and plot it against the pressure drop.

8–105 The mass flow rate of air at 20°C ($\rho = 1.204$ kg/m³) through a 15-cm-diameter duct is measured with a Venturi meter equipped with a water manometer. The Venturi neck has a diameter of 6 cm, and the manometer has a maximum differential height of 40 cm. Taking the discharge coefficient to be 0.98, determine the maximum mass flow rate of air this Venturi meter can measure. *Answer:* 0.273 kg/s
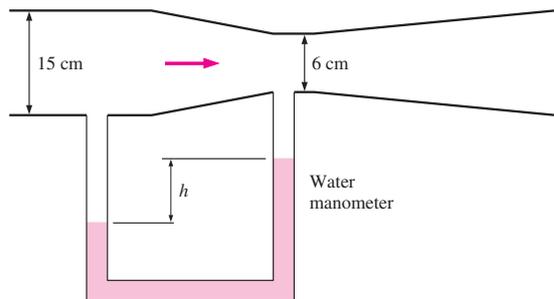
FIGURE P8–105

8–106 Repeat Prob. 8–105 for a Venturi neck diameter of 7.5 cm.

8–107 A vertical Venturi meter equipped with a differential pressure gage shown in Fig. P8–107 is used to measure the
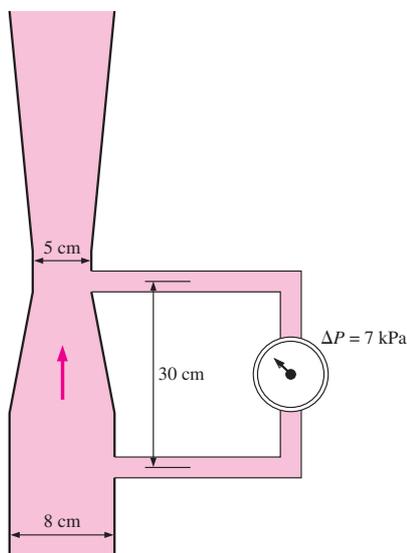
FIGURE P8–107

flow rate of liquid propane at 10°C ($\rho = 514.7$ kg/m³) through an 8-cm-diameter vertical pipe. For a discharge coefficient of 0.98, determine the volume flow rate of propane through the pipe.

8–108 A flow nozzle equipped with a differential pressure gage is used to measure the flow rate of water at 10°C ($\rho = 999.7$ kg/m³ and $\mu = 1.307 \times 10^{-3}$ kg/m · s) through a 3-cm-diameter horizontal pipe. The nozzle exit diameter is 1.5 cm, and the measured pressure drop is 3 kPa. Determine the volume flow rate of water, the average velocity through the pipe, and the head loss.
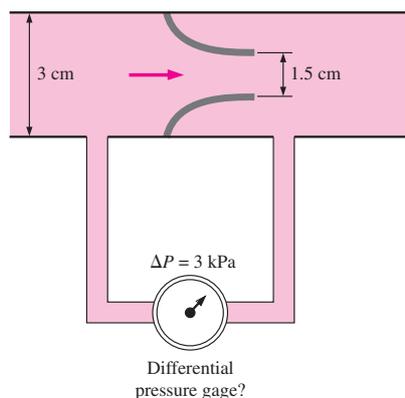
FIGURE P8–108

8–109 A 16-L kerosene tank ($\rho = 820$ kg/m³) is filled with a 2-cm-diameter hose equipped with a 1.5-cm-diameter nozzle meter. If it takes 20 s to fill the tank, determine the pressure difference indicated by the nozzle meter.

8–110 The flow rate of water at 20°C ($\rho = 998$ kg/m³ and $\mu = 1.002 \times 10^{-3}$ kg/m · s) through a 4-cm-diameter pipe is measured with a 2-cm-diameter nozzle meter equipped with an inverted air–water manometer. If the manometer indicates
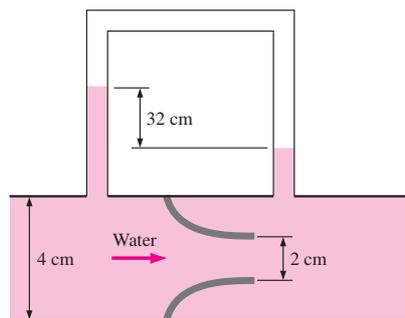
FIGURE P8–110

a differential water height of 32 cm, determine the volume flow rate of water and the head loss caused by the nozzle meter.

8–111E The volume flow rate of liquid refrigerant-134a at 10°F ($\rho = 83.31$ lbm/ft^3) is to be measured with a horizontal Venturi meter with a diameter of 5 in at the inlet and 2 in at the throat. If a differential pressure meter indicates a pressure drop of 7.4 psi, determine the flow rate of the refrigerant. Take the discharge coefficient of the Venturi meter to be 0.98.

Review Problems

8–112 The compressed air requirements of a manufacturing facility are met by a 150-hp compressor that draws in air from the outside through an 8-m-long, 20-cm-diameter duct made of thin galvanized iron sheets. The compressor takes in air at a rate of 0.27 m^3/s at the outdoor conditions of 15°C and 95 kPa. Disregarding any minor losses, determine the useful power used by the compressor to overcome the frictional losses in this duct. *Answer:* 9.66 W
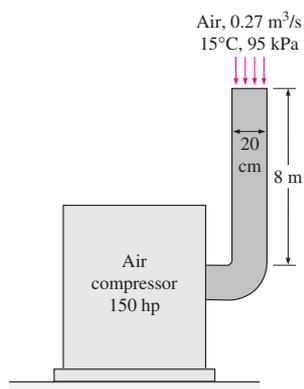
FIGURE P8–112

8–113 A house built on a riverside is to be cooled in summer by utilizing the cool water of the river. A 15-m-long sec-
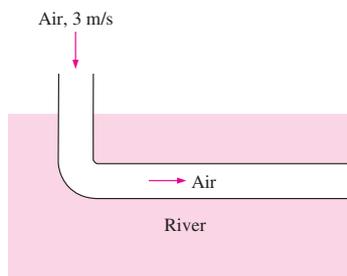
FIGURE P8–113

tion of a circular stainless-steel duct of 20-cm diameter passes through the water. Air flows through the underwater section of the duct at 3 m/s at an average temperature of 15°C. For an overall fan efficiency of 62 percent, determine the fan power needed to overcome the flow resistance in this section of the duct.

8–114 The velocity profile in fully developed laminar flow in a circular pipe, in m/s, is given by $u(r) = 6(1 - 100r^2)$, where r is the radial distance from the centerline of the pipe in m. Determine (*a*) the radius of the pipe, (*b*) the average velocity through the pipe, and (*c*) the maximum velocity in the pipe.

8–115E The velocity profile in a fully developed laminar flow of water at 40°F in a 80-ft-long horizontal circular pipe, in ft/s, is given by $u(r) = 0.8(1 - 625r^2)$, where r is the radial distance from the centerline of the pipe in ft. Determine (*a*) the volume flow rate of water through the pipe, (*b*) the pressure drop across the pipe, and (*c*) the useful pumping power required to overcome this pressure drop.

8–116E Repeat Prob. 8–115E assuming the pipe is inclined 12° from the horizontal and the flow is uphill.

8–117 Consider flow from a reservoir through a horizontal pipe of length *L* and diameter *D* that penetrates into the side wall at a vertical distance *H* from the free surface. The flow rate through an actual pipe with a reentrant section ($K_L = 0.8$) will be considerably less than the flow rate through the hole calculated assuming "frictionless" flow and thus zero loss. Obtain a relation for the "equivalent diameter" of the reentrant pipe for use in relations for frictionless flow through a hole and determine its value for a pipe friction factor, length, and diameter of 0.018, 10 m, and 0.04 m, respectively. Assume the friction factor of the pipe to remain constant and the effect of the kinetic energy correction factor to be negligible.

8–118 Water is to be withdrawn from a 5-m-high water reservoir by drilling a well-rounded 3-cm-diameter hole with negligible loss at the bottom surface and attaching a horizontal 90° bend of negligible length. Taking the kinetic energy correction factor to be 1.05, determine the flow rate of water through the bend if (*a*) the bend is a flanged smooth bend
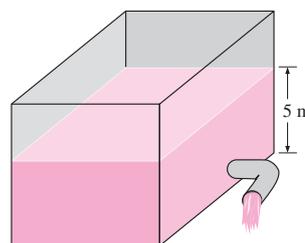
FIGURE P8–118

and (*b*) the bend is a miter bend without vanes. *Answers:* (*a*) 0.00603 m³/s, (*b*) 0.00478 m³/s

8–119 In a geothermal district heating system, 10,000 kg/s of hot water must be delivered a distance of 10 km in a horizontal pipe. The minor losses are negligible, and the only significant energy loss will arise from pipe friction. The friction factor can be taken to be 0.015. Specifying a larger-diameter pipe would reduce water velocity, velocity head, pipe friction, and thus power consumption. But a larger pipe would also cost more money initially to purchase and install. Otherwise stated, there is an optimum pipe diameter that will minimize the sum of pipe cost and future electric power cost.

Assume the system will run 24 h/day, every day, for 30 years. During this time the cost of electricity will remain constant at $0.06/kWh. Assume system performance stays constant over the decades (this may not be true, especially if highly mineralized water is passed through the pipeline—scale may form). The pump has an overall efficiency of 80 percent. The cost to purchase, install, and insulate a 10-km pipe depends on the diameter *D* and is given by *Cost* = \$10⁶ *D*², where *D* is in m. Assuming zero inflation and interest rate for simplicity and zero salvage value and zero maintenance cost, determine the optimum pipe diameter.

8–120 Water at 15°C is to be discharged from a reservoir at a rate of 18 L/s using two horizontal cast iron pipes connected in series and a pump between them. The first pipe is 20 m long and has a 6-cm diameter, while the second pipe is 35 m long and has a 4-cm diameter. The water level in the reservoir is 30 m above the centerline of the pipe. The pipe entrance is sharp-edged, and losses associated with the connection of the pump are negligible. Neglecting the effect of the kinetic energy correction factor, determine the required pumping head and the minimum pumping power to maintain the indicated flow rate.
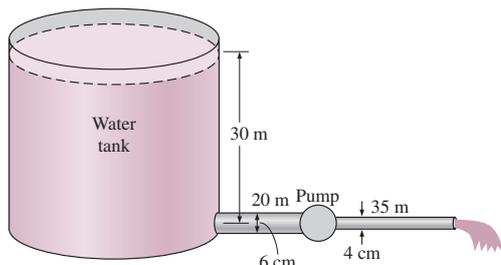
FIGURE P8–120

8–121 Reconsider Prob. 8–120. Using EES (or other) software, investigate the effect of the second pipe diameter on the required pumping head to maintain the

indicated flow rate. Let the diameter vary from 1 to 10 cm in increments of 1 cm. Tabulate and plot the results.

8–122 Two pipes of identical diameter and material are connected in parallel. The length of pipe *A* is twice the length of pipe *B*. Assuming the flow is fully turbulent in both pipes and thus the friction factor is independent of the Reynolds number and disregarding minor losses, determine the ratio of the flow rates in the two pipes. *Answer:* 0.707

8–123 A pipeline that transports oil at 40°C at a rate of 3 m³/s branches out into two parallel pipes made of commercial steel that reconnect downstream. Pipe *A* is 500 m long and has a diameter of 30 cm while pipe *B* is 800 m long and has a diameter of 45 cm. The minor losses are considered to be negligible. Determine the flow rate through each of the parallel pipes.
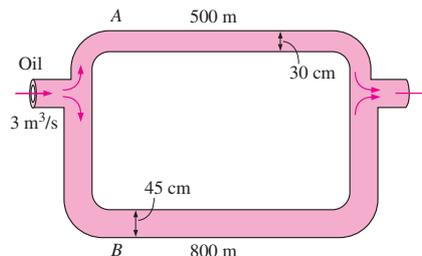
FIGURE P8–123

8–124 Repeat Prob. 8–123 for hot-water flow of a district heating system at 100°C.

8–125E A water fountain is to be installed at a remote location by attaching a cast iron pipe directly to a water main through which water is flowing at 70°F and 60 psig. The entrance to the pipe is sharp-edged, and the 50-ft-long piping system involves three 90° miter bends without vanes, a fully open gate valve, and an angle valve with a loss coefficient of 5 when fully open. If the system is to provide water at a rate of 20 gal/min and the elevation difference between the pipe and the fountain is negligible, determine the minimum diameter of the piping system. *Answer:* 0.76 in
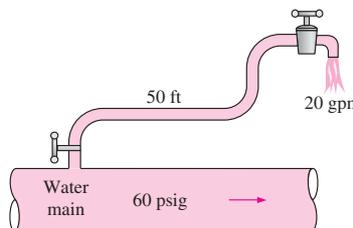
FIGURE P8–125E

8–126E Repeat Prob. 8–125E for plastic pipes.

8–127 In a hydroelectric power plant, water at 20°C is supplied to the turbine at a rate of 0.8 m³/s through a 200-m-long, 0.35-m-diameter cast iron pipe. The elevation difference between the free surface of the reservoir and the turbine discharge is 70 m, and the combined turbine–generator efficiency is 84 percent. Disregarding the minor losses because of the large length-to-diameter ratio, determine the electric power output of this plant.

8–128 In Prob. 8–127, the pipe diameter is tripled in order to reduce the pipe losses. Determine the percent increase in the net power output as a result of this modification.

8–129E The drinking water needs of an office are met by large water bottles. One end of a 0.35-in-diameter, 6-ft-long plastic hose is inserted into the bottle placed on a high stand, while the other end with an on/off valve is maintained 3 ft below the bottom of the bottle. If the water level in the bottle is 1 ft when it is full, determine how long it will take to fill an 8-oz glass ($= 0.00835$ ft³) (*a*) when the bottle is first opened and (*b*) when the bottle is almost empty. Take the total minor loss coefficient, including the on/off valve, to be 2.8 when it is fully open. Assume the water temperature to be the same as the room temperature of 70°F. *Answers: (a)* 2.4 s, *(b)* 2.8 s
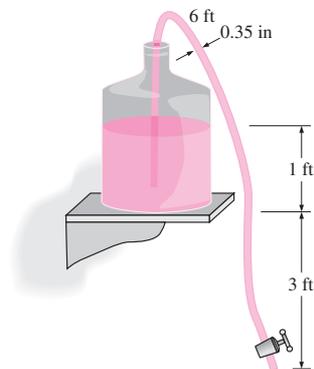
FIGURE P8–129E

8–130E Reconsider Prob. 8–129E. Using EES (or other) software, investigate the effect of the hose diameter on the time required to fill a glass when the bottle is full. Let the diameter vary from 0.2 to 2 in, in increments of 0.2 in. Tabulate and plot the results.

8–131E Reconsider Prob. 8–129E. The office worker who set up the siphoning system purchased a 12-ft-long reel of the plastic tube and wanted to use the whole thing to avoid cutting it in pieces, thinking that it is the elevation difference that makes siphoning work, and the length of the tube is not important. So he used the entire 12-ft-long tube. Assuming the turns or constrictions in the tube are not significant (being very optimistic) and the same elevation is maintained, determine the time it takes to fill a glass of water for both cases.

8–132 A circular water pipe has an abrupt expansion from diameter $D_1 = 15$ cm to $D_2 = 20$ cm. The pressure and the average water velocity in the smaller pipe are $P_1 = 120$ kPa and 10 m/s, respectively, and the flow is turbulent. By applying the continuity, momentum, and energy equations and disregarding the effects of the kinetic energy and momentum-flux correction factors, show that the loss coefficient for sudden expansion is $K_L = (1 - D_1^2/D_2^2)^2$, and calculate K_L and P_2 for the given case.
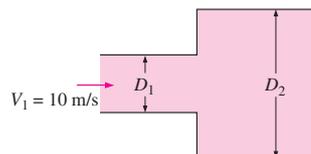
FIGURE P8–132

8–133 The water at 20°C in a 10-m-diameter, 2-m-high aboveground swimming pool is to be emptied by unplugging a 3-cm-diameter, 25-m-long horizontal plastic pipe attached to the bottom of the pool. Determine the initial rate of discharge of water through the pipe and the time it will take to empty the swimming pool completely assuming the entrance to the pipe is well-rounded with negligible loss. Take the friction factor of the pipe to be 0.022. Using the initial discharge velocity, check if this is a reasonable value for the friction factor. *Answers:* 1.01 L/s, 86.7 *h*
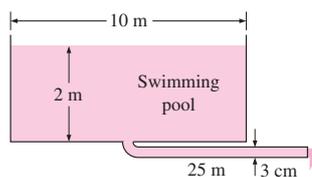
FIGURE P8–133

8–134 Reconsider Prob. 8–133. Using EES (or other) software, investigate the effect of the discharge pipe diameter on the time required to empty the pool completely. Let the diameter vary from 1 to 10 cm, in increments of 1 cm. Tabulate and plot the results.

8–135 Repeat Prob. 8–133 for a sharp-edged entrance to the pipe with $K_L = 0.5$. Is this "minor loss" truly "minor" or not?

8–136 A system that consists of two interconnected cylindrical tanks with $D_1 = 30$ cm and $D_2 = 12$ cm is to be used to determine the discharge coefficient of a short $D_0 = 5$ mm diameter orifice. At the beginning ($t = 0$ s), the fluid heights in the tanks are $h_1 = 50$ cm and $h_2 = 15$ cm, as shown in Fig. P8–136. If it takes 170 s for the fluid levels in the two tanks to equalize and the flow to stop, determine the discharge coefficient of the orifice. Disregard any other losses associated with this flow.
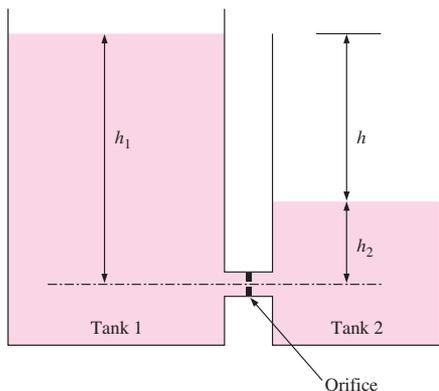
FIGURE P8–136

8–137 A highly viscous liquid discharges from a large container through a small-diameter tube in laminar flow. Disre-

FIGURE P8–137

garding entrance effects and velocity heads, obtain a relation for the variation of fluid depth in the tank with time.

8–138 A student is to determine the kinematic viscosity of an oil using the system shown in Prob. 8–137. The initial fluid height in the tank is $H = 40$ cm, the tube diameter is $d = 6$ mm, the tube length is $L = 0.65$ m, and the tank diameter is $D = 0.63$ m. The student observes that it takes 2842 s for the fluid level in the tank to drop to 36 cm. Find the fluid viscosity.

Design and Essay Problems

8–139 Electronic boxes such as computers are commonly cooled by a fan. Write an essay on forced air cooling of electronic boxes and on the selection of the fan for electronic devices.

8–140 Design an experiment to measure the viscosity of liquids using a vertical funnel with a cylindrical reservoir of height h and a narrow flow section of diameter D and length L. Making appropriate assumptions, obtain a relation for viscosity in terms of easily measurable quantities such as density and volume flow rate. Is there a need for the use of a correction factor?

8–141 A pump is to be selected for a waterfall in a garden. The water collects in a pond at the bottom, and the elevation difference between the free surface of the pond and the location where the water is discharged is 3 m. The flow rate of water is to be at least 8 L/s. Select an appropriate motor–pump unit for this job and identify three manufacturers with product model numbers and prices. Make a selection and explain why you selected that particular product. Also estimate the cost of annual power consumption of this unit assuming continuous operation.

8–142 During a camping trip you notice that water is discharged from a high reservoir to a stream in the valley through a 30-cm-diameter plastic pipe. The elevation difference between the free surface of the reservoir and the stream is 70 m. You conceive the idea of generating power from this water. Design a power plant that will produce the most power from this resource. Also, investigate the effect of power generation on the discharge rate of water. What discharge rate will maximize the power production?